AWARD NUMBER: W81XWH-18-1-0669

TITLE: Linking Cerebral Hemodynamics and Neuroinflammation to Alzheimer's Pathology in Repetitive Mild Traumatic Brain Injury

PRINCIPAL INVESTIGATOR: Levi B. Wood

CONTRACTING ORGANIZATION: Georgia Tech Research Corporation

REPORT DATE: July 2023

TYPE OF REPORT: Final

PREPARED FOR: U.S. Army Medical Research and Development Command
Fort Detrick, Maryland 21702-5012

DISTRIBUTION STATEMENT: Approved for public release; distribution is unlimited.

The views, opinions and/or findings contained in this report are those of the author(s) and should not be construed as an official Department of the Army position, policy or decision unless so designated by other documentation.

REPORT DOCUMENTATION PAGE

Form Approved
OMB No. 0704-0188

Public reporting burden for this collection of information is estimated to average 1 hour per response, including the time for reviewing instructions, searching existing data sources, gathering and maintaining the data needed, and completing and reviewing this collection of information. Send comments regarding this burden estimate or any other aspect of this collection of information, including suggestions for reducing this burden to Department of Defense, Washington Headquarters Services, Directorate for Information Operations and Reports (0704-0188), 1215 Jefferson Davis Highway, Suite 1204, Arlington, VA 22202-4302. Respondents should be aware that notwithstanding any other provision of law, no person shall be subject to any penalty for failing to comply with a collection of information if it does not display a currently valid OMB control number. **PLEASE DO NOT RETURN YOUR FORM TO THE ABOVE ADDRESS.**

1. REPORT DATE	2. REPORT TYPE	3. DATES COVERED
JULY 2023	Final	15SEPT2018 - 14MAR2023

4. TITLE AND SUBTITLE

Linking Cerebral Hemodynamics and Neuroinflammation to Alzheimer's Pathology in Repetitive Mild Traumatic Brain Injury

5a. CONTRACT NUMBER
W81XWH-18-1-0669

5b. GRANT NUMBER

5c. PROGRAM ELEMENT NUMBER

6. AUTHOR(S)

Levi B Wood and Erin Buckley

E-Mail: levi.wood@me.gatech.edu

5d. PROJECT NUMBER

5e. TASK NUMBER

5f. WORK UNIT NUMBER

7. PERFORMING ORGANIZATION NAME(S) AND ADDRESS(ES)
GEORGIA TECH RESEARCH CORPORATION
505 10th St NW
Atlanta, GA 30318

8. PERFORMING ORGANIZATION REPORT NUMBER

9. SPONSORING / MONITORING AGENCY NAME(S) AND ADDRESS(ES)

U.S. Army Medical Research and Development Command
Fort Detrick, Maryland 21702-5012

10. SPONSOR/MONITOR'S ACRONYM(S)

11. SPONSOR/MONITOR'S REPORT NUMBER(S)

12. DISTRIBUTION / AVAILABILITY STATEMENT
Approved for public release; distribution is unlimited.

13. SUPPLEMENTARY NOTES

14. ABSTRACT

Project Purpose and Goals: Repetitive mild traumatic brain injuries (rmTBI) not only take a toll on a patient's immediate well-being, but are also associated with increased risk of neurodegenerative disease. In the current study, we quantified cerebral blood flow together with immune protein and transcriptional profiling in 3xTg-AD mice to identify the effects of rmTBI and relationships among cerebral blood flow, immune markers, and transcripts (**Aim 1**). We also modulated p38 MAPK immune signaling to determine its role in regulating brain immunity and pathological markers (**Aim 2**).
Major Findings. The key outcome of this study is the identification of a neuroimmune cascade of mild traumatic brain injury in 3xTg-AD mice, consisting of i) an immediate decrease in neuronal homeostatic gene expression and an elevation of AD-associated genes after a single injury, ii) elevation of a subset of cortical cytokines that co-label with neurons after each successive injury in correlation with phosphorylated tau, and iii) increased expression of non-neuronal genes suggesting glial reactivity within days of repeated injury. We provide resolution of these acute protein and transcriptional changes at a previously uncharacterized minutes-to-days time scale alongside the key experimental variables of sex, brain region, and number of injuries.

15. SUBJECT TERMS
Traumatic brain injury, cerebral blood flow, hemodynamics, cytokines, phospho-proteins, signaling, amyloid beta, tau, Alzheimer's disease.

16. SECURITY CLASSIFICATION OF:			17. LIMITATION OF ABSTRACT	18. NUMBER OF PAGES	19a. NAME OF RESPONSIBLE PERSON
a. REPORT	b. ABSTRACT	c. THIS PAGE			USAMRDC
U	U	U	UU	78	19b. TELEPHONE NUMBER *(include area code)*

TABLE OF CONTENTS

	Page
1. Introduction	1
2. Keywords	1
3. Accomplishments	1
4. Impact	15
5. Changes/Problems	16
6. Products	16
7. Participants & Other Collaborating Organizations	19
8. Special Reporting Requirements	23
9. Appendices	23

1. INTRODUCTION:

Repetitive mild traumatic brain injuries (rmTBI) not only take a toll on a patient's immediate well-being, but are also associated with increased risk of neurodegenerative disease. The long-term consequence of repetitive TBI were recently emphasized by the report that 177 of 202 American football players possessed molecular hallmarks of dementia, including amyloid beta (Aβ) plaques and neurofibrillary tangles (NFTs) associated with Alzheimer's disease (AD) (Mez et al, JAMA. 2017; 318(4):360-70). The discovery of robust biomarkers capable of predicting long-term cognitive and pathological outcome after mTBI would address an unmet clinical need calling for objective methods of evaluating prognosis, assessing treatment efficacy, and managing injury-risk exposure. We have investigated the potential of cerebral blood flow (CBF) as a biomarker of cognitive outcome after rmTBI in a well-controlled and well-established mouse model. Using diffuse correlation spectroscopy (DCS) to quantify cerebral blood flow, our published findings suggest that low cerebral blood flow measured either before or early on in the evolution of injury caused by repetitive closed head injury (rCHI) may predict poor cognitive outcome after repetitive injuries. This result gives us the unique capacity to explore molecular mechanisms driving poor outcome by first measuring CBF prior to injury, which predicts long-term cognitive outcome. Then we can relate these predicted cognitive outcomes to pathological assessment of tissues taken acutely after rCHI. One pathologic mechanism that has received limited attention in rmTBI is neuroinflammation. In this project, we expanded our preliminary results to investigate the effects of rmTBI and inter-relationships between CBF, panels of protein markers of inflammation and pathology, and transcriptional profiles using the 3xTg-AD Alzheimer's mouse model (**Aim 1**). Further, we modulated p38 MAPK immune signaling in an effort to relate MAPK signaling to cytokine production and pathological markers (**Aim 2**).

2. KEYWORDS:

Traumatic brain injury, cerebral blood flow, hemodynamics, cytokines, phospho-proteins, signaling, amyloid beta, tau, Alzheimer's disease.

3. ACCOMPLISHMENTS:

What were the major goals of the project?

<u>Aim 1, BIOMARKERS:</u> Test if deranged cerebral blood flow, oxygen metabolism, and/or cerebrovascular reactivity predicts chronic tissue pathology after repetitive closed head injury.

Specific Aim 1	**Timeline** (Months)	**Percent Complete**
Major Task 1: Legwork		
<u>Subtask 1:</u> Obtain IACUC and ACURO project approval.	1-3	100%
<u>Subtask 2</u>: Breeding and aging 3xTg-AD mouse colony.	3-9	100%

Subtask 3: Establish IHC quantification workflow using existing tissues in the Wood lab.	1-9	100%
Milestones Achieved: IACUC/ACURO approved, colony of aged/aging 3xTg-AD mice ready for use.	Total: 9	100%
Major Task 2: Data Collection		
Subtask 1: Measure blood flow for up to 1 month after 1xCHI, 3xCHI, and 5xCHI.	9-12	100%
Subtask 2: Measure cerebrovascular reactivity for up to 1 month after 1xCHI, 3xCHI, and 5xCHI.	13-18	100%
Subtask 3: Extract & prep brains to assess pathological, biochemical, transcriptional markers of injury.	9-21	100%
Milestone(s) Achieved: Aim 1 data collected.	Total: 12	100%
Major Task 3: Data Analysis		
Subtask 1: Analyze blood flow, metabolism, and vascular reactivity time series data.	12-21	100%
Subtask 2: Process brain samples, analyze temporal evolution of pathological markers.	8-26	100%
Subtask 3: Identify hemodynamic biomarkers of AD pathology, inflammation, and transcriptional changes.	20-28	100%
Milestone(s) Achieved: Detailed temporal analysis of changes in hemodynamic markers and molecular changes.	Total: 16	100%
Major Task 4: Manuscript preparation		
Subtask 1: Prepare manuscript.	24-30	100
Subtask 2: Report data	31-32	100%
Milestone(s) Achieved: Manuscript published, data disseminated to the research community.	Total: 8	100%

Aim 2, MECHANISMS: Determine if inflammatory p38 MAPK and Jak/Stat pathway signaling drives outcome after repetitive closed head injury.

Specific Aim 2 (MECHANISMS)	**Timeline** (Months)	**Percent Complete**
Major Task 1: Establish pre-treatment timing		
Subtask 1: Treat mice with p38 or Jak/Stat kinase inhibitors.	3-5	100%
Subtask 2: Quantify p38 and Jak/Stat phosphorylation from mouse tissues. Identify	5-6	100%

optimal timing of pre-treatments to induce > 4h sustained kinase inhibition.		
Milestones Achieved: Identify drugs that yield sustained kinase inhibition	Total: 3	100%
Major Task 2: Pre-treat to inhibit neuroinflammation		
Subtask 1: Test up to 4 potential inhibitors, assess AD pathological outcome after 1 month. Process data to identify most promising pre-treatment inhibitor.	21-27	100%
Subtask 2: Using most promising inhibitor, assess effects on AD pathology and neuroinflammation 1 & 4h post 5xCHI. Process brain samples, statistical analysis.	28-30	100%
Milestone(s) Achieved: Determine if kinase inhibitors modulate Aβ and NFT pathology, microglial & astrocyte activation, cytokine expression, and blood flow.	Total: 9	100%
Major Task 3: Manuscript preparation		
Subtask 1: Prepare manuscript detailing how modulating inflammatory signaling modulates hemodynamics, pathology, and behavior.	30-36	-
Subtask 2: Report data	35-36	100%
Milestone(s) Achieved: Manuscript submitted, data disseminated to the research community.	Total: 6	100%

What was accomplished under these goals?

Accomplishments. To our knowledge, the data from this project contribute the most comprehensive view to date of the relationship between neuroimmune proteins (cytokines, phospho-proteins, glial markers), pathological markers (amyloid beta, total tau, phosphorylated tau), hemodynamics, and transcriptional profile in response to successive repetitive closed head injuries (CHIs). This work has resulted in numerous talks, poster presentations, one published methods paper (Brothers et al, 2022), and one pre-print that is in submission (Pybus et al, 2023). It has also resulted in the deposition of one RNAseq dataset to NCBI GEO and three datasets submitted to the Open Data Commons for Traumatic Brain Injury that include combined protein data spanning cytokines, phospho-proteins, and glial markers, together with cerebral blood flow data, so that others may extend on our own analysis of the data. As noted below, Drs. Wood and Buckley have also obtained new funding that continue this work in multiple directions spanning traumatic brain injury and Alzheimer's disease.

Major Findings. The key outcome of this study is the identification of a neuroimmune cascade of mild traumatic brain injury in 3xTg-AD mice, consisting of i) an immediate decrease in neuronal homeostatic gene expression and an elevation of AD-associated genes after a single injury, ii)

elevation of a subset of cortical cytokines that co-label with neurons after each successive injury in correlation with phosphorylated tau, and iii) increased expression of non-neuronal genes suggesting glial reactivity within days of repeated injury. We provide resolution of these acute protein and transcriptional changes at a previously uncharacterized minutes-to-days time scale alongside the key experimental variables of sex, brain region, and number of injuries. Moreover, pronounced changes in neuronal gene expression that correlated with inflammatory protein expression and co-labeling of injury-elevated cytokines and MAPK phospho-proteins with neuronal marker NeuN suggest a key role for neurons in the modulation of neuroimmune activity following brain injury. Further, the association of phospho-Mek1 and phospho-Atf2, cytokines, and phospho-tau T181 after injury may represent a future therapeutic avenue for regulating inflammation and acute pathological mechanisms.

In relation to our Specific Aims:

1. **Aim 1**: We found that repetitive CHIs did not significantly affect cerebral blood flow at either acute or 1 month (mo) time points after injury. However, we did find that CHI yielded an increase in certain cytokines and MAPK phospho-proteins, and a time point of maximal expression or activation that depended on the number of injuries. These were accompanied by transcriptional changes in neurons after 1xCHI and increasing transcriptional changes in glia with successive injuries. Moreover, we identified a weak correlation between cerebral blood flow measured at acute time points and cytokines and pathological markers at 1mo after injury.
2. **Aim 2**: Our CHI model of repetitive mild TBI showed minimal changes in amyloid beta (Aβ) and tau pathological markers. Moreover, our top candidate drug, VX-745, targeting p38 MAPK exacerbated cytokine expression in 3xTg-AD mice exposed to repetitive mild TBI, suggesting that our initial targets are not effective in 3xTg-AD mice. In concert with our detailed analysis spanning multiple injuries and time points in Aim 1, we now believe that the targets relevant to wild-type vs. Alzheimer's pathology mice may be different. Indeed, we have identified phosphorylated Mek and Atf2 as being elevated after CHI in 3xTg AD mice, while our ongoing work in wild-type mice suggests that targeting p38 MAPK may be effective. These findings, although in progress, emphasize the importance of genotype and pre-existing pathology in determining the tissue and cellular response to TBI.

<u>Aim 1, BIOMARKERS:</u> Test if deranged cerebral blood flow, oxygen metabolism, and/or cerebrovascular reactivity predicts chronic tissue pathology after repetitive closed head injury.

We were able to reliably quantify cerebral blood flow as our primary hemodynamic biomarker via our noninvasive optical sensor, as well as panels of cytokines, pro-inflammatory MAPK phosphor-proteins, together with markers of microglial activation (CD68), glial reactivity (GFAP), Aβ1-40, Aβ1-42, total tau, phospho-tauT181 and phosphor-tauS262 (immunohistochemistry). Because the 3xTg-AD strain of mouse did not reliably perform in behavioral assays, we focused our analysis on CBF and molecular measures. We executed these studies in 2-4mo 3xTg mice to model the effect of repetitive injury on young adults (i.e., relevant to football players or military service personnel). Moreover, we collected data after 1x, 3x, and 5xCHI with time points spanning 30min, 4hr, 24hr, and 1mo after injury. Below, we detail some of the central findings of this study. Please also see the manuscript pre-print (**Appendix)** for further analyses and discussion.

Immune, glial, and pathological markers differed between male and female 3xTg-AD mice

Since prior reports showed pronounced differences in pathological burden between male and female 3xTg-AD mice, we began the current study by evaluating sex differences among all protein measures: cytokines, MAPK phospho-proteins, glial markers, phosphorylated and total tau, and Aβ40/42. Data were adjusted for batch effects as needed using linear models of technical replicates (**Appendix**). We first obtained a holistic view of variation within the data using a principal component analysis (PCA), which revealed a pronounced effect of sex within both brain regions (**Fig. 1A**). Female replicate samples from the male batches grouped with female batch samples and separately from male samples, emphasizing that the effects of sex were biological, rather than technical (purple points, **Fig. 1A**).

To define the specific effects of sex versus injury and time point, we conducted multiple linear regression of all quantified proteins and phospho-proteins using sex, injury number, and time point as independent variables. This analysis revealed that sex, as compared to all other variables in the model, had the most significant effect (**Appendix Fig. S1)**. We next conducted comparisons between sex for each measured protein in 1) sham-injured animals only (**Fig. 1B**) and 2) all sham and injured animals (**Appendix Fig. S1A**). Importantly, all proteins determined to be significantly different between sexes based on the sham animals alone were also significantly different between sexes when all samples were used, regardless of injury condition (**Fig. 1C**). An additional 12 and 17 significantly different proteins were identified in the frontal cortex and hippocampus, respectively, when all animals across injury conditions were compared (**Fig. 1C**). Many of these effects remained despite adjusting for Aβ42 levels (see **Appendix**).

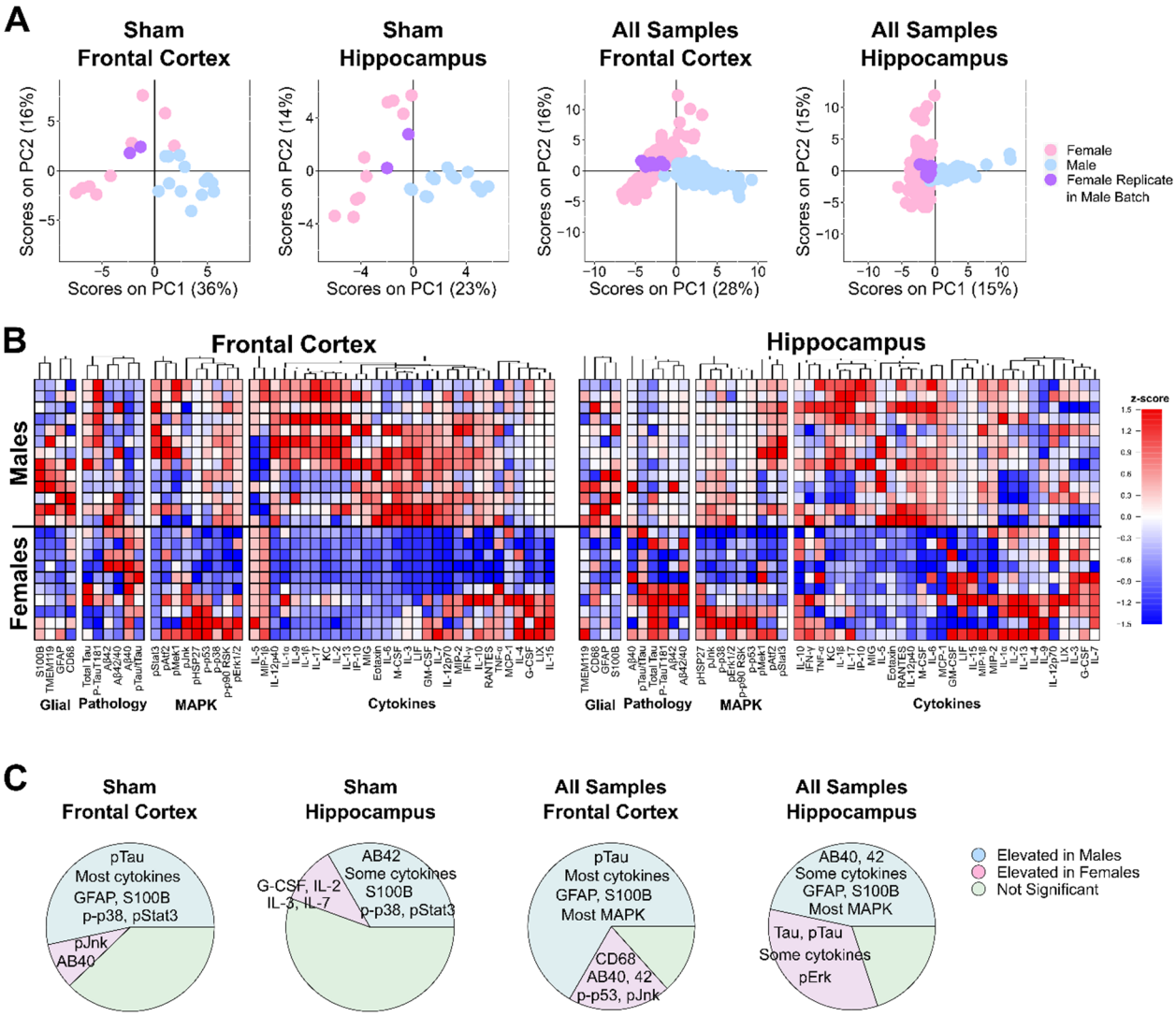


Figure 1. Pronounced sexual dimorphism of immune signaling, glial markers, and molecular markers of pathology in 3xTg-AD mice. A) Principal component analysis of combined protein data across sham-injured animals (left) and all injuries and time points (right) reveals strong separation between male and female mice on the first two PCs. Female replicate samples measured in male batch assays are shown in purple. Percent variance described by each PC is annotated in parentheses. **B**) Uninjured control mice show distinct baseline sex differences in expression of glial markers, pathological markers, MAPK signaling, and cytokines. Proteins are categorized by function then clustered by Euclidean distance within each category. Red to blue indicates relatively high to low expression among all sham animals (n=13 males, n=10 females). Of the 46 measured immune and pathological marker proteins in sham-injured animals, 37 from the frontal cortex (80%) and 30 from the hippocampus (65%) had higher average expression in males compared to females. **C**) Pie charts for each region and sample set (just sham on left, all animals combined on right) show high proportions of all analytes measured (4 glial markers, 4 pathological markers, 9 MAPK, 30 cytokines) that are significantly elevated ($p<0.05$, Wilcoxon rank-sum) in males (blue) or females (pink).

Cytokines and MAPK phospho-proteins are elevated after each closed-head injury

To identify patterns of co-varying cytokines and phospho-proteins with injury and time point, we next conducted hierarchical clustering within each sex and brain region (**Appendix**). We found that females exhibited robust variation of these signaling proteins with both number of injuries and time

point. The clustering identified a group of injury-induced cytokines (IL-9, IL-17, KC, IL-1α, IL-2, IL-1β, IL-13) and MAPK phospho-proteins (phospho-Atf2, phospho-Mek1) that tightly clustered together within the frontal cortex data from female mice (**"Group 1"**). Proteins within this group were significantly increased at 24h after 1x, 2x, and 3xCHI, showed mild increases 24h after 4xCHI, and returned to baseline sham levels 24h after 5xCHI (**Fig. 2**), suggesting a dysregulated immune response after four or more injuries. Interestingly, these proteins were elevated 4h post-5xCHI compared to sham, 4h post-1xCHI, and 4h post-3xCHI animals (**Fig. 2**), indicating an earlier response after multiple injuries consistent with a "primed" immune state. Although many of the same cytokines and phospho-proteins from Group 1 again clustered together within the female hippocampus (**Appendix**) and male frontal cortex and hippocampus (**Appendix**), this same trend of an injury-dependent increase was only noted in the female frontal cortex. Together, these data indicate the importance of evaluating multiple time points after injury to fully define the immune response and emphasize the need to evaluate males and females separately. Finally, we note that many of the Group 1 proteins co-label with the neuronal marker NeuN (**Appendix Fig. 4**), strongly suggesting a neuronal role in driving immune signaling.

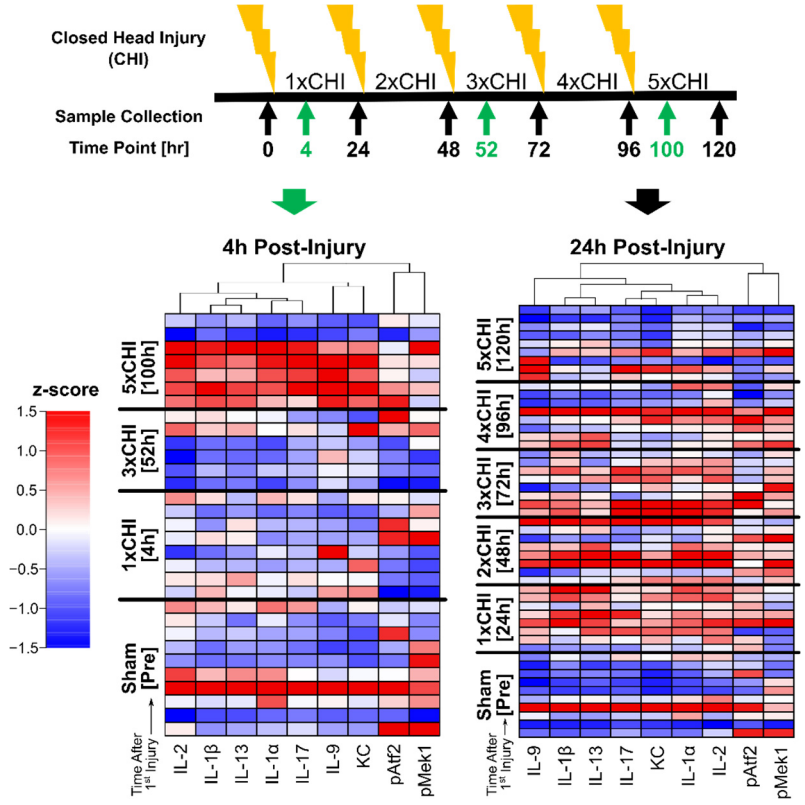


Figure 2. Cytokines and MAPK phospho-proteins are elevated after each closed-head injury in females. Hierarchical clustering of cytokines and MAPK phospho-proteins (**Appendix Fig. S4, "Group 1"**) from the frontal cortex of female 2-4mo 3xTg sham-injured mice and 4hr (left) or 24hr (right) after 1-5x closed head injuries (CHI). Each row represents data from an individual mouse z-scored along each column.

Acute cerebral blood flow shows trending correlations with 1-month molecular changes

Our previous work in wild type mice has shown that cerebral blood flow: 1) acutely decreases after repeated CHI, 2) is associated with cognitive outcome assessed 72h after five once-daily CHI, and 3)

is correlated to increased neuroinflammation 4hr after three once-daily CHI. We therefore hypothesized that we would see similar results in 3xTg-AD mice while using the same injury model.

We first looked at acute time points, and found that CBF measured 30m, 4h, and 24h post-1x, 3x, and 5xCHI was not significantly different from CBF of sham-injured mice for either male or female populations (**Fig. 3A**), although we did see trends of decreased CBF in male mice 4hr post-3xCHI (p=0.06, Wilcoxon rank-sum). Lastly, we conducted a correlation analysis of CBF vs 48 concurrently measured neuroimmune and pathological protein markers (**Fig. 3B**). We found no significant correlations in Sham-injured samples and very few in post-injury samples, with inconsistent trends across injury number and time point. Interestingly, both male and female frontal cortex samples showed broad negative correlation trends between CBF and protein markers 24h post-5xCHI, with more variable trends at all earlier time points.

We next evaluated the relationship between CBF measured at multiple time points after injury (4hr post 3xCHI, 4hr post 5xCHI, 24hr post 5xCHI, and 1mo post 5xCHI) and 1mo molecular measurements of cytokines, Aβ, and tau (**Fig. 4**) in the frontal cortices of female animals. As with acute CBF measurements, we found no differences between sham and injured groups at any of the quantified time points (**Fig. 4A**). However, there were multiple significant and trending correlations between 1month molecular markers and CBF at distinct time points in both sham (**Fig. 4B**) and injured groups (**Fig. 4C**). Interestingly, in sham mice, lower CBF (e.g., at 4hr after 3xCHI) is associated with increased pro-inflammatory cytokines (IL-9, IL-1a, IP-10), whereas in injured mice lower CBF (at 24hr post 5xCHI) is associated with other increased IL-17 and increased Aβ1-40. Importantly, increased IL-17, was associated with lower CBF in our prior work in wild-type mice, suggesting it warrants further study. Together, these data suggest a weak relationship between CBF and molecular markers that shifts between sham and injured mice.

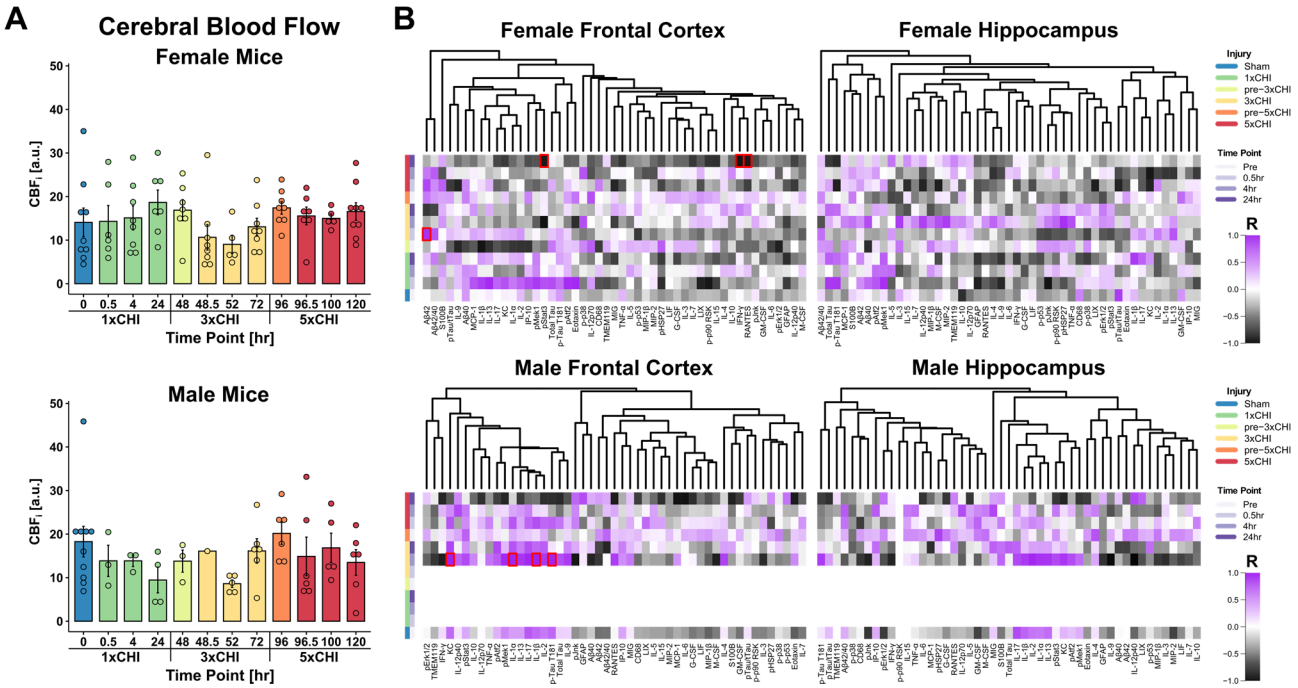


Figure 3: Correlation between cerebral blood flow measured 30m, 4hr, and 24hr after 1x, 3x, and 5x weight drop closed-head injuries and neuroimmune markers in 3xTg mice. CBF was non-invasively

measured from isoflurane-anesthetized mice with an optical sensor at 3mm depth using diffuse correlation spectroscopy. Immediately following CBF measurement, frontal cortex and hippocampus tissue was extracted to quantify 48 neuroimmune and pathological protein markers by single and Luminex ELISA. CBF and proteins were both quantified from the left hemisphere. **A**) CBF was not significantly different between sham-injured (blue) and injured groups for either female (top) or male (bottom) 3xTg mice (mean±SE). **B**) Neuroimmune and pathological protein markers showed inconsistent correlation with CBF both before and after injury. Each row indicates an injury time point group (groups of n<5 excluded) and each column indicates a measured protein, with color corresponding to Pearson's correlation coefficient R against CBF. Red boxes indicate p<0.05, ordinary least squares regression. Proteins are clustered by Euclidean distance using unweighted pair group method with arithmetic mean.

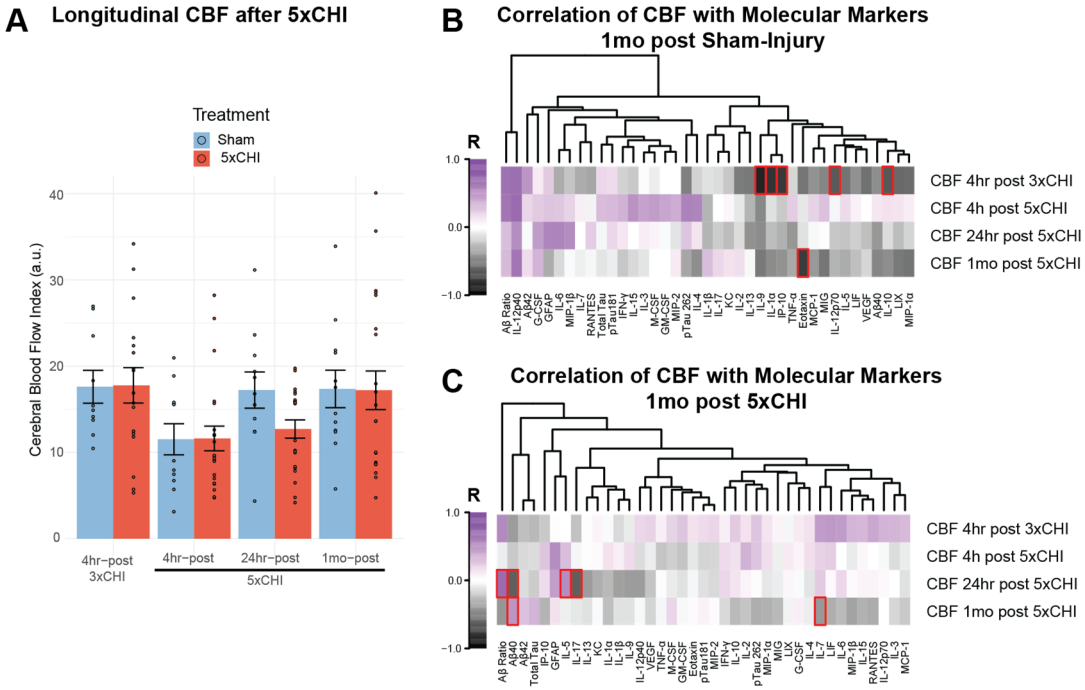


Figure 4: Correlation between cerebral blood flow measured at 4hr after 3xCHI and 4hr, 24hr, and 1mo after 5xCHI with cytokines and pathological markers quantified 1mo after 5xCHI in 3xTg-AD females. CBF was non-invasively measured from isoflurane-anesthetized mice with an optical sensor at 3mm depth using diffuse correlation spectroscopy. 1mo after injury, frontal cortical tissues were extracted to quantify 32 cytokines, and four pathological markers via Luminex analysis. **A**) CBF was not significantly different between sham or injury groups at any time point (mean±SE, two-tailed t-test at each time point, N=10-12 sham, 17-21 injured). **B**) Neuroimmune and pathological protein markers showed some correlation. Each row indicates correlation of 1mo molecular data with CBF measured at the indicated time point and each column indicates a measured protein, with color corresponding to Pearson's correlation coefficient R against CBF. Red boxes indicate p<0.05, ordinary least squares regression. Proteins are clustered by Euclidean distance using unweighted pair group method with arithmetic mean.

Bulk RNAseq analysis reveals the effect of injury on pathology- and cell type-associated gene modules.

To illuminate the broad effects of repetitive mTBI on cortical transcriptional networks, we next conducted network analysis on the same subset of 40 female cortical samples (somatomotor cortex, adjacent to the frontal cortex sections used for protein analysis), sampled from all acute injury groups and time points (n=3-4 per group). To obtain an unbiased view of expression patterns within the data, we first conducted WGCNA (**Methods**), which identified 14 distinct modules of co-varying genes (**Fig. 5A**). A module eigengene (ME) was computed for each module as its first principal component, and expression scores of each ME were displayed for each sample across all injury and time point groups (**Fig. 5B**). Due to small sample sizes and relatively low variation within time points of each injury group (**Fig. 5B**), we combined post-injury time points (30m, 4hr, 24hr) into one group per injury number and compared module expression across number of injuries. The two modules comprised of the largest number of genes, ME1 (turquoise) and ME2 (blue), rapidly changed after 1xCHI, with ME1 showing a significant increase ($p<0.05$) and ME2 showing trending decreases ($p=0.054$) post-injury. In contrast, ME9 (magenta) progressively increased with successive injuries (**Fig. 5C**) and tracked closely with ME7 and ME8 (black, pink) after 2-5xCHI. Moreover, ME3 (brown) and ME6 (red) were increased after 1xCHI then decreased compared to sham after 5xCHI, while ME10 (purple) and ME11 (green-yellow) peaked after 2xCHI, then returned to sham levels. These modules therefore define changes associated with rapid (ME1, ME2), transient (ME3, ME6, ME10, ME11) and gradual time scales (ME7, 8, 9).

To understand the biological relevance of each module, we used gene ontology (GO, via PANTHER) to identify top GO terms enriched in each module (**Fig. 5D**). Importantly, the rapidly changing ME2 (blue) was enriched for genes related to nervous system development, suggesting a rapid downregulation of homeostatic neuronal functions. The gradually changing modules, ME7, ME8, and ME9 (black, pink, magenta), were enriched for GO terms associated with wound healing, cytokine response, gliogenesis, and regulation of the immune response, suggesting a multi-day response that involves immune processes and healing. Importantly, those modules that increase with injury were all correlated with immune proteins (inflammatory cytokines, MAPK activation, and GFAP) quantified in the frontal cortex of the same animals (ME1, 7, 9; "Trait Correlations" **Fig. 5E**), whereas ME2, which shows decreasing trends after injury and is associated with neuronal function, was inversely correlated with immune proteins (**Fig. 5E**).

We next conducted a cell-type enrichment analysis for genes with high specificity in neurons, oligodendrocytes, endothelia, astrocytes, and microglia derived from published cell type specific mouse brain proteome and transcriptome studies (**Fig. 5F,** see **Appendix** for details). We found that ME2 (blue), which decreases after a single injury and was inversely correlated with immune protein markers, was significantly enriched for neuronal genes. In contrast, ME7, 8, and 9 (black, pink, magenta), which show gradual increasing trends with successive injuries and (with the exception of ME8) correlate with immune protein markers, were enriched for endothelial, astrocyte, and microglial genes, respectively.

We concluded this unbiased analysis by asking if specific modules were associated with AD-related genes. To test this, we used a Multi-marker Analysis of GenoMic Annotation (MAGMA) analysis to determine if AD genes were significantly over-represented within specific gene modules. Indeed, AD genes were enriched in ME1 (i.e. *Pfdn5*, *Rps11*, *Rpl13a*, *Lamtor4*, *Rpl14*), which increases with a single injury and correlates significantly to several inflammatory proteins. AD genes were also enriched in ME9 (i.e. *Hepacam*, *Vav1*, *Hexb*, *Grn*, *Laptm5*), which increases gradually, correlates with inflammatory proteins, and is enriched for microglial genes (**Fig. 5G**). Taken together,

these data suggest an early inflammatory response associated with AD genes (ME1) and a concomitant neuronal decrease in homeostatic functions (ME2) after a single injury. Moreover, multiple injuries progressively increased gene expression profiles associated with wound healing and regulation of inflammation within endothelia, astrocytes, and microglia.

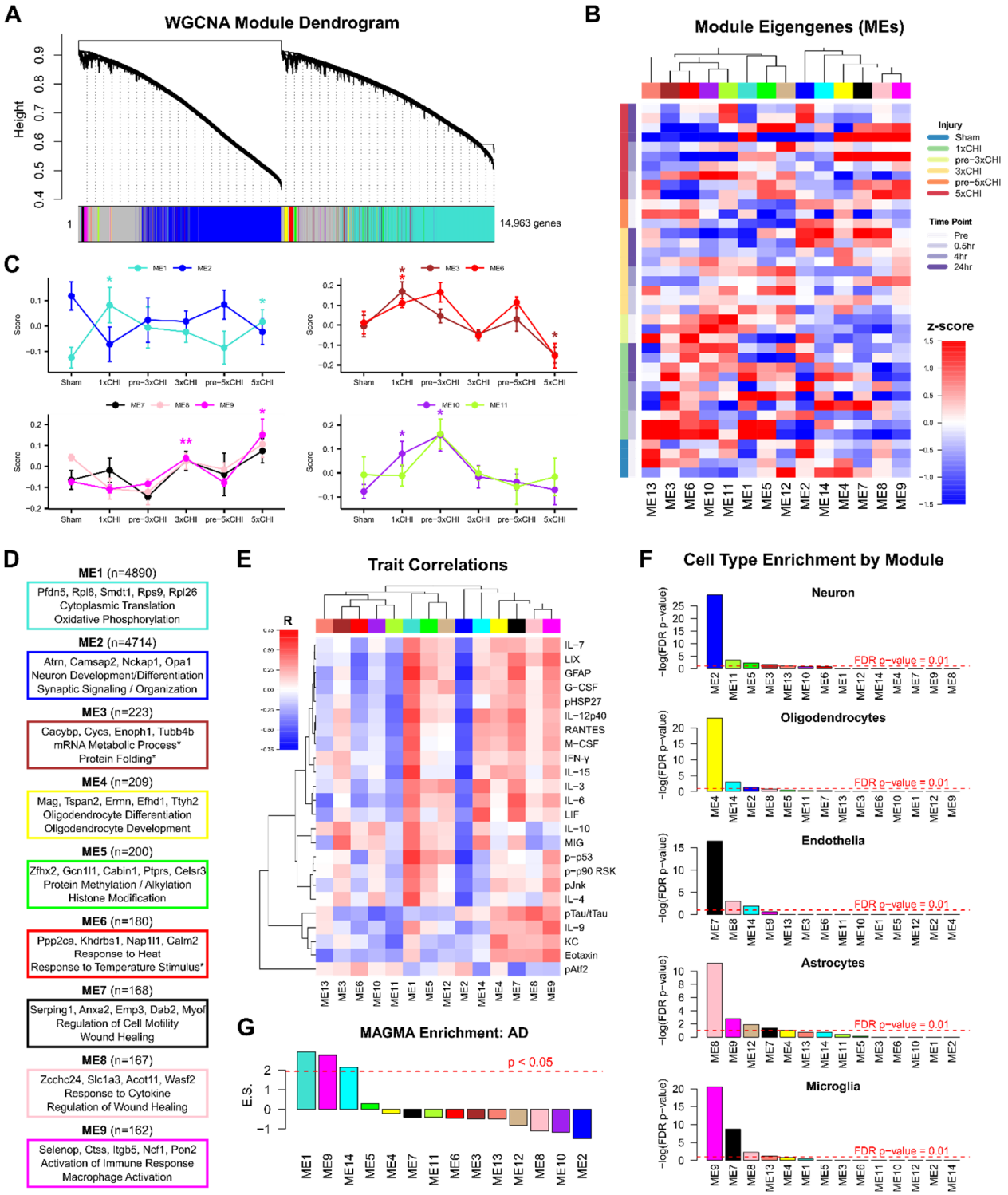


Figure 5. WGCNA of somatomotor cortex transcriptome identifies modules of co-expressed genes associated with injury, GO biological processes, inflammatory protein expression, brain cell types, and AD genetic risk factors. A) WGCNA identified 14 modules of co-expressed genes. **B**) Expression scores for the 14 module eigengenes (MEs, the first principal component of each module) for each sample. MEs are clustered by Euclidean distance (columns) and expression scores are displayed by increasing injury number and time point from bottom to top of the heatmap (rows). **C**) Line plots show changing ME expression scores over increasing numbers of injuries. Time points for 30min, 4hr, and 24hr after each injury (1x, 3x, 5xCHI)

are combined due to low sample sizes (n=2-4). ME1 (turquoise) and ME2 (blue) show opposite behavior after 1xCHI, with ME1 significantly increasing alongside trending decreases in ME2 after a single injury. ME 9 (magenta) shows significant increases after successive injuries that track closely with ME7 and 8 (black and pink) (*p<0.05, **p<0.01, permutation tests compared to sham, see **Methods**) (mean ± SEM). **D**) Gene ontology enrichment of biological processes was conducted for each module (Fisher's exact test with FDR-corrected p-value <0.05). ME3 and ME6 had fewer than two significant GO sets. Sets marked with asterisks had FDR-corrected p>0.05 but uncorrected p<0.0001. **E**) Protein expression data from the frontal cortex of the same animals were correlated against each ME. Selected proteins showed a correlation p-value of at least 0.01 against at least one ME. Red indicates a positive Pearson's correlation coefficient (R) while blue indicates negative correlation. **F**) Cell type enrichment analysis showed significant enrichment of neuronal genes in ME2 (blue), oligodendrocyte genes in ME4 (yellow), endothelia genes in ME7 (black), astrocyte genes in ME8 (pink), and microglial genes in ME9 (magenta). **G**) MAGMA enrichment for GWAS AD genes showed significant over-representation within ME1 (turquoise), ME9 (magenta), and ME14 (cyan). The dotted red line indicates an enrichment z-score of 1.96, above which a module is considered significantly enriched (normal distribution, p<0.05).

<u>Aim 2, MECHANISMS:</u> Determine if inflammatory p38 MAPK and Jak/Stat pathway signaling drives outcome after repetitive closed head injury.

Our preliminary data in wild-type mice had identified several possible intracellular phosphoproteins associated with reduced cognitive outcomes, including Stat1and p38. Although neither of these were as robustly associated with injury in our extensive kinetic analysis in the current study (**Fig. 2, Appendix Fig S4**), we elected to evaluate the effects of p38 MAPK inhibition on 1mo molecular outcomes because of the established pro-inflammatory role of p38 MAPK. Thus, we treated 3xTg-AD mice with the translationally relevant p38 MAPK signaling inhibitor VX-745 after each successive injury to determine if inhibition of p38 MAPK signaling would modulate 1mo cytokine expression or pathological markers. Neither the injury nor the drug significantly impacted Luminex measurements of Aβ1-40, Aβ1-42, or tau pathology (**Fig. 6A**) in the frontal cortex at the 1mo time point. However, clustering of the cytokines data indicates that a group of pro-inflammatory cytokines and chemokines were elevated by VX-745 (**Fig. 6B**, IL-17, KC, MIG, IL-1b, Eotaxin, MCP-1, VEGF), suggesting that inhibition of p38 MAPK is not relevant for treatment of TBI in mice with prior pathology. Our acute signaling data suggest that Mek signaling may be a relevant future target, but this is part of the canonical portion of the MAPK that is a key regulator of cell survival. Thus, a sophisticated approach would be needed to target Mek signaling for TBI without toxicity. Evaluation of this pathway for treatment of Alzheimer's disease is part of an ongoing study in the Wood lab.

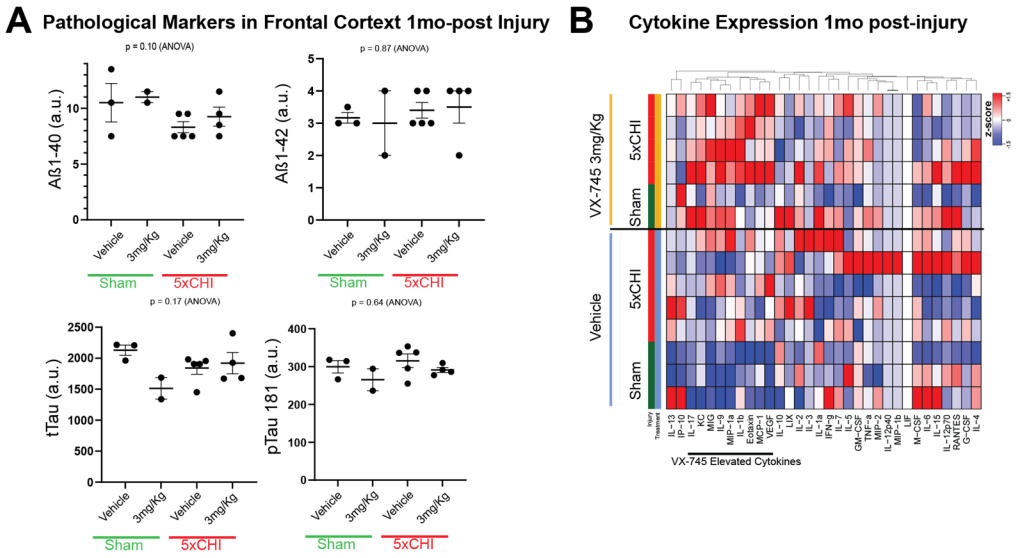


Figure 6: p38 inhibitor VX-745 accentuated cytokine expression in 3xTg mice post 5xCHI. **A**) Luminex analysis of pathological markers after 5xCHI injury and VX-745 did not significantly change Aβ or tau 1 month after 5xCHI. **B**) Luminex analysis of cortical cytokine expression 1 month after 5xCHI suggests that some pro-inflammatory cytokines (e.g., IL-1b, MCP-1) may be exacerbated by p38 inhibition in 3xTg mice.

Ongoing and Future Directions. Our research group continues our study of repetitive mild TBI informed by what we learned from this study. Indeed, we are continuing our mechanistic study of the role of pro-inflammatory p38 MAPK signaling in wild-type mice, using a combination of drugging and transgenic cell-type specific knockout. Our ongoing data collection in the Wood and Buckley labs suggests that inhibition of this pathway has the potential to be effective in wild-type mice for ameliorating both immune and behavioral changes after repetitive CHI. Additionally, we have mounting preliminary evidence that much longer time points >6mo are needed fully define the long-term effects of injury and whether interventions are therapeutic. Finally, Dr. Wood is pursuing the role of Mek signaling in models of Alzheimer's disease. These ongoing studies have all been enabled by the groundwork in the current project.

What opportunities for training and professional development has the project provided?

- Alyssa Pybus attended a webinar hosted by the National Neurotrauma Society, "Behavioral Testing after Experimental Neurotrauma: Tips, Advice and Live Q&A.", April 2021.
- Ms. Pybus defended her Ph.D. thesis in Spring, 2023.

How were the results disseminated to communities of interest?

- Since 2018, Dr. Wood and his team have given annual presentations, after school workshops, and summer camps on brain health to Hispanic and Black elementary and middle school students in partnership with Corners Academy, located in the greater Atlanta area. Our teaching modules include discussing the function of the brain, what different areas are responsible for, how it is made up of different kinds of cells, and how it is effected by traumatic brain injury. A regular part of these discussions is the importance of wearing helmets. The

students are extremely enthusiastic during each of our visits, and through this same program we have recently been engaging with high school students interested in paths to college, and careers in science, engineering, and neuroscience.

- The Buckley lab has participated in several science outreach events in conjunction with SmartHeart, a program founded by Michael Davis in the Department of Biomedical Engineering at Emory University, that aims to educate children and parents about cardiac diseases and cutting-edge cardiovascular research. The format of these events ranges in scope, from personalized lab tours for elementary school classrooms to short presentations to topic-related activities. Over the course of 2018-2019, we participated in 5 different events with SmartHeart to share our work on non-invasive brain monitoring with the community.

What do you plan to do during the next reporting period to accomplish the goals?

Nothing to Report.

4. **IMPACT:** D*escribe distinctive contributions, major accomplishments, innovations, successes, or any change in practice or behavior that has come about as a result of the project relative to:*

What was the impact on the development of the principal discipline(s) of the project?

This project yielded two key findings critical to our understanding of neurotrauma in humans and to the study of traumatic brain injury research in mice. The first is that there are essential differences in molecules that regulate brain immunity between males and females, both in response to injury, as well as even in the absence of injury. Females showed a more pronounced change in immune molecules, known as cytokines, which is consistent with prior studies in humans showing that women can be more susceptible to injury. Our second key finding is that repetitive brain injuries appear to affect all the major cell types in the brain over the course of days, with neurons showing the earliest signs of stress after a single injury and other immune and supporting cells, called glia, reacting over multiple injuries. Our data suggest that the immune cells, which are the critical processing cells required for the brain to work, have the potential to trigger the immune cells to respond improperly. Thus, neurons may be a critical target for new treatments.

What was the impact on other disciplines?
Nothing to Report.

What was the impact on technology transfer?
Nothing to Report.

What was the impact on society beyond science and technology?
Nothing to Report.

5. CHANGES/PROBLEMS:

Changes in approach and reasons for change
Nothing to report. The limited changes to experimental design, e.g., age of animals, etc, were approved by the program officer and all work was done with pre-approval of the local IACUC and ACURO.

Actual or anticipated problems or delays and actions or plans to resolve them
This project was substantially delayed by COVID19, due to the need to 1) the requirement to substantially shrink our animal colony during the lockdown period and 2) limit staff access to our labs, with total disruptions of more than a year. The no-cost extension period enabled us to complete the vast majority of our planned experimental cohorts, yielding an interpretable and publishable dataset.

Changes that had a significant impact on expenditures
Nothing to Report.

Significant changes in use or care of human subjects, vertebrate animals, biohazards, and/or select agents

Significant changes in use or care of human subjects
Nothing to Report. This project did not involve human subjects.

Significant changes in use or care of vertebrate animals
Nothing to Report. All animal work conducted during this projected was approved by ACURO (first approval was on 11/20/2018), the Emory University IACUC, the Georgia Tech IACUC. All adjustments made to the protocol during the award were approve by the program officer, and each of these offices and committees prior to implementation. The most recent ACURO approval was obtained after the IACUC triennial renewal on 08/03/2021.

Significant changes in use of biohazards and/or select agents
Nothing to Report.

6. PRODUCTS: *List any products resulting from the project during the reporting period. If there is nothing to report under a particular item, state "Nothing to Report."*

- **Publications, conference papers, and presentations**
  Report only the major publication(s) resulting from the work under this award.

Journal publications.
Brothers, R., Bitarafan, S., Pybus, A., Wood, L. Buckley, E., 2022. *Systems Analysis of the Neuroinflammatory and Hemodynamic Response to Traumatic Brain Injury,* Journal of Visualized Experiments, e61504:10.3791/61504. PMID: 35695529. Federal support from this grant was acknowledged.

Pybus, A., Bitarafan, S., Brothers, R., Rohrer, L., Khaitan, A., Rivera, F., Udeshi, K., Davies, B., Triplett, S., Dammer, E., Rangaraju, S., Buckley, E., Wood, L., 2023. *Profiling the Neuroimmune Cascade after Repetitive Mild Traumatic Brain Injury*, Georgia Institute of Technology, April 2022. Posted to bioRxiv under https://doi.org/10.1101/2023.06.13.544838. Being submitted to *Journal of Neuroinflammation* special collection on traumatic brain injury. Federal support from this grant was acknowledged.

Books or other non-periodical, one-time publications.
Pybus, A., *Profiling the Neuroimmune Cascade after Repetitive Mild Traumatic Brain Injury*, Ph.D. Dissertation, Georgia Institute of Technology, April 2023. Federal support from this grant was acknowledged.

Other publications, conference papers and presentations. *Identify any other Poster presentations*

1. Bitarafan, S., Brothers, R., Pybus, A., Ortiz, E., Wood, L, Buckley, E., *Cerebral blood flow as a biomarker of pathological outcome after repetitive mild traumatic brain injury*, Neurotrauma, July 2021, Virtual.

2. Pybus, A., Bitarafan, S., Brothers, R., Ortiz, E., Buckley, E., Wood, L, *Repetitive mild traumatic brain injuries prolong activation of the MAPK neural immune pathway and modulate cytokine expression compared to a single injury*, Neurotrauma, July 2021, Virtual.

3. Pybus, A., Bitarafan, S., Brothers, R., Ortiz, E., Rohrer, A, Buckley, E., Wood, L, *Repetitive Mild Traumatic Brain Injuries Prolong Activation of the MAPK Neural Immune Pathway*, Biomedical Engeneering Society Conference, Orlando Fl and Virtual, October 2021.

4. Pybus A., Bitarafan, S., Brothers, R., Rohrer A., Udeshi, D., Khaitan, A., Buckley, E., Wood., L. *Repetitive mild traumatic brain injury increases tau phosphorylation, cytokine expression, and phospho-protein signaling in the 3xTg mouse model of Alzheimer's disease*. National Neurotrauma Society Conference, Atlanta, GA, June, 2022.

5. Pybus A., Bitarafan, S., Brothers, R., Rohrer A., Khaitan, A., Rivera Moctezuma, F., Udeshi, D., Davies, B., Buckley, E., Wood., L. *Repetitive mild traumatic brain injury increases tau phosphorylation, cytokine expression, and phospho-protein signaling in the 3xTg mouse model of Alzheimer's disease*. Biomedical Engineering Society Conference, San Antonio, TX, October, 2022.

6. Pybus A., Bitarafan, S., Brothers, R., Rohrer A., Rivera Moctezuma, F., Udeshi, D., Khaitan, Davies, B., Triplett, S., Li, Chenxing, Dammer, E., Buckley, E., Wood., L. *Profiling the Neuroimmune Cascade in 3xTg Mice Exposed to Successive Mild Traumatic Brain Injuries*. National Neurotrauma Society Conference, Austin, Tx, June, 2023.

Seminars

1. Wood, L, *Systems Analysis Identifies Neuronal Inflammatory Signaling after Repetitive Mild TBI in Mice*, Neurotrauma, July 2021, Virtual.

2. Wood, L., *Systems Analysis of Neural Immune Signaling in Neurodegenerative Diseases*, Emory University Neuroscience Seminar Series, September, 2021

3. Wood, L., *Systems analysis of neural immune signaling in neurodegenerative diseases*, Emory Cardiovascular Seminar Series, Oct, 2021.

4. Wood, L., *Systems analysis of neural immune signaling in neurodegenerative diseases*, Pennsylvania State, Oct, 2021.

- **Website(s) or other Internet site(s)**
  Nothing to Report.

- **Technologies or techniques**
  Nothing to Report.

- **Inventions, patent applications, and/or licenses**
  Nothing to Report.

- **Other Products**
  1. RNAseq data are posted to the NCBI Gene Expression Omnibus under accession number: GSE226838.

  2. Structured protein data, including cytokines, glial markers, and cerebral blood flow measurements are posted to the Open Data Commons for Traumatic Brain Injury repository under dataset the following dataset ID's:
     a. ODC-TBI ID 861: *Acute neuroimmune and pathological protein data from 3xTg-AD cortex and hippocampus after rmTBI* (Editor approved)

b. ODC-TBI ID 928: *1 month neuroimmune, cerebral blood flow, and pathological protein data from 3xTg mice after rmTBI* (Awaiting approval)
c. ODC-TBI ID 927: *1 month neuroimmune and pathological protein data from 3xTg-AD Cortex after rmTBI and treatment with MAPK inhibitor VX-745* (Awaiting approval)

7. PARTICIPANTS & OTHER COLLABORATING ORGANIZATIONS

What individuals have worked on the project?

Name: Dr. Levi Wood
Project Role: Principal Investigator
Researcher Identifier (e.g. ORCID ID): ORCID ID: 0000-0002-4248-0888
Nearest person month worked: 6
Contribution to Project: Dr. Wood worked on project oversight, data analysis, and manuscript preparation.

Name: Dr. Erin Buckley
Project Role: Co-Principal Investigator
Researcher Identifier (e.g. ORCID ID): ORCID ID: 0000-0003-1068-8411
Nearest person month worked: 8
Contribution to Project: Dr. Buckley worked on project oversight, experimental design, manuscript preparation.

Name: Ms. Alyssa Pybus
Project Role: Graduate Student
Researcher Identifier (e.g. ORCID ID): ORCID ID: 0000-0002-9722-3977
Nearest person month worked: 27
Contribution to Project: Ms. Pybus worked on acute signaling, immunohistochemistry, data analysis and manuscript preparation.
Funding Support: Ms. Pybus was primarily funded by an NIH T32 Training grant.

Name: Mr. Junho Yoo
Project Role: Graduate Student
Researcher Identifier (e.g. ORCID ID): ORCID ID: 0000-0002-9720-6827.
Nearest person month worked: 4
Contribution to Project: Mr. Yoo worked on immunohistochemistry workflow and learned and conducted MAPK signaling analysis.
Funding Support: Mr. Yoo was funded in part by this award and by NIH R21NS104801

Name: Mr. Rowan Brothers

Project Role: Research Technician
Researcher Identifier (e.g. ORCID ID): ORCID ID: 0000-0003-0587-4578
Nearest person month worked: 11
Contribution to Project: Mr. Brothers contributed to mouse colony maintenance and injury paradigm.
Funding Support: NIH R21NS104801, NIH R01HD046922

Name: Ms. Sara Bitarafan
Project Role: Research Technician/Graduate Student
Researcher Identifier (e.g. ORCID ID): ORCID ID: 0000-0003-4584-1420
Nearest person month worked: 5
Contribution to Project: Ms. Bitarafan worked on analysis of cytokines, Aβ, and tau.
Funding Support: Ms. Bitarafan was funded in part by this award, by a grant from the Coins for Alzheimer's Research Trust, and by NIH R33 ES025661 S1, NIH R01 NS115994

Name: Ms. Alivia Rohrer
Project Role: Research Specialist
Researcher Identifier (e.g. ORCID ID): ORCID ID: 0000-0002-4676-3906
Nearest person month worked: 5
Contribution to Project: Ms. Rohrer contributed to mouse colony maintenance and injury paradigm
Funding Support: Ms. Rohrer was funded by NIH R01 NS115994

Has there been a change in the active other support of the PD/PI(s) or senior/key personnel since the last reporting period?
As summarized, in the annual and quarterly reports, Drs. Wood and Buckley have had changes in support during the term of this award. These grants did not overlap with this work and did not change their effort on this project:

- Dr. Wood

  Coins for Alzheimer's Research Trust (Wood) 07/01/19-06/30/21 0.25 Summer
  Coins for Alzheimer's Research Trust, Role: PI
  Controlling gene expression patterns in Alzheimer's disease that enhance learning, cell survival, and immunity using precise sensory stimulation
  This proposal will create a map linking exposure of mice to different frequencies and durations of sensory audio/visual stimulation to expression of genes that promote healthy neuronal or neural immune function.
  Overlap: None.

  1944053 Wood (PI) 09/01/20-08/31/25 0.5 Summer Months
  National Science Foundation, Role: Principal Investigator
  CAREER: Closing the Loop on Neuroinflammation.

The objective of this award is to use dynamic modeling and open- and closed-loop control methods to modulate microglial activity, thereby establishing a new paradigm for treating and regulating neuroinflammation.
Overlap: None.

NIH 1R01NS114130-01 Rangaraju (PI) 04/01/19-03/31/25 0.25 Summer
NIH/NIA, Role: Co-Investigator
Targeting Kv1.3 potassium channels for neuro-immunomodulation in Alzheimer's Disease
The goal of this work is to determine if Kv1.3 channels in microglia can be targeted to ameliorate neuroinflammation in Alzheimer's disease
Overlap: None.

P50 AG025688, ADRC Seed Grant (Rangaraju/Wood Co-PI)
07/01/2020 – 06/30/2021 0 Months
NIH, Donor, Role: Co-PI Annual Cost at Georgia Tech Site
Therapeutic efficacy and biomarkers of ERK attenuation in an Alzheimer's mouse model
The goal of this seed grant is to determine if ERK signaling in mice can be targeted to change microglial phenotype in a manner that is detectable in the cerebrospinal fluid.
Overlap: None.

1 R01 NS115899 (Jang) 04/01/2021 – 03/31/2026 0.5 Summer
NIH/NHLBI, Role: co-I Direct costs to Wood lab
Engineered Heterochronic Parabiosis on 3D Microphysiological Systems
Role: Co-I
The goal of this proposal is to engineer a physiologically relevant 3D platform for studying interactions between young and aged cells.
Overlap: None.

R44 AG071138 (Graudejus) 09/01/2021 – 08/31/2022 0.5 Academic
NIH/NHLBI, Role co-I at Georgia Tech site
The first adaptable, 3D-formfitting microelectrode array for organoid-based models of neurological and neurodegenerative diseases
Role: Co-I
This SBIR grant will create a novel 3D microelectrode system to take electrophysiology data from organoids.
Overlap: None.

1R01AG075820 (Rangaraju/Seyfried/Wood) 09/30/2020-05/31/2026 1 Academic
NIH/NIA, Role: MPI Direct costs to Wood lab
Neuron and microglia-specific proteomic signatures of ERK mediated mechanisms of Alzheimer's disease
This work will utilize a combination of Cre-lox and small molecule inhibition experiments to identify the role of microglial and neuronal ERK signaling in Alzheimer's disease. This work takes advantage of a novel Cre-mediating proteomic labeling strategy, TurboID, to identify cell-type specific proteomes from whole tissues.
Overlap: None.

R44 AG071138 (Graudejus) 09/01/2022 – 08/31/2025 1 Academic
NIH/NHLBI Total costs to Wood lab
A physiologically relevant pre-clinical drug screening platform for Alzheimer's Disease and traumatic brain injury with integrated stretchable microelectrodes
Role: Co-I
The goal of this proposal is to create a 3D cell co-culture system to study the interplay between traumatic brain injury and Alzheimer's disease.
Overlap: None.

1R01DE031271 (Goudy) 07/01/2022 – 06/30/2027 0.5 Academic
NIH/NHLBI, Role: Co-I Total costs to Georgia Tech
Jagged1-based craniofacial bone regeneration
The goal of this proposal is to utilize Jagged1 ligand as a novel strategy to promote craniofacial bone regeneration by stimulating non-canonical NOTCH signaling
Overlap: None.

Seed Grant (Wood/Marklein) 09/01/2022 – 08/31/2023 0 Academic
Regenerative Engineering Seed Grant, Role: Co-PI Total costs to Georgia Tech
Mitochondrial Transfer from MSC-derived Extracellular Vesicles as a Novel Paradigm to Modulate Microglia Metabolism in Alzheimer's Disease
The goal of this seed grant is to create preliminary data showing if MSC-derived extracellular vesicles can infiltrate the brain and modulate brain immunity
Overlap: None.

5R25EB025783 (Wood) 06/01/2023 – 05/31/2024 1 Academic
NIH/NIBIB, Role: PI total cost
Georgia Tech ESTEEMED
Georgia Tech (GT) ESTEEMED is an integrated plan and pipeline to prepare underrepresented students for a Ph.D. or M.D./Ph.D.
Overlap: None.

- Dr. Buckley

1 R01 NS115994-01A1 (Wood/Buckley, M-PI) 09/01/2020-06/30/2025 3 Calendar
NIH/NINDS, Role: Multiple-PI
Role of neuronal p38 MAPK after repetitive mild TBI
This proposal will use genetic and pharmacologic interventions to test the hypothesis that mechanical stress associated with repetitive mild traumatic brain injury induces acute changes in neuronal p38 MAPK signaling that promotes neuroinflammation, reduces cerebral blood flow, and ultimately leads to functional deficits in wild-type mice.
Overlap: None.

1R01HL152322-01A1(Buckley/Gee/Khemani) 01/01/2021 – 12/31/2024 2.4 Cal Months

NIH/NHLBI, Role MPI Total Costs *Diffuse optical spectroscopies to assess cerebral hemodynamics in pediatric sickle cell disease*
This proposal will (1) validate our DCS hematocrit-correction against "gold-standard" perfusion MRI, (2) determine if FDNIRS/DCS is sensitive to cerebral hemodynamic abnormalities in patients with silent infarcts, and (3) demonstrate FDNIRS/DCS can assess real-time changes in cerebral hemodynamics during transfusion, which reduces silent infarct risk in SCD patients.
Overlap: None.

R01NS130036-01 (Sadan) 09/01/2022 – 08/31/2027 1.2 Cal Months
NIH/NHLBI, Role co-I Total Costs
Development of biomarkers to optimize intrathecal nicardipine treatment for cerebral vasospasm and delayed cerebral ischemia after subarachnoid hemorrhage
Our overall objective is to develop biomarkers of outcome after SAH that can help optimize treatment strategies and improve outcomes.
Overlap: None.

GBT021601-BUC (Buckley) 06/01/2021 – 11/30/2023 0.58 Cal Months
Global Blood Therapeutics, Role PI Total Costs
Hemodynamic Response In Children At Risk For Cerebral Injury (VoxSCAN)
This project will assess the effect of voxelotor, a novel therapeutic for sickle cell disease, on cerebral blood flow, oxygen extraction, and oxygen metabolism
Overlap: None.

PO/009603 (Buckley) 03/01/2023 – 03/01/2024 0.66 Cal Months
Global Blood Therapeutics, Role PI Total Costs
GBT021601-BUC
We will perform the optical measurements at the Visionaries site as defined by protocol.
Overlap: None.

What other organizations were involved as partners?
Nothing to Report.

8. SPECIAL REPORTING REQUIREMENTS

QUAD CHARTS: Final Quad Chart is submitted with this final report and attached at the end.

9. APPENDICES: *Manuscript pre-print is attached:*

Pybus, A., Bitarafan, S., Brothers, R., Rohrer, L., Khaitan, A., Rivera, F., Udeshi, K., Davies, B., Triplett, S., Dammer, E., Rangaraju, S., Buckley, E., Wood, L., "*Profiling the neuroimmune cascade in 3xTg mice exposed to successive mild traumatic brain injuries*," https://doi.org/10.1101/2023.06.13.544838.

Linking Cerebral Hemodynamics and Neuroinflammation to Alzheimer's Pathology in Repetitive Mild Traumatic Brain Injury

Log Number: AZ170073

Award Number: W81XWH-18-1-0669

PI: Levi Wood, co-PI: Erin Buckley **Org:** Georgia Institute of Technology **Award Amount:** $500,000

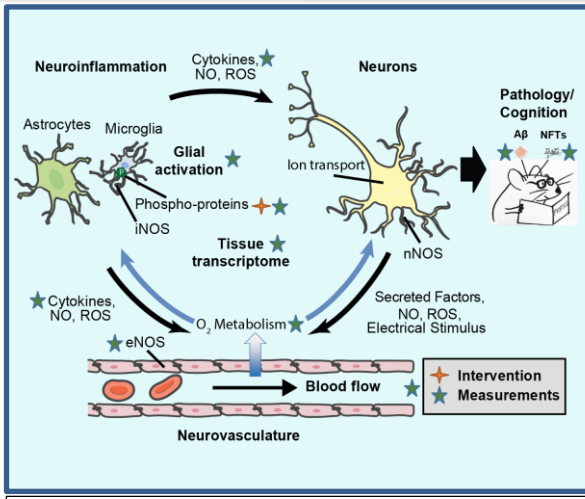
Study/Product Aim(s)

- Aim 1 BIOMARKERS: Test if deranged cerebral blood flow, oxygen metabolism, and/or cerebrovascular reactivity predicts chronic tissue pathology after repetitive closed head injury.

- Aim 2 MECHANISMS: Determine if inflammatory p38 MAPK and Jak/Stat pathway signaling drives outcome after repetitive closed head injury.

Approach

We are using novel optical hemodynamic sensors to identify prognostic biomarkers of pathological outcome associated with repetitive mTBI, specifically amyloid beta plaques and neurofibrillary tangles, using the 3xTg Alzheimer's mouse model (Aim 1). Further, we will modulate inflammatory signaling in order to elucidate the mechanistic link between hemodynamics, neuroinflammation, and subsequent neurodegeneration after repetitive mTBI (Aim 2).



We hypothesize that hemodynamic markers, such as CBF, are linked to molecular outcomes, such as eNOS, neuroinflammation, and pathology after repetitive mild traumatic brain injury are linked (Aim1). We will use pharmacologic interventions to test if inflammatory signaling is a causal mechanism (Aim 2).

Accomplishment: We have established a large molecular dataset consisting of cytokine, phospho-signaling, pathology, and RNAseq data with paired CBF data at acute and chronic time points. Manuscript submitted to bioRxiv and being submitted to journal.

Timeline and Cost

Activities CY	18	19	20	21	22	23
Task 1: Legwork						
Task 2: Data Collection						
Task 3: Data Analysis						
Task 4: Manuscript preparation						
Estimated Budget ($K)	**$0**	**$140**	**$185**	**$175**		

Updated: 07/12/2023

Goals/Milestones

CY18 Goal – Preliminary legwork

☑ IACUC/ACURO approval

☑ Establish 3xTg mouse breeding

CY19 Goals – Data collection

☑ Hemodynamic measurements in mice after 1, 3, and 5 once daily injuries

☑ Preliminary treatment of mice with signaling inhibitors

CY20 Goal – Predictive capacity of hemodynamic markers

☑ Quantify hemodynamic maker predictive capacity/submit paper

CY21 Goal – Determine role of inflammatory signaling

☑ Define immune signaling after mTBI

Comments/Challenges/Issues/Concerns

- This project was impacted by COVID-19, still made important impact on understanding of effects of repetitive closed head injury

Budget Expenditure to Date

Projected Expenditure: $500,000

Actual Expenditure: $500,000

Profiling the neuroimmune cascade in 3xTg mice exposed to successive mild traumatic brain injuries

Alyssa F. Pybus[1], Sara Bitarafan[2], Rowan O. Brothers[1], Alivia Rohrer[1], Arushi Khaitan[1], Felix Rivera Moctezuma[2], Kareena Udeshi[2], Brae Davies[2], Sydney Triplett[1], Eric Dammer[3], Srikant Rangaraju[4], Erin M. Buckley[1,5,6,¥,], Levi B. Wood[1,2,6,¥,] *

[1]Wallace H. Coulter Department of Biomedical Engineering, Georgia Institute of Technology and Emory University
[2]George W. Woodruff School of Mechanical Engineering, Georgia Institute of Technology
[3]Center for Neurodegenerative Diseases, School of Medicine, Emory University
[4]Department of Neurology, School of Medicine, Emory University
[5]Department of Pediatrics, School of Medicine, Emory University
[6]Parker H. Petit Institute for Bioengineering and Bioscience, Georgia Institute of Technology

[¥]*Equally contributing corresponding authors*
**To whom correspondence should be addressed*

Erin M. Buckley, PhD[¥, *] Assistant Professor Wallace H. Coulter Department of Biomedical Engineering, Georgia Institute of Technology and Emory University; Department of Pediatrics, School of Medicine, Emory University 1760 Haygood Dr NE Atlanta, GA 30322	**Levi B. Wood**, PhD [¥, *] Assistant Professor George W. Woodruff School of Mechanical Engineering, Wallace H. Coulter Department of Biomedical Engineering, and Parker H. Petit Institute for Bioengineering and Bioscience, Georgia Institute of Technology 315 Ferst Dr, Rm 3311 Atlanta, GA 30322

ABSTRACT

Repetitive mild traumatic brain injuries (rmTBI) sustained within a window of vulnerability can result in long term cognitive deficits, depression, and eventual neurodegeneration associated with tau pathology, amyloid beta (Aβ) plaques, gliosis, and neuronal and functional loss. However, we have limited understanding of how successive injuries acutely affect the brain to result in these devastating long-term consequences. In the current study, we addressed the question of how repeated injuries affect the brain in the acute phase of injury (<24hr) by exposing the 3xTg-AD mouse model of tau and Aβ pathology to successive (1x, 3x, 5x) once-daily weight drop closed-head injuries and quantifying immune markers, pathological markers, and transcriptional profiles at 30min, 4hr, and 24hr after each injury. We used young adult mice (2-4 months old) to model the effects of rmTBI relevant to young adult athletes, and in the absence of significant tau and Aβ pathology. Importantly, we identified pronounced sexual dimorphism, with females eliciting more differentially expressed proteins after injury compared to males. Specifically, females showed: 1) a single injury caused a decrease in neuron-enriched genes inversely correlated with inflammatory protein expression as well as an increase in AD-related genes within 24hr, 2) each injury significantly increased expression of a group of cortical cytokines (IL-1α, IL-1β, IL-2, IL-9, IL-13, IL-17, KC) and MAPK phospho-proteins (phospho-Atf2, phospho-Mek1), several of which were co-labeled with neurons and correlated with phospho-tau, and 3) repetitive injury caused increased expression of genes associated with astrocyte reactivity and immune function. Collectively our data suggest that neurons respond to a single injury within 24h, while other cell types including astrocytes transition to inflammatory phenotypes within days of repetitive injury.

Keywords: traumatic brain injury; mild traumatic brain injury; Alzheimer's pathology; cytokines; neuroinflammation; MAPK; 3xTg-AD; astrocyte reactivity

INTRODUCTION

Traumatic brain injury (TBI) results in approximately 2.5 million emergency department visits every year in the Unites States alone. Approximately 75% of TBI cases are classified as mild (mTBI), and these mild cases carry an annual cost burden of $17 billion (1,2). An estimated 10-40% of mTBIs are associated with persistent cognitive impairment lasting longer than one month and in some cases up to a year (3–6). Moreover, repeated mTBIs (rmTBIs) sustained within a window of vulnerability can intensify pathological and functional consequences (7,8). These repeated injuries, which are often observed among athletes in high contact sports such as American football and boxing, can result in the development of Alzheimer's disease-like pathology, including neurofibrillary tangles and amyloid beta (Aβ) plaques (9). Current treatment paradigms for (r)mTBI are severely lacking and focus on the alleviation of symptoms, rather than targeting the underlying mechanisms of injury. There is thus an urgent need to illuminate the post-injury neuro-molecular sequelae for development of targeted therapies.

Mounting evidence suggests the involvement of brain immune signaling as a key driver of long-term outcome following mTBI. Brain immune signaling is implicated in several neurodegenerative diseases associated with mTBI, including Alzheimer's disease (AD) (10–12) and Parkinson's disease (PD) (13–15). Moreover, the roles of immune signaling in driving pathology following severe TBI have been relatively well-studied (16–20), and preliminary evidence shows similar patterns in (r)mTBI (16,21–25). Indeed, prior research from our own group has identified correlations between lower cerebral blood flow (a potential biomarker of worse cognitive outcome) and increased mitogen-activated protein kinase (MAPK) signaling, cytokine expression, and microglial activation after repetitive closed-head injuries (CHI) in wild type mice, supporting an essential relationship between brain immune signaling and outcome after mTBI. However, a comprehensive study relating acute changes in immune signaling and glial activation to neuronal changes and pathological markers after single and repetitive mTBIs is currently lacking and would provide a much-needed perspective to guide the search for new therapies.

The acute pathophysiology of mTBI has previously been defined by the "neurometabolic cascade of concussion," in which neurons undergo axonal injury and dysfunction, altered neurotransmission, ionic flux, and indiscriminate release of glutamate, while many brain cells undergo a hyperglycolysis energy crisis to restore homeostasis (26,27). When the neurometabolic cascade was defined in 2014, relatively little was known about mTBI-induced inflammatory changes, but research over the last decade has more fully defined changes in immune signaling, microglial activation, and astrocyte reactivity, as well as their effects on secondary injury after TBI (16,28–31). For example, recent studies suggest that astrocytes rapidly respond to mechanical stress after injury, potentially via opening of mechanosensitive ion channels, leading to activation of MAPK signaling, ATP release, and reactive astrogliosis (28,32–38). Here we propose to similarly define the acute "neuroimmune cascade" of mTBI. These clear changes in microglial and astrocyte responses post-mTBI suggest a broad and complex neuroimmune response to mTBI. Thus, a comprehensive understanding of neuroimmune signaling and its hypothesized relationship to neuronal, glial, and pathogenic changes after injury is critical to identifying drivers of secondary injury as well as determining therapeutic targets to mitigate adverse cognitive and pathological outcomes.

In the current study, we sought to define the neuroimmune cascade of rmTBI by profiling protein and transcriptomic changes associated with immune signaling, pathology, and the neuronal, microglial, and astrocytic compartments. We specifically hypothesized that mTBI would drive

brain immune signaling in a manner correlated with markers of neurodegeneration, such as tau, Aβ, astrocyte reactivity, and microglial activation. Because wild-type mice show inconsistent evidence of pathological changes after TBI (39–41), we used the triple transgenic model of Alzheimer's-like pathology (3xTg-AD), which contains human mutant forms of genes in the Aβ processing pathway (*APP*, *PSEN1*) and tau (*MAPT*). This model is widely used to study AD and is increasingly utilized in brain injury research (42–49). Here, we sought to concomitantly define the effects of successively increasing mild traumatic brain injuries on the following molecular outcomes in the frontal cortex and hippocampus: 1) the kinetics of brain immune signaling and cytokine expression, 2) tau phosphorylation and Aβ burden, 3) markers of astrocyte reactivity and microglial activation, and 4) transcriptional profiling of the somatomotor cortex (females only). Our data analyses revealed pronounced effects of repetitive injury on all molecular outcomes. Further, the inclusion of both male and female 3xTg-AD mice in our study revealed strong effects of sexual dimorphism in this model across all outcomes, with males showing higher basal levels of immune signaling but females showing more pronounced changes in response to injury.

MATERIALS AND METHODS

Study Protocol

3xTg-AD on C57BL/6J mice (Jackson Laboratory, strain 033930) were aged 2-4 months (98 females, 86 males). All protocols were approved by the U.S. Army Medical Research and Development Command Animal Care and Use Review Office (ACURO) and the Emory University Institutional Animal Care and Use Committee (IACUC) in accordance with National Institutes of Health guidelines. Mice were housed in a pathogen free facility with a twelve-hour light/dark cycle. Food and water were provided *ad libitum*. Mice were randomly assigned to one of four injury groups: sham-injured controls, one closed head injury (1xCHI), three closed-head injuries spaced once daily (3xCHI), and five closed-head injuries spaced once daily (5xCHI). Animals were sacrificed, and the brain was harvested for molecular and pathological assessment at the following time points for each group: pre-injury, 30 minutes, 4 hours, and 24 hours post-injury. Sample sizes (n=6-8 per injury time point group in protein data, n=2-4 in RNAseq data) are provided in **Table S1**.

Closed Head Injury Model

This work was conducted using a previously characterized weight drop closed-head injury (CHI) model (50,51). Animals were anesthetized using 4.5% isoflurane (1 L/min, 70/30 nitric oxide/oxygen) prior to injury. The injury was delivered by dropping a 54 g bolt down a 0.96 m guide tube (49035K85, McMaster-Carr, Elmhurst IL) onto the dorsal aspect of the head (skull intact), targeting between the approximate location of the coronal and lambdoid structures. The anesthetized animal was positioned under the guide tube on a Kimwipes® task wipe (Kimberly-Clark, Irving, TX). The animal was grasped by the base of the tail so that on impact, the mouse penetrated the task wipe and underwent rapid, unrestricted rotation of the head in the anterior-posterior plane. Control, sham-injured mice were age- and sex- matched and received the same exposure to anesthesia but were not subject to closed-head injury.

Quantification of Immune and Pathological Proteins

To comprehensively profile the immune signaling kinetics after repeated CHI in 3xTg-AD male and female mice, we quantified four classes of proteins: glial phenotypic markers (astrocyte

reactivity markers GFAP and S100B; microglial activation marker CD68 and homeostatic marker TMEM119), molecular markers of pathology (Aβ40, Aβ42, total tau, and phospho-tau T181), nine MAPK phospho-proteins, and 30 cytokines (in total 47 measured proteins, plus ratios Aβ42/40 and pTau/tTau). We collected frontal cortex and hippocampal samples from the left hemisphere of the three injury groups (1xCHI, 3xCHI, and 5xCHI) across four time points each (pre-injury and 30min, 4h, 24h post-injury), where the pre-injury 1xCHI group represents sham-injured controls. For analysis purposes, pre-3xCHI and pre-5xCHI are sometimes referred to as the 24h post-2xCHI and 24h post-4xCHI groups, respectively. In total, data was collected from 98 female mice and 86 male mice. Two female and three male mice were excluded from our analysis after Mahalanobis outlier detection using all protein data from the same sex and region ($\alpha<0.001$), leaving n=96 females and n=83 males.

Cortical and hippocampal brain tissue sections were lysed using the Bio-Plex cell lysis kit (Bio-Rad Laboratories #171304011) and protein concentrations were determined using a Pierce BCA Protein Assay (Thermo Fisher #23225). Multiplexed cytokine quantification was conducted using the Milliplex® MAP Mouse Cytokine/Chemokine 32-Plex kit (Eotaxin, G-CSF, GM-CSF, IFN-γ, IL-1α, IL-1β, IL-2, IL-3, IL-4, IL-5, IL-6, IL-7, IL-9, IL-10, IL-12p40, IL-12p70, IL-13, IL-15, IL-17, IP-10, KC, LIF, LIX, MCP-1, M-CSF, MIG, MIP-1α*, MIP-1β, MIP-2, RANTES, TNF-α, and VEGF*) (Millipore Sigma MCYTMAG-70K-PX32). Cytokines marked with an asterisk did not fall within a linear range and were not included in our analysis. Multiplexed phospho-protein quantification was conducted for the MAPK signaling pathway using the Bio-Plex Pro™ Cell Signaling MAPK Panel 9-plex kit (phospho-Atf2 T71, phospho-Erk1/2 T202/Y204 T185/Y187, phospho-HSP27 S78, phospho-JNK T183/Y185, phospho-Mek1 S217/S221, phospho-p38 MAPK T180/Y182, phospho-p53 S15, phospho-p90 RSK S380, phospho-Stat3 S727) (Bio-Rad Laboratories LQ00000S6KL81S). Prior to analysis, lysates were thawed on ice and centrifuged at 4°C for 10 min at 15,500g. Protein concentrations were normalized with Milliplex® MAP Assay Buffer (EMD Millipore, Billerica, MA) to 6 μg protein per 12.5 μL for cytokine analysis and 1 μg protein per 12.5 μL for the MAPK pathway analysis. These protein concentrations were selected because they fell within the linear range of bead fluorescent intensity vs. protein concentration for detectable analytes. Quantification of pathological markers was conducted for total tau, phospho-tau (T181), Aβ 1-40, and Aβ 1-42 using the Milliplex® MAP Human Amyloid Beta and Tau Multiplex Assay kit (Millipore Sigma HNABTMAG-68K). All kits were read on a MAGPIX® system (Luminex, Austin, TX).

We quantified astrocyte reactivity markers glial fibrillary acidic protein (GFAP) and S100 calcium binding protein B (S100B) as well as macrophage and microglia activation marker cluster of differentiation 68 (CD68) and microglial homeostatic marker transmembrane protein 119 (TMEM119) via enzyme-linked immunosorbent assay (ELISA). Protein concentrations were normalized with respective assay diluents from each kit to 2.5 μg/ml in 50 μL for the GFAP ELISA kit (Abcam ab233621), 50 μg/ml in 50 μL for the S100B ELISA kit (Abcam ab234573), and 0.1 μg/μL in 50ul for the CD68 and TMEM119 ELISA kits (Lifespan Biosciences LS-F11095 and LS-F52734). These protein concentrations were selected because they fell within the linear range of absorbance vs. protein concentration for detectable analytes.

Data Analysis and Visualization

Data was analyzed and figures were generated in RStudio (Boston, MA) using the R programming language. Data processing was conducted using the `tidyverse` collection of packages (52). Heatmaps were generated using the R package `heatmap3` (53), bar graphs and regression plots were created using the packages `ggplot2` (54) and `ggpubr` (55), and gene set

variation analysis was conducted using the `gsva` package (56) available on Bioconductor. For each molecular assay, we collected background measurements using assay buffer in the absence of biological samples. We subtracted average background measurements from each sample measurement and set negative values to zero. Clustering was conducted using the `hclust` function of the `stats` package in R using Euclidean distance in the unweighted pair group method with arithmetic mean. Outlier detection was conducted in R by calculating Mahalanobis distance of each point from the data's centroid within each grouping of sex and region (female frontal cortex, female hippocampus, male frontal cortex, and male hippocampus) using the `ClassDiscovery` (57) package. Two female and three male hippocampus samples were outside the cutoff threshold of α=0.001 and all data from those animals was discarded in both the frontal cortex and hippocampus sets.

Adjustment for Batch Effect and Pathology

Male and female data were collected simultaneously for S100B, CD68, and TMEM119 by ELISA, but separated into different batches for all other protein measurements. Eight female sample replicates were included in each male batch assay and then used to transform the male data into the female space via a linear model for each protein. Computations were conducted using the lm() function in R.

To adjust data for the effects of pathology, linear models were calculated using neuroimmune proteins as dependent variables with the following combinations of independent variables: total tau and phospho-tau T181; Aβ40 and Aβ42; or total tau, phospho-tau T181, Aβ40, and Aβ42. Residuals of each linear model were defined as the pathology-adjusted (tau-adjusted, Aβ-adjusted, or total pathology-adjusted) neuroimmune protein data. Computations were conducted using the lm() function in R.

Immunohistochemistry

Immunohistochemistry was performed to investigate GFAP, NeuN, IL-1α, IL-1β, IL-13, KC, phospho-Atf2 (T71), phospho-Mek1/2 (S217/S221), and phospho-tau (S262/T263). Right brain hemispheres from each animal were fixed in 4% paraformaldehyde then processed and embedded in paraffin. Tissue slices were cut into 10 µm thick sagittal sections using a rotary microtome (Thermo Fisher) and affixed onto glass microscopy slides (Electron Microscopy Sciences, Hatfield, PA). Tissue slices were deparafinized in xylene and rehydrated by washing with 100% ethanol, 95% ethanol, and deionized water. Antigen retrieval was performed in a microwave by boiling slides in 10mM sodium citrate buffer at pH 6.0. Slides were rinsed in tris-buffered saline with 0.01% tween (TBST). A hydrophobic ring was drawn around each individual tissue slice using an immunohistochemistry PAP pen (Enzo Life Sciences, Farmingdale, NY), after which samples were blocked for 2 hr in blocking buffer, 5% w/v Bovine Serum Albumin (BSA) or 50% goat serum (Sigma-Aldrich) in TBST. Samples were incubated at 4°C overnight with primary antibodies diluted in blocking buffer: GFAP (1:100, Diagnostic Biosystems Mob064), NeuN (1:200, Abcam ab104224), IL-1α (1:50, Thermo Fisher PA5-89037), IL-1β (1:500, Abcam ab283818), IL-13 (1:100, Abcam ab106732), KC (1:50, Thermo Fisher PA5-86508), phospho-Atf2 T71 (1:50, Thermo Fisher PA5-97332), phospho-Mek1/2 S217/S221 (1:50, Themo Fisher PA5-1057), or phospho-tau S262/T263 (1:100, Abcam ab92627), as appropriate. Slides were rinsed again in TBST and incubated with either Alexa Fluor 555 and/or Alexa Fluor 488 secondary antibodies (Thermo Fisher) diluted 1:200 in blocking buffer. Slides were counterstained with 1 µg/mL DAPI, rinsed in water, and mounted with VECTASHIELD Antifade Mounting Medium

(Vector Laboratories, Burlingame, CA). Samples were imaged using epifluorescent microscopy on a Zeiss Axio Observer Z.1 inverted microscope.

Bulk Tissue RNA Sequencing and Analysis

We conducted RNA sequencing on a representative subset of 40 female left somato-motor cortex samples selected from the original 96 for bulk tissue RNA sequencing (available on the NCBI Gene Expression Omnibus under accession number GSE226838). One sample was removed post-sequencing after identification as an outlier animal within the protein data. RNA was extracted using the miRNeasy Micro kit (Qiagen #217084). Extracted RNA was sent to Admera Health, LLC (South Plainfield, NJ) for sequencing, alignment, and calculation of the count matrix. The count matrix yielded 32,807 non-zero features. Features with fewer than 10 counts in more than four samples (~10%) were filtered out of the analysis (17,844 features). The remaining 14,963 features were normalized by ratio of median method then variance-stabilized in R using the `DESeq2` package, available on Bioconductor (58).

Weighted gene co-expression network analysis (WGCNA) was conducted in R using the `WGCNA` package (59) available on the Comprehensive R Archive Network (CRAN). A WGCNA threshold power of 4 was chosen since it was the smallest threshold that resulted in a scale-free R^2 value greater than 0.80. We constructed our network in a single block using blockwiseModules() with the following parameters: threshold power of 4, signed modules, a minimum module size of 20, a merge cut height of 0.07, a reassignment threshold of 0.05, a "bicor" correlation type, and a "mean" TOM denominator. Significance of module eigengene (ME) expression between sham and injured samples was assessed by permutation test, in which ME values for both populations were randomly re-assigned to either group then permutated mean difference was compared to the true mean difference across 10,000 iterations. Original sample sizes were maintained. Groups were considered significantly different if the true mean difference was greater than or equal to the permutated mean difference in at least 95% of iterations.

Gene ontology was conducted for each of the 14 resulting WGCNA modules using PANTHER overrepresentation test on PANTHER 17.0, available on the Gene Ontology Resource. We used the mm10 GO biological process complete annotation set with Fisher's exact test and false discovery rate (FDR) corrected p-values. The test was applied using all genes with a network kME, or module connectivity (59), of at least 0.60 and a background of the 14,963 features used to construct the network.

Cell type enrichment was conducted using protocol as published in (60–62). Briefly, a cell type marker list was created for neurons, oligodendrocytes, endothelia, astrocytes, and microglia from cell type specific mouse brain proteome and transcriptome studies Sharma *et al.* (63) and Zhang *et al.* (64). Fisher exact tests with FDR correction were performed to determine enrichment for each cell type marker list within each WGCNA network module. We used R scripts by Eric Dammer and Divya Nandakumar (Emory University School of Medicine) freely available on GitHub at https://github.com/edammer/CellTypeFET.

Multi-marker Analysis of GenoMic Annotation (MAGMA)(65) was conducted to identify modules with significant enrichment for genes related to Alzheimer's disease (AD) as identified in genome-wide association studies (GWAS) (66–68). To implement MAGMA, we used R scripts by Eric Dammer as used in Seyfried *et al*. (62), freely available on GitHub at https://github.com/edammer/MAGMA.SPA.

Gene set variation analysis (GSVA) was conducted on the normalized and variance-stabilized count matrix in R using the `gsva` package, also available on Bioconductor (56). Gene sets used for GSVA included the C2 curated gene sets collection from the Molecular Signatures Database (69,70) as well as our previously published astrocyte-enriched gene sets (71).

RESULTS

Immune, glial, and pathological markers differed between male and female 3xTg-AD mice

Since prior reports showed pronounced differences in pathological burden between male and female 3xTg-AD mice (72,73), we began the current study by evaluating sex differences among all protein measures: cytokines, MAPK phospho-proteins, glial markers, phosphorylated and total tau, and Aβ40/42. Data were adjusted for batch effects as needed using linear models of technical replicates (**Methods**). We first obtained a holistic view of variation within the data using a principal component analysis (PCA), which revealed a pronounced effect of sex within both brain regions (**Fig. 1A**). Female replicate samples from the male batches grouped with female batch samples and separately from male samples, emphasizing that the effects of sex were biological, rather than technical (purple points, **Fig. 1A**).

To define the specific effects of sex versus injury and time point, we conducted multiple linear regression of all quantified proteins and phospho-proteins using sex, injury number, and time point as independent variables, revealing that sex, as compared to all other variables in the model, had the most significant effect (**Fig. S1)**. We next conducted comparisons between sex for each measured protein in 1) sham-injured animals only (**Fig. 1B**) and 2) all sham and injured animals (**Fig. S1A**). Importantly, all proteins determined to be significantly different between sexes based on the sham animals alone were also significantly different between sexes when all samples were used, regardless of injury condition (**Fig. 1C**, **Fig. S2**, **Table S2**). An additional 12 and 17 significantly different proteins were identified in the frontal cortex and hippocampus, respectively, when all animals across injury conditions were compared (**Fig. 1C, Fig. S2**, **Table S2**).

Importantly, female samples showed significantly higher levels of Aβ42 in the frontal cortex compared to males, and higher total and phosphorylated tau at a pathologically relevant residue (T181) (74) in the hippocampus compared to male samples ($p<0.0001$, Wilcoxon rank-sum; **Fig. 1C**, **Table S2**). This matches most prior studies in 3xTg-AD mice, as reviewed in (72). Interestingly, we found significantly higher phospho-tau T181 in male compared to female frontal cortices ($p<0.0001$, Wilcoxon rank-sum). While our findings of sex differences are consistent with prior reports in 3xTg AD mice (72), there have been no reports evaluating sex differences in immune signaling or glial activation. Here, we found that the majority of the 46 measured immune and pathological marker proteins in both brain regions showed higher average levels in males compared to females (**Fig 1B**, **Fig S1A**). Of those, 31 from the frontal cortex (24 in sham-only) and 21 from the hippocampus (15 in sham-only) reached statistical significance ($p<0.05$, Wilcoxon rank-sum; **Fig. 1C**, **Fig. S2**, **Table S2**). Importantly, the astrocyte reactivity markers GFAP and S100B were significantly elevated in the male frontal cortex and hippocampus, indicating increased astrocyte reactivity in males. Taken together, these data suggest an elevated immune signaling baseline in young (2-4mo) male 3xTg-AD mice compared to their age-matched female counterparts.

To determine if differences in immune markers between male and female mice could be explained by the well-documented disparities in Aβ and tau in this model (72), we adjusted our data for effects related to Aβ (Aβ40 and Aβ42), tau (total tau and phospho-tau T181), or both (**Methods, Fig. S3, Table S3**). Adjustment for all pathological markers in the frontal cortex reduced the number of differentially expressed proteins from 31 to 15 elevated in males and from 9 to 3 elevated in females, suggesting that approximately half of all differentially expressed proteins can be explained by pathology. A similar effect is seen in the hippocampus after adjustment: from 21 to 12 proteins elevated in males and 16 to 8 in females. Interestingly, the removal of only Aβ-related effects (Aβ40 + Aβ42) in the hippocampus only accounted for 2 differentially expressed proteins (**Table S3**). The persistence of sexual dimorphism among immune markers (mostly cytokines) after adjustment for pathological measures suggests inherent differences in baseline immune signaling of young male and female 3xTg-AD mice independent of their stage of pathogenesis. Thus, we analyzed male and female data separately in this study.

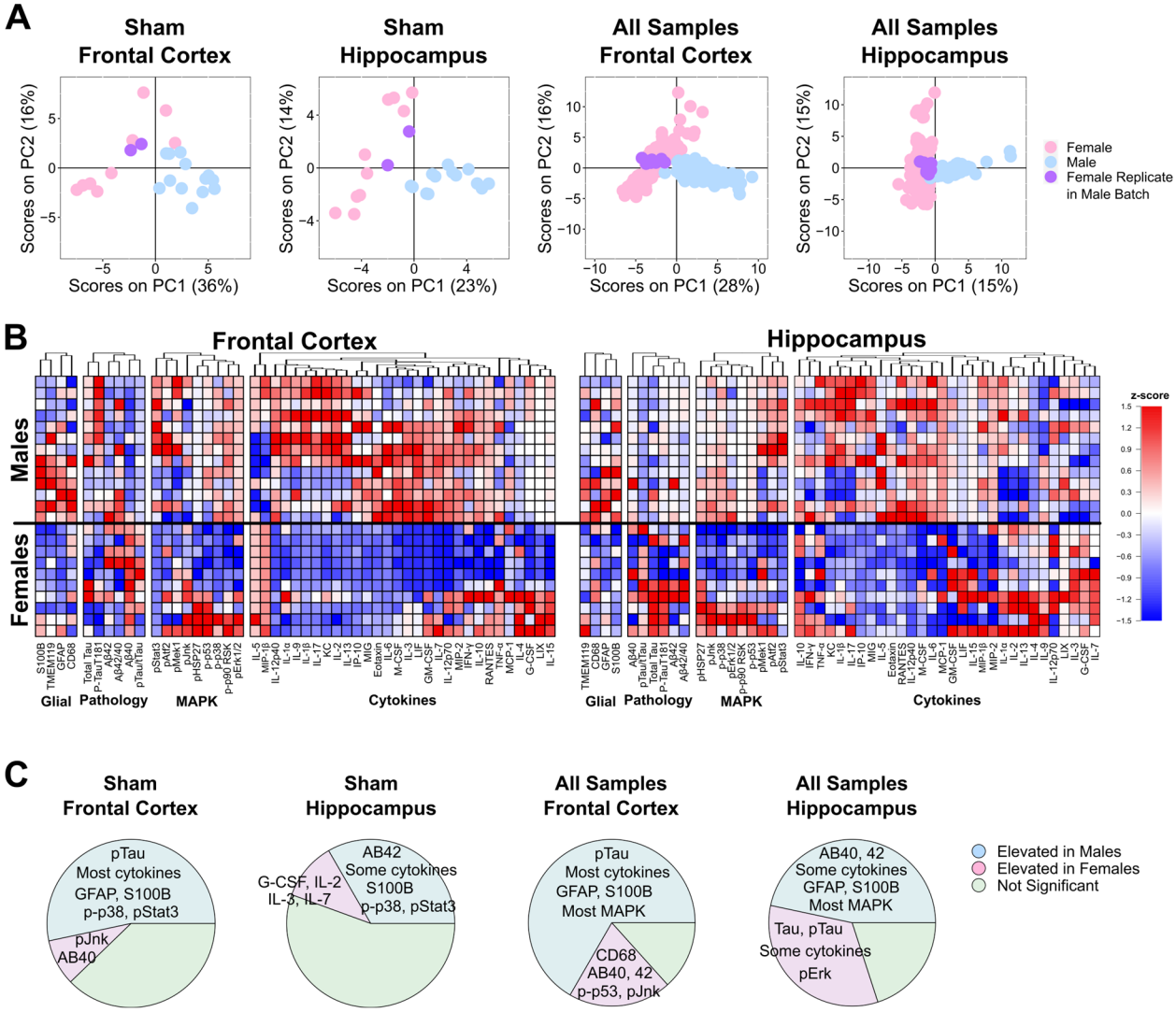


Figure 1. Pronounced sexual dimorphism of immune signaling, glial markers, and molecular markers of pathology in 3xTg-AD mice. A) Principal component analysis of combined protein data across sham-injured animals (left) and all injuries and time points (right) reveals strong separation between male and

female mice on the first two PCs. Female replicate samples measured in male batch assays are shown in purple. Percent variance described by each PC is annotated in parentheses. **B**) Uninjured control mice show distinct baseline sex differences in expression of glial markers, pathological markers, MAPK signaling, and cytokines. Proteins are categorized by function then clustered by Euclidean distance within each category. Red to blue indicates relatively high to low expression among all sham animals (n=13 males, n=10 females). Of the 46 measured immune and pathological marker proteins in sham-injured animals, 37 from the frontal cortex (80%) and 30 from the hippocampus (65%) had higher average expression in males compared to females. **C**) Pie charts for each region and sample set (just sham on left, all animals combined on right) show high proportions of all analytes measured (4 glial markers, 4 pathological markers, 9 MAPK, 30 cytokines) that are significantly elevated ($p<0.05$, Wilcoxon rank-sum) in males (blue) or females (pink). See summary of significant differences in **Table S2**.

Cytokines and MAPK phospho-proteins are elevated after each closed-head injury

To identify patterns of co-varying cytokines and phospho-proteins with injury and time point, we next conducted hierarchical clustering within each sex and brain region (**Methods, Fig. S4-5**). Importantly, we found that females exhibited robust variation of these signaling proteins with both number of injuries and time point. The clustering identified a group of injury-induced cytokines (IL-9, IL-17, KC, IL-1α, IL-2, IL-1β, IL-13) and MAPK phospho-proteins (phospho-Atf2, phospho-Mek1) that tightly clustered together within the frontal cortex data from female mice (**Fig. S4, "Group 1"**). Proteins within this group were significantly increased at 24h after 1x, 2x, and 3xCHI, showed mild increases 24h after 4xCHI, and returned to baseline sham levels 24h after 5xCHI (**Fig. 2**), suggesting a dysregulated immune response after four or more injuries. Interestingly, these proteins were elevated 4h post-5xCHI compared to sham, 4h post-1xCHI, and 4h post-3xCHI animals (**Fig. 2**), indicating an earlier response after multiple injuries consistent with a "primed" immune state (75). Although many of the same cytokines and phospho-proteins from Group 1 again clustered together within the female hippocampus (**Fig. S4**) and male frontal cortex and hippocampus (**Fig. S5**), this same trend of an injury-dependent increase was only noted in the female frontal cortex. Together, these data indicate the importance of evaluating multiple time points after injury to fully define the immune response and emphasize the need to evaluate males and females separately.

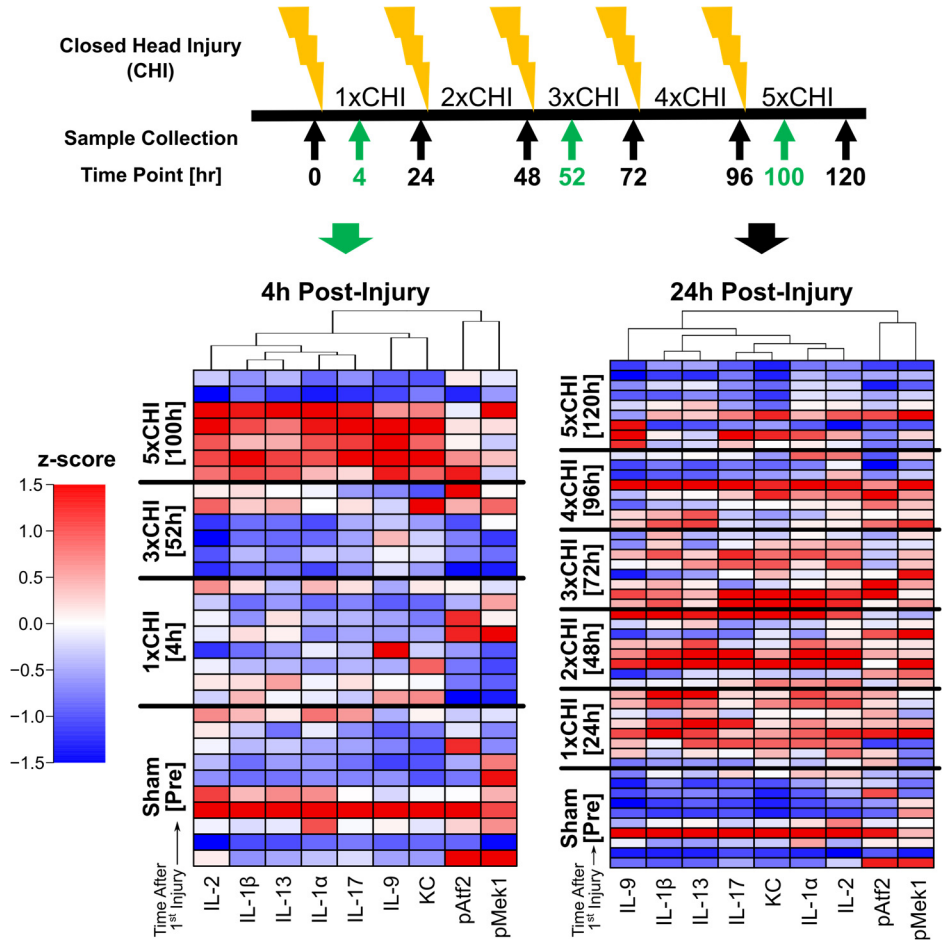


Figure 2. Cytokines and MAPK phospho-proteins are elevated after each closed-head injury in females. Hierarchical clustering of cytokines and MAPK phospho-proteins (subset from **Fig. S4, "Group 1"**) from the frontal cortex of female 2-4mo 3xTg sham-injured mice and 4hr (left) or 24hr (right) after 1-5x closed head injuries (CHI). Each row represents data from an individual mouse z-scored along each column.

Protein and transcript markers of pathology are elevated after injury

Our motivation for conducting this study in 3xTg-AD mice was to identify relationships between immune signaling and molecular markers associated with AD-related pathology. In particular, TBI is known to cause neurodegenerative pathologies, such as neurofibrillary tangles associated with hyperphosphorylated tau as well as the build-up of Aβ plaques. To assess the relationship between our injury-elevated Group 1 immune signals and pathology-associated proteins, we quantified total tau, phospho-tau (T181), Aβ 1-40, and Aβ 1-42 by Luminex ELISA, then conducted clustering and correlation analyses. Few significant acute changes in Aβ or correlation with Group 1 proteins were observed in either region or sex (**Figs. S8-9**). Interestingly, however, in both brain regions and both sexes, the Group 1 immune markers clustered with phospho-tau with few exceptions (**Fig. S4-5**), suggesting a connection between cytokines and pathologically relevant tau phosphorylation (74). Pearson's correlation coefficients between phospho-tau T181 and each cortical immune marker within each injury group (**Fig. 3A**) revealed that the majority of immune signals in Group 1 were correlated (|R|>0.50) across multiple time

points. These data thus suggest that injury drives acute cytokine and MAPK immune signaling associated with increased phosphorylated tau.

Interestingly we observed these pronounced correlations in the frontal cortex despite only finding group-wise elevation of phospho-tau at 24h post-3xCHI in female frontal cortices (**Fig. S6**) and no group-wise changes in males. However, total tau and phospho-tau (T181) were elevated at multiple time points after 3x and 5xCHI (**Fig. 3B**). These data thus indicate that our CHI model induces acute pathological changes in a region-dependent manner, and that Group 1 immune signaling correlates with phosphorylated tau even in the absence of group changes in total or phosphorylated tau.

Due to the observed increases in total and phospho-tau in injured animals, we hypothesized that genes associated with AD pathogenesis may also become upregulated after rmTBI. To test this, we conducted bulk RNAseq on a subset of 40 females (somatomotor cortex, n=3-4 per group), then conducted gene set variation analysis (GSVA) using the Alzheimer's disease-related gene set from the Molecular Signatures Database (MSigDB) C2 curated gene sets collection. Importantly, this gene set was significantly enriched after a single injury and remained enriched with subsequent injuries (**Fig. 3C, Fig. S10**). Thus, our protein and transcriptional data together indicate that pathological markers increase after injury and are correlated with neuroimmune markers.

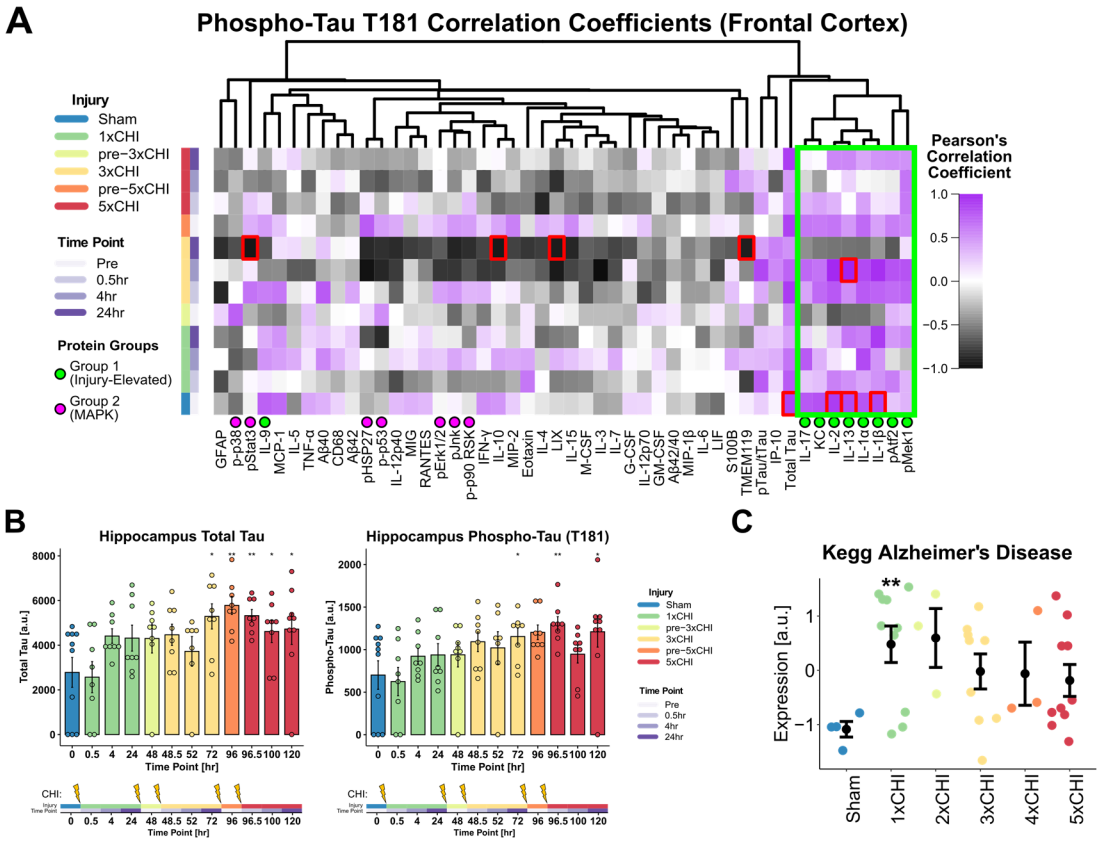


Figure 3. Total and phospho-tau increase with successive injuries in the hippocampus, AD-related genes increase in the somatomotor cortex after 1xCHI. A) Heatmap of Pearson's correlation coefficient of cortical phospho-tau T181 versus each measured cortical protein (columns) within each injury group and time point (rows); red boxes indicate FDR-adjusted p<0.05; green and purple dots represent Group 1 and 2

proteins, respectively. Green box shows eight out of nine Group 1 proteins cluster together and show correlation coefficients R>0.50 with phospho-tau T181. **B**) Total tau is significantly upregulated in the hippocampus at 24hr post-3xCHI and each successive time point compared to sham-injured animals (*p<0.05, **p<0.01 Wilcox). Phospho-tau (T181) is significantly upregulated in the hippocampus 30min and 24hr post-5xCHI compared to sham-injured animals (*p<0.05, **p<0.01 Wilcox) (mean ± SEM). **C**) Expression of the gene set "Kegg Alzheimer's Disease" significantly increases after 1xCHI (**p<0.01, t-test with Bonferroni correction) (mean ± SEM). See individual gene changes in **Fig. S10**.

Cytokines and MAPK phospho-proteins elevated after injury co-label with neurons

Having found that Group 1 proteins correlated with phospho-tau, which is a primarily a neuronal protein (**Fig. 3A**), we next asked if Group 1 signaling would be associated with neurons or other cell types. To this end, we conducted immunohistochemistry for various Group 1 proteins together with markers for neurons (NeuN) and astrocytes (GFAP) at the 24h time point in mice exposed to 1x or 3xCHI. We found that IL-1α, IL-1β, IL-13, phospho-Atf2, and phospho-Mek1/2 co-localized with the neuronal marker NeuN in the cortex and hippocampus after injury, suggesting neuronal involvement in post-rmTBI immune signaling (**Fig. 4, Fig. S11**). Additionally, IL-1β, IL-13, KC, phospho-Atf2, and phospho-Mek1/2 did not co-localize with the astrocyte marker GFAP in the cortex (**Fig. S12**) or hippocampus (**Fig. S13**).

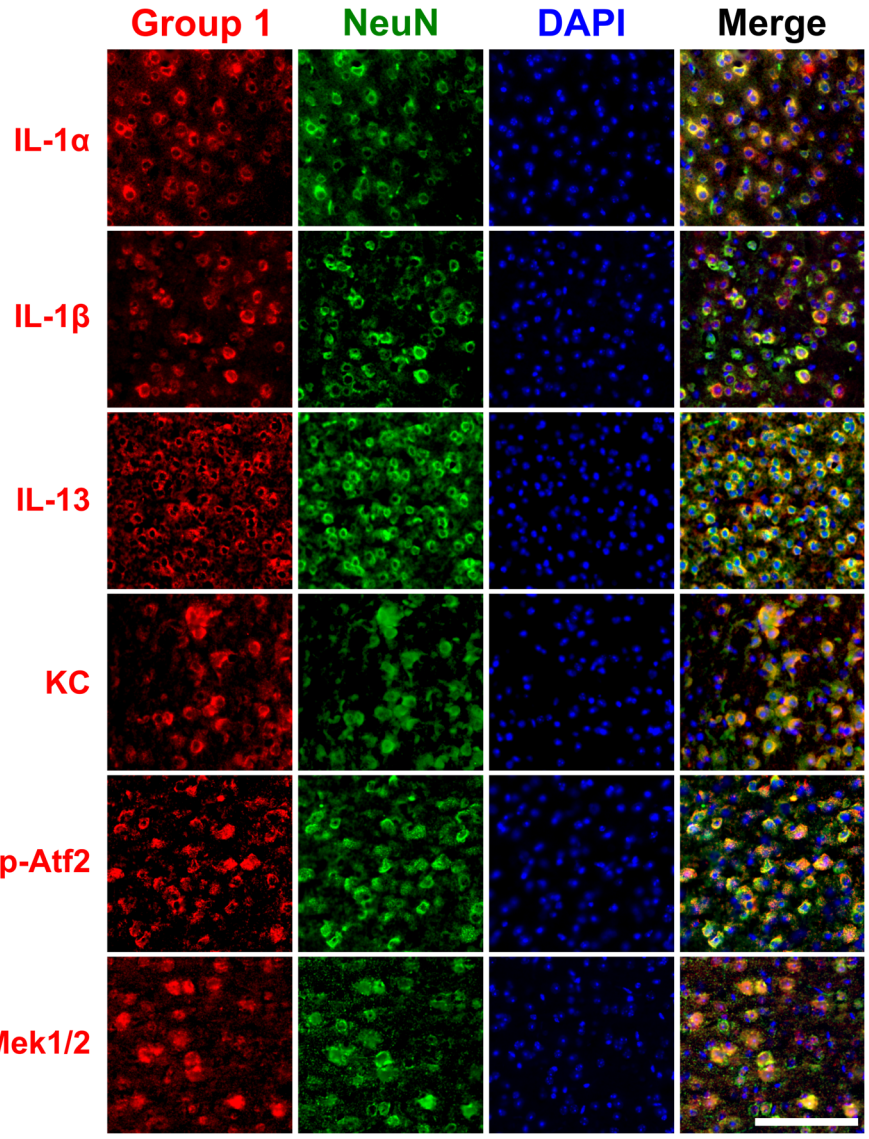


Figure 4. Group 1 cytokines and phospho-proteins co-label with NeuN in frontal cortex 24hr post-CHI. Group 1 cytokines (IL-1α, IL-1β, IL-13, and KC) and MAPK phospho-proteins (phospho-Atf2 and phospho-Mek1/2) (red) co-stained with NeuN (green) and DAPI (blue) show neuronal localization in the frontal cortex 24h post-CHI in female 3xTg mice aged 2-4mo (scale bar: 500μm).

Bulk RNAseq analysis reveals the effect of injury on pathology- and cell type-associated gene modules

To illuminate the broad effects of repetitive mTBI on cortical transcriptional networks, we next conducted network analysis on the same subset of 40 female cortical samples (somatomotor cortex, adjacent to the frontal cortex sections used for protein analysis) used in **Fig. 3C**, sampled from all injury groups and time points (n=3-4 per group). One sample was removed from the analysis due to its outlier status and exclusion within the protein data (Mahalanobis multivariate outlier detector with $\alpha<0.001$, **Methods**).

To obtain an unbiased view of expression patterns within the data, we first conducted WGCNA (**Methods**), which identified 14 distinct modules of co-varying genes (**Fig. 5A**). A module eigengene (ME) was computed for each module as its first principal component, and expression scores of each ME were displayed for each sample across all injury and time point groups (**Fig. 5B**). Due to small sample sizes and relatively low variation within time points of each injury group (**Fig. 5B**), we combined post-injury time points (30m, 4h, 24h) into one group per injury number and compared module expression across number of injuries. The two modules comprised of the largest number of genes, ME1 (turquoise) and ME2 (blue), rapidly changed after 1xCHI, with ME1 showing a significant increase ($p<0.05$) and ME2 showing trending decreases ($p=0.054$) post-injury. In contrast, ME9 (magenta) progressively increased with successive injuries (**Fig. 5C**) and tracked closely with ME7 and ME8 (black, pink) after 2-5xCHI. Moreover, ME3 (brown) and ME6 (red) were increased after 1xCHI then decreased compared to sham after 5xCHI, while ME10 (purple) and ME11 (green-yellow) peaked after 2xCHI, then returned to sham levels. These modules therefore define changes associated with rapid (ME1, ME2), transient (ME3, ME6, ME10, ME11) and gradual time scales (ME7, 8, 9).

To understand the biological relevance of each module, we used gene ontology (GO, via PANTHER) to identify top GO terms enriched in each module (**Fig. 5D**). Importantly, the rapidly changing ME2 (blue) was enriched for genes related to nervous system development, suggesting a rapid downregulation of homeostatic neuronal functions. The gradually changing modules, ME7, ME8, and ME9 (black, pink, magenta), were enriched for GO terms associated with wound healing, cytokine response, gliogenesis, and regulation of the immune response, suggesting a multi-day response that involves immune processes and healing. Importantly, those modules that increase with injury were all correlated with immune proteins (inflammatory cytokines, MAPK activation, and GFAP) quantified in the frontal cortex of the same animals (ME1, 7, 9; "Trait Correlations" **Fig. 5E**), whereas ME2, which shows decreasing trends after injury and is associated with neuronal function, was inversely correlated with immune proteins (**Fig. 5E**).

We next conducted a cell-type enrichment analysis for genes with high specificity in neurons, oligodendrocytes, endothelia, astrocytes, and microglia derived from cell type specific mouse brain proteome and transcriptome studies Sharma et. al. (63) and Zhang et. al. (64) (**Fig. 5F**). We found that ME2 (blue), which decreases after a single injury and is inversely correlated with immune protein markers, was significantly enriched for neuronal genes. In contrast, ME7, 8, and 9 (black, pink, magenta), which show gradual increasing trends with successive injuries and (with the exception of ME8) correlate with immune protein markers, were enriched for endothelial, astrocyte, and microglial genes, respectively.

We concluded this unbiased analysis by asking if specific modules were associated with AD-related gene expression. To test this, we used a Multi-marker Analysis of GenoMic Annotation (MAGMA) analysis to determine if disease risk associated with AD-related genes was significantly elevated within specific gene modules. In this analysis, each module is evaluated for AD-enriched genes (previously identified by GWAS, 66–68) weighted by their associated risk factor for AD. Indeed, AD risk was significantly elevated in ME1 (i.e. *Pfdn5*, *Rps11*, *Rpl13a*, *Lamtor4*, *Rpl14*), which increases with a single injury and correlates significantly to several inflammatory proteins. AD risk was also elevated in ME9 (i.e. *Hepacam*, *Vav1*, *Hexb*, *Grn*, *Laptm5*), which increases gradually, correlates with inflammatory proteins, and is enriched for microglial genes (**Fig. 5G**). Taken together, these data suggest an early inflammatory response associated with AD genes (ME1) and a concomitant, trending, neuronal decrease in homeostatic functions (ME2) after a single injury. Moreover, multiple injuries progressively increased gene

expression profiles associated with wound healing and regulation of inflammation within endothelia, astrocytes, and microglia.

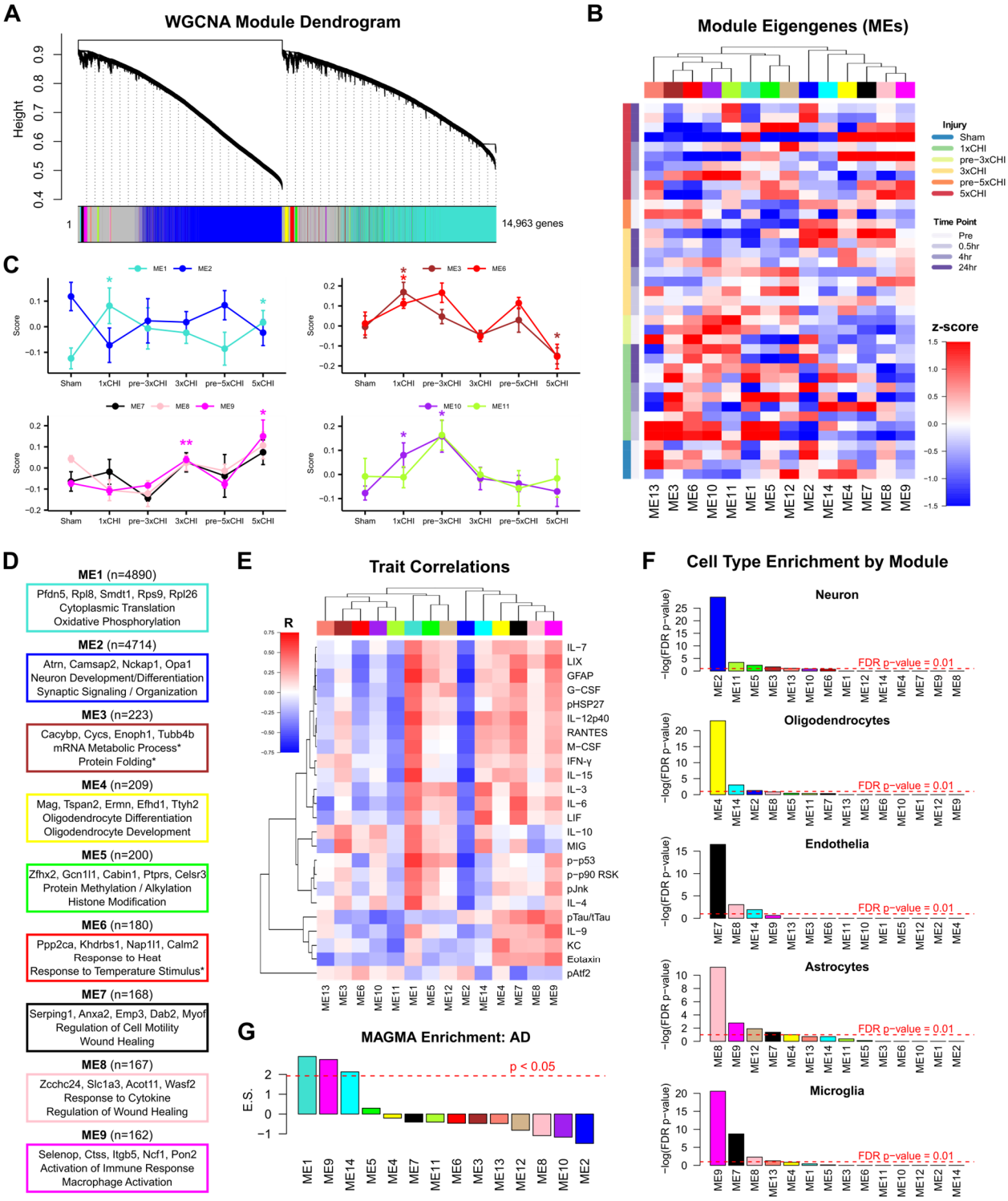


Figure 5. WGCNA of somatomotor cortex transcriptomes identifies modules of co-expressed genes associated with injury, GO biological processes, inflammatory protein expression, brain cell types,

and AD genetic risk factors. A) WGCNA identified 14 modules of co-expressed genes. **B**) Expression scores for the 14 module eigengenes (MEs, the first principal component of each module) for each sample. MEs are clustered by Euclidean distance (columns) and expression scores are displayed by increasing injury number and time point from bottom to top of the heatmap (rows). **C**) Line plots show changing ME expression scores over increasing numbers of injuries. Time points for 30min, 4hr, and 24hr after each injury (1x, 3x, 5xCHI) are combined due to low sample sizes (n=2-4). ME1 (turquoise) and ME2 (blue) show opposite behavior after 1xCHI, with ME1 significantly increasing alongside trending decreases in ME2 after a single injury. ME 9 (magenta) shows significant increases after successive injuries that track closely with ME7 and 8 (black and pink) (*$p<0.05$, **$p<0.01$, permutation tests compared to sham, see **Methods**) (mean ± SEM). **D**) Gene ontology enrichment of biological processes was conducted for each module (Fisher's exact test with FDR-corrected p-value <0.05). ME3 and ME6 had fewer than two significant GO sets. Sets marked with asterisks had FDR-corrected $p>0.05$ but uncorrected $p<0.0001$. **E**) Protein expression data from the frontal cortex of the same animals were correlated against each ME. Selected proteins showed a correlation p-value of at least 0.01 against at least one ME. Red indicates a positive Pearson's correlation coefficient (R) while blue indicates negative correlation. **F**) Cell type enrichment analysis showed significant enrichment of neuronal genes in ME2 (blue), oligodendrocyte genes in ME4 (yellow), endothelia genes in ME7 (black), astrocyte genes in ME8 (pink), and microglial genes in ME9 (magenta). **G**) MAGMA enrichment for GWAS AD risk showed significant over-representation within ME1 (turquoise), ME9 (magenta), and ME14 (cyan). The dotted red line indicates an enrichment z-score of 1.96, above which a module is considered significantly enriched (normal distribution, $p<0.05$).

Transcriptional and protein markers of astrocyte reactivity are increased after repetitive closed head injury

Astrocyte reactivity is a central phenotype of brain injury. Several studies have reported elevated expression of the astrocyte reactivity marker GFAP within hours, and up to 1mo, after TBI. Moreover, GFAP is being evaluated as a CSF biomarker for TBI diagnosis and prognosis (76–80). We therefore hypothesized that astrocyte reactivity would be increased in 3xTg mice exposed to successive mTBIs. To analyze possible changes in astrocyte phenotypes and function following injury, we conducted a gene set variation analysis (GSVA) (56,69) of custom-annotated astrocyte gene sets that define astrocyte homeostatic and reactive functions (1,740 genes spanning 17 gene sets plus the A1 and A2 gene sets (81)) from our prior work (71) (**Fig. 6A**). To define the specific effects of injury and time point on astrocyte transcriptional profiles, we conducted multiple linear regression of the enrichment scores of all 17 astrocyte gene sets using number of injuries, time point after injury, and a binary injury variable (injured or sham) as independent variables. Consistent with our WGCNA, this analysis revealed that the number of injuries had a greater effect on gene set enrichment than the post-injury time point (**Fig. 6B**). We therefore combined post-injury time points (30min, 4h, 24h) to create a single group for each number of injuries 1-5xCHI, improving our ability to analyze differences despite our small sample sizes (n=3-4 per time point).

Interestingly, clustering of sample enrichment scores for the 17 astrocyte gene sets revealed two distinct patterns of expression after repeated injury (**Fig. 6A**). First, twelve astrocyte gene sets formed a cluster characterized by rapid decreases in enrichment following the first CHI, as represented by the Gliotransmission and Plasticity sets (**Fig. 6C**). These sets mostly showed recovery of expression to sham-levels by 24hr post-4/5xCHI. Many of these sets represent normal homeostatic astrocytic functions, such as gliotransmission, plasticity, gene expression, and the perisynaptic astrocyte process (PAP). A rapid decrease in expression of these sets following 1xCHI suggests astrocytes first respond to injury by altering their homeostatic functions. The second

response pattern, represented by Stress Response and General Metabolism (**Fig. 6D**), shows a gradual increase in expression after 3-5xCHI. Coloring data points according to *Gfap* revealed an association between astrocyte reactivity and elevated Stress Response and General Metabolism gene sets. Other gene sets exhibiting this trend of a gradual increase include the A1 and A2 phenotypes and Carbohydrate Metabolism, which are functions that are generally related to astrocyte reactivity (81,82). These data therefore suggest elevated astrocyte reactivity by 3-5xCHI, 72-120hr after the first daily injury.

Since the RNAseq analysis suggested increased astrocyte reactivity at the transcriptional level, we next analyzed astrocyte reactivity at the protein level. To do so, we quantified astrocyte reactivity markers glial fibrillary acidic protein (GFAP) and S100 calcium binding protein B (S100B) by ELISA in the frontal cortex and hippocampus of all female mice exposed to 1x, 3x, or 5x once daily CHIs. To assess the behavior of GFAP in our injury model, we conducted a multiple linear regression analysis with dependent variables of time point following injury (pre-injury vs 30min, 4hr, or 24hr post-injury) and total number of injuries. Across female frontal cortex samples, we found that post-injury samples were significantly upregulated from pre-injury samples at both 30min and 4hr, but not 24hr post-injury (**Fig. 6E**), and that the total number of injuries was not a significant predictor of GFAP levels. In a parallel analysis, multiple linear regression of cortical S100B in female mice similarly revealed statistically significant upregulation 30min post-injury vs pre-injury but not after 4hr or 24hr (**Fig. S14**). Taken together, these data indicate a rapid, transient state of astrocyte reactivity following each repeated CHI that begins as early as 30min, but returns to basal levels by 24hr. Due to the significant increases after successive injuries in microglial-enriched and AD-GWAS-enriched ME9 (**Fig. 5**), we also quantified microglial activation marker CD68 but found that changes were minimal and inconsistent between sex and region (**Fig. S15**).

Because astrocyte reactivity is a key component of the brain's response to stress and injury, we next analyzed the relationships between GFAP protein levels, cytokine expression, and MAPK signaling activity. Among both female cortical and hippocampal samples, a group of MAPK phospho-proteins, termed "Group 2" (phospho-Stat3, phospho-Jnk, phospho-HSP27, phospho-p38, phospho-p90 RSK, phospho-Erk1/2, and phospho-p53), clustered tightly together across all injury groups and closely with GFAP (**Fig. S4-5**), indicating potential involvement of astrocyte reactivity in both brain regions. Therefore, we next computed Pearson's correlation coefficients between GFAP and each measured immune marker within each injury and time group (**Fig. 6F**) and found broad positive correlations both before and after injury, emphasizing the involvement of astrocytes in brain immune signaling.

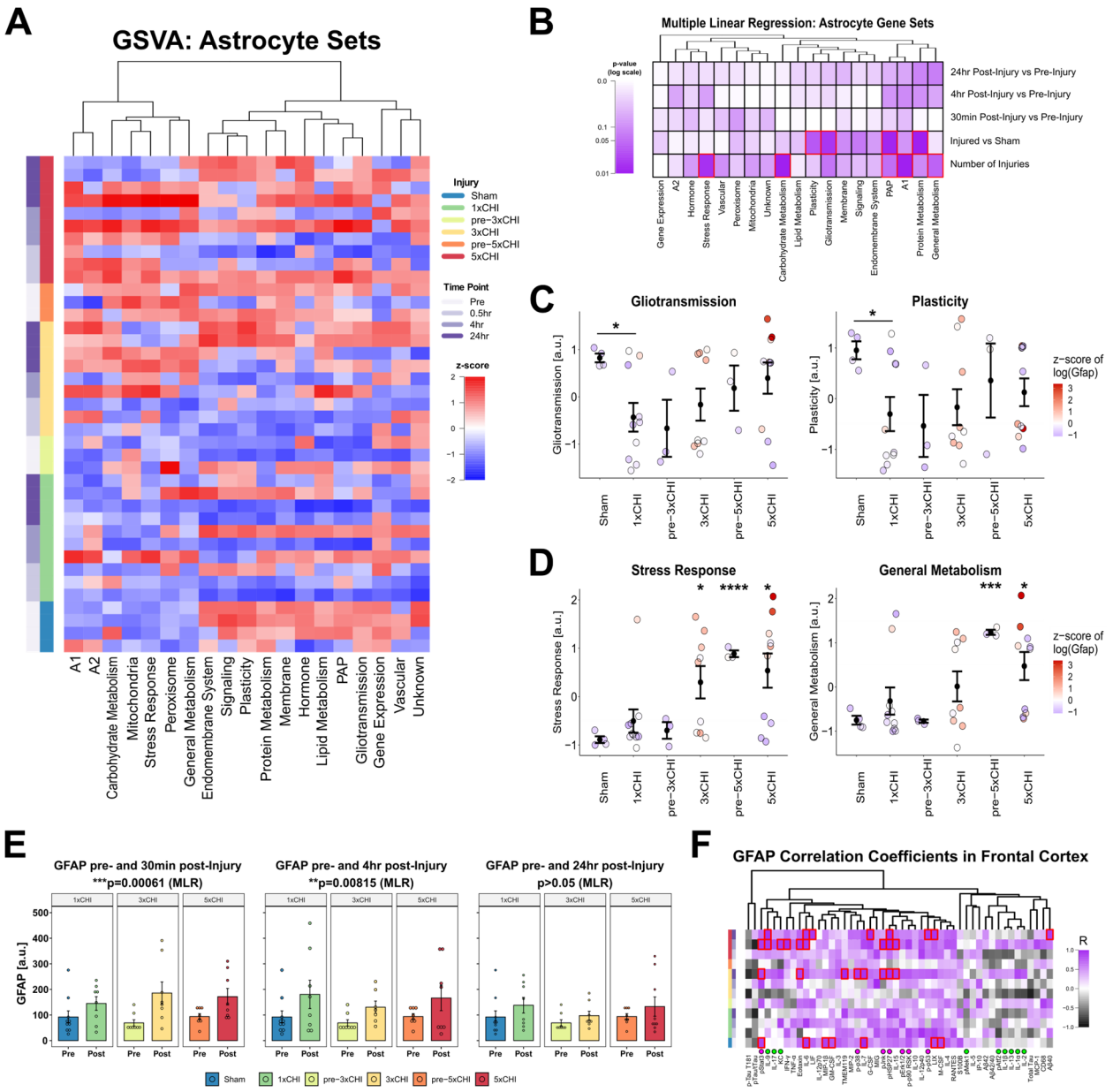


Figure 6. Cortical astrocytes become reactive following mild TBI. A) Gene set variation of custom-curated astrocyte gene sets (columns) across injury and time point groups (rows) reveals two distinct expression patterns: gradual increase by 3-5xCHI (left cluster) and rapid decrease after 1xCHI (right cluster). Gene sets are z-scored and clustered by Euclidean distance. **B**) Multiple linear regression models were calculated for each gene set using fixed effects of time point after most recent injury, binary injury status (injured, sham), and number of injuries. The model shows that the effects of injury (both numeric and binary) outweigh time-dependent changes for most gene sets. Red boxes indicate statistical significance ($p<0.05$). **C**) Astrocyte gene sets Gliotransmission and Plasticity are representative of right cluster, displaying a decrease after 1xCHI followed by return to sham levels by 4-5xCHI (*$p<0.05$, t-test with Bonferroni adjustment) (mean ± SEM). Data points are colored by the z-score of the log of astrocyte reactivity marker gene *Gfap*. **D**) Astrocyte gene sets Stress Response and A1 are representative of left cluster, displaying a gradual increase after 3-5xCHI (*$p<0.05$, ***$p<0.001$, ****$p<0.0001$; t-test with Bonferroni adjustment) (mean ± SEM). Data points are colored by the z-score of the log of astrocyte reactivity marker gene *Gfap*, which is associated with high expression in either set. **E**) Glial fibrillary

acidic protein (GFAP) is significantly upregulated 30min and 4hr post-injury vs pre-injury (***p<0.001, **p<0.01; multiple linear regression model, pre/post and number of injuries) (mean ± SEM). **F**) Heatmap of Pearson's correlation coefficient of cortical GFAP versus each measured cortical protein (columns) within each injury group and time point (rows); red boxes indicate FDR-corrected p<0.05. Panels A-D represent transcriptional data from female somatomotor cortex. Panels E-F represent protein data from female frontal cortex.

DISCUSSION

In this study, we comprehensively profiled immune and pathological responses to rmTBI in the brains of 3xTg-AD mice using a combination of targeted protein panels and RNA sequencing. We hypothesized that repeated mTBI drives progressive changes in immune signaling together with markers of astrocyte reactivity, microglial activation, and changes in tau and Aβ. Because wild type mice do not develop plaques and tangles associated with AD or brain injury-induced pathology, we employed the triple transgenic model of AD (3xTg-AD) in the present study to evaluate relationships between injury, pathological hallmarks, and markers of immune response across multiple acute time points. To our knowledge, this study is the first to define the temporal evolution of immune and pathological responses to rmTBI at both the protein and transcriptional levels in a mouse model capable of displaying both Aβ plaques and neurofibrillary tangles.

While sex differences in pathology and cognitive outcomes after injury in 3xTg mice have been extensively studied (72), few studies have evaluated sex differences in immune signaling. Indeed, to our knowledge all published brain injury studies which make use of the 3xTg-AD model report only male mice or combined-sex experimental groups. Sexual dimorphism of brain immune signaling in both humans and other mouse models is well-documented, generally showing a stronger immune response in females (83). Female 3x-Tg AD mice are reported to have increased Aβ pathology, possibly due to increased β-secretase processing (73,84,85) while male 3xTg AD mice and have been reported to have increased systemic autoimmunity (86), emphasizing the need to evaluate the role of sex. Indeed, we found that 40 out of 46 measured proteins were significantly different between males and females in the frontal cortex, as well as 37 out of 46 in the hippocampus. Further, we determined that total tau, phospho-tau T181, Aβ40, and Aβ42 accounted for only half of the differentially expressed proteins. In particular, pathology-adjusted data left 18 significantly different proteins in the frontal cortex and 20 in the hippocampus. These findings indicate that male and female samples should be analyzed separately. Indeed, dichotomizing our protein data into male and female datasets revealed that females exhibited a much stronger response to injury (**Fig. S4, Fig S5**). For this reason, we focused our analysis on females.

A key finding of our work is that many of the quantified cytokines and phospho-protein signaling molecules co-labeled with NeuN. Neurons are known to express a plethora of cytokine receptors and undergo phospho-protein signaling cascades (i.e., MAPK and NF-κB, among others) in response to inflammation (87–92), but an increasing body of work suggests that neurons also participate in cytokine secretion in both homeostatic and pathological conditions (93–104). Indeed, prior work from our own group has found increased MAPK and NF-κB signaling and expression of cytokines that co-label with neurons following rmTBI in male wild type mice (105). Moreover, multiple studies have reported evidence of co-localization of immune signaling proteins and/or their transcripts with neurons in most of our "Group 1" proteins, which are elevated in the cortex in females following each CHI: IL-1α (93,94), IL-1β (95,96), IL-2 (97,98), IL-9 (99), IL-13 (100–

102), and KC. Importantly, our IHC in the current study revealed prominent neuronal co-localization of four cytokines (IL-1α, IL-1β, IL-13, and KC) and both MAPK phospho-proteins (phospho-Atf2 and phospho-Mek1) within "Group 1," which is consistent with prior literature. Our data together with prior literature therefore support a role for neurons in orchestrating an immune signaling response post-rmTBI.

To our knowledge, our work is the first to conduct transcriptional profiling after successive mTBIs in a transgenic mouse model. We used WGCNA to provide an unbiased summary of gene expression trends in the data, then assessed each identified gene module for enhanced expression of specific biological processes (gene ontology), cell type specific markers, and GWAS-identified markers of AD, as well as correlation with paired protein expression (**Fig. 5**). Indeed, we identified an early inflammatory response associated with AD-GWAS gene expression and protein translation after a single injury, paired with a concomitant decrease in neuronal-enriched functions associated with neuronal development and synaptic signaling. Within days of repeated injury, there was a gradual increase of endothelia-, astrocyte-, and microglia-enriched gene modules associated with wound healing and regulation of inflammation. Interestingly, we also found a significant enrichment of AD-GWAS risk genes within the microglia-enriched gene modules, suggesting microglial involvement in acute pathogenesis after injury. Collectively, these data suggest that even a single mTBI elicits a change in genes associated with lost neuronal homeostasis, whereas repeated daily mTBIs yield changes that propagate into astrocytes, microglia, and endothelial cells.

Interestingly, our protein data showed that the astrocyte reactivity markers GFAP and S100B are transiently elevated at 30min after each repetitive mTBI in the female frontal cortex. Although few studies have characterized such rapid changes in reactivity markers following closed-head injury, elevated GFAP and GFAP breakdown products are detectable in serum less than one hour after mild-to-severe TBI in mice (76–78). This parallels findings in human patients, where serum GFAP levels rapidly increase within an hour then decline within 24-72hr following mild-to-severe injury (78–80,106–108) as well as some mouse studies (109,110), but is in contrast to several other studies in rodents showing sustained GFAP elevation up to two weeks post-injury (111–114). Differences in rodent and injury models, sample type (serum, CSF, tissue lysate), and sex composition of experimental groups may account for some of these conflicting results. On the transcriptional level, we found that astrocyte-specific gene sets for stress response, general metabolism, and immune-related phenotypes A1 and A2 (81) showed gradual increases compared to sham after 3-5xCHI, while homeostatic sets associated with gliotransmission and astrocyte plasticity showed decreased expression compared to sham after just 1xCHI. These findings mirror previous studies which have identified elevated immune response genes in astrocytes 7 days post-severe TBI (115) and the lack of astrocyte-specific inflammatory gene changes 24h after mild TBI (116). Combined, our protein and transcriptional data indicate that astrocytes are responsive to mTBI as early as 30min after injury, while transcriptional changes in stress response pathways persist on the order of days.

The MAPK intracellular signaling pathway is a known mediator of astrocyte reactivity (117–119), including after a traumatic brain injury (35). The clustering of female cortical GFAP and multiple MAPK phospho-proteins suggests that MAPK signaling may be responsible for the phenotypic transition to a reactive state in our model. Further, GFAP also correlates with a host of cytokines such as LIX, IL-7, IL-3, IL-12p40, RANTES, IL-15, M-CSF, G-CSF. These relationships generally exist independently of injury and suggest involvement within reactive astrocyte signaling, which peaks on a time scale of minutes-to-hours after each injury. Further studies should investigate the effect of MAPK signaling in astrocyte response to brain injury.

The current study has several limitations requiring future work. First, while the 3xTg-AD mouse model is becoming relatively popular for brain injury research (42–49), its predisposition towards spontaneous development of pathology due to the expression of three causal neurodegenerative transgenes is not genetically representative of most human TBI patients. The use of human transgenes is necessary due to the lack of pathogenicity of native mouse tau and Aβ, while the use of mutations specifically associated with dementia is justified by the short life span of mice. Here, we mitigated the potential effects of pre-existing pathology on injury outcomes by using mice aged to 2-4 months, well before the reported build-up of Aβ and phosphorylated tau at 6 and 12 months, respectively (120,121). Second, while bulk tissue processing enabled appropriate sample sizes and comparison between 12 injury and time point groups, it also limited our ability to draw conclusions at the level of a single cell. Our bulk analysis highlights injury groups and time points of interest to be interrogated in future work for single cell analysis. Single cell profiling would identify how subtypes of neurons, glia, and other cells respond to successive mTBIs at a higher resolution than can be inferred by network analysis of bulk transcriptomic data. Specifically, single cell analysis may help clarify the extent to which neurons may be involved in immune signaling through cytokine expression and MAPK activation as seen in the injury-driven "Group 1". Third, our findings are purely correlative. While we have established evidence of a relationship between elevated neuroimmune signaling and outcome, future studies are required to establish whether this signaling indeed drives pathogenesis after rmTBI, or is merely correlated.

CONCLUSIONS

In total, our data define an acute neuroimmune cascade of mild traumatic brain injury in 3xTg-AD mice, consisting of i) an immediate decrease in neuronal homeostatic gene expression and an elevation of AD-associated genes after a single injury, ii) elevation of a subset of cortical cytokines that co-label with neurons and correlated with phosphorylated tau, and iii) increased expression of non-neuronal genes suggesting glial reactivity within days of repeated injury. We provide resolution of these acute protein and transcriptional changes at a previously uncharacterized minutes-to-days time scale alongside the key experimental variables of sex, brain region, and number of injuries. Pronounced changes in neuronal gene expression that correlate with inflammatory protein expression and co-labeling of injury-elevated cytokines and MAPK phospho-proteins with neuronal marker NeuN suggest a key role for neurons in the modulation of neuroimmune activity following brain injury. Further, the association of phospho-Mek1 and phospho-Atf2, cytokines, and phospho-tau T181 after injury may represent a therapeutic avenue for regulating inflammation and acute pathological mechanisms. Future work should explore the causal functions of these key molecular signals.

DATA AVAILABILITY

The gene expression FASTQ files and count matrix that support the findings of this study have been deposited in the Gene Expression Omnibus (GEO) repository under series record GSE226838. Protein expression data and mouse metadata has been deposited in the Open Data Commons for Traumatic Brain Injury repository.

ABBREVIATIONS

3xTg-AD: Triple transgenic Alzheimer's disease mouse model

Aβ: Amyloid beta

ACURO: Animal Care and Use Review Office (U.S. Army MRDC)
AD: Alzheimer's disease
APP: Amyloid precursor protein
ARRIVE: Animal Research: Reporting of *In Vivo* Experiments
ATP: Adenosine triphosphate
BSA: Bovine serum albuminCD68: Cluster of differentiation 68
CHI: Closed-head injury
CRAN: Comprehensive R Archive Network
DAPI: 4′,6-diamidino-2-phenylindole
ELISA: Enzyme-linked immunosorbent assay
FDR: False discovery rate
G-CSF: Granulocyte colony-stimulating factor
GEO: Gene expression omnibus
GFAP: Glial fibrillary acidic protein
GM-CSF: Granulocyte macrophage colony-stimulating factor
GSVA: Gene set variation analysis
GWAS: Genome-wide association study
IACUC: Institutional Animal Care and Use Committee
Iba1: Ionized calcium binding adaptor molecule 1
IFN-γ: Interferon gamma
IHC: Immunohistochemistry
IL: Interleukin
IP-10: Interferon gamma-induced protein 10
KC: Keratinocyte chemoattractant
LIF: Leukemia inhibitory factor
LIX: Lipopolysaccharide-induced CXC chemokine
MAGMA: Multi-marker Analysis of GenoMic Annotation
MAPK: Mitogen-activated protein kinase
MAPT: Microtubule-associated protein tau
MCP-1: Monocyte chemoattractant protein 1
M-CSF: Macrophage colony-stimulating factor
MIG: Monokine induced by interferon gamma
MIP: Macrophage inflammatory protein
MRDC: Medical Research and Development Command (U.S. Army)
NCBI: National Center for Biotechnology Information
mTBI: Mild traumatic brain injury

PAP: Perisynaptic astrocyte processes
PCA: Principal component analysis
PD: Parkinson's disease
PSEN1: Presenilin 1
pTau: Phospho-tau
RANTES: Regulated upon activation, normal T cell expressed and presumably secreted
rmTBI: Repetitive traumatic brain injury
RNA: Ribonucleic acid
S100B: S100 calcium binding protein B
TBI: Traumatic brain injury
TBST: Tris-buffered saline with tween
TMEM119: Transmembrane protein 119
TNF-α: Tumor necrosis factor α
tTau: Total tau
WGCNA: Weighted gene co-expression network analysis

REFERENCES

1. US Department of Health & Human Services; Centers for Disease Control (CDC); National Center for Injury Prevention and Control. Report to Congress on Mild Traumatic Brain Injury in the United States: Steps to Prevent a Serious Public Health Problem: (371602004-001) [Internet]. American Psychological Association; 2003 [cited 2021 Jan 9]. Available from: http://doi.apa.org/get-pe-doi.cfm?doi=10.1037/e371602004-001

2. Surveillance Report of Traumatic Brain Injury-related Emergency Department Visits, Hospitalizations, and Deaths. :24.

3. Iraji A, Benson RR, Welch RD, O'Neil BJ, Woodard JL, Ayaz SI, et al. Resting State Functional Connectivity in Mild Traumatic Brain Injury at the Acute Stage: Independent Component and Seed-Based Analyses. J Neurotrauma. 2015 07-15;32(14):1031–45.

4. McCrory P, Meeuwisse W, Aubry M, Cantu B, Dvorak J, Echemendia RJ, et al. Consensus statement on concussion in sport–the 4th International Conference on Concussion in Sport held in Zurich, November 2012. Clin J Sport Med. 2013 03;23(2):89–117.

5. Belanger HG, Vanderploeg RD, Curtiss G, Warden DL. Recent neuroimaging techniques in mild traumatic brain injury. J Neuropsychiatry Clin Neurosci. 2007;19(1):5–20.

6. Sours C, Zhuo J, Roys S, Shanmuganathan K, Gullapalli RP. Disruptions in Resting State Functional Connectivity and Cerebral Blood Flow in Mild Traumatic Brain Injury Patients. PLoS ONE. 2015;10(8):e0134019.

7. Guskiewicz KM, McCrea M, Marshall SW, Cantu RC, Randolph C, Barr W, et al. Cumulative effects associated with recurrent concussion in collegiate football players: the NCAA Concussion Study. Jama. 2003 11-19;290(19):2549–55.

8. Longhi L, Saatman KE, Fujimoto S, Raghupathi R, Meaney DF, Davis J, et al. Temporal window of vulnerability to repetitive experimental concussive brain injury. Neurosurgery. 2005 Feb;56(2):364–74; discussion 364-374.

9. Mez J, Daneshvar DH, Kiernan PT, Abdolmohammadi B, Alvarez VE, Huber BR, et al. Clinicopathological Evaluation of Chronic Traumatic Encephalopathy in Players of American Football. JAMA. 2017 Jul 25;318(4):360–70.

10. Fleminger S, Oliver DL, Lovestone S, Rabe-Hesketh S, Giora A. Head injury as a risk factor for Alzheimer's disease: the evidence 10 years on; a partial replication. J Neurol Neurosurg Psychiatry. 2003 Jul;74(7):857–62.

11. Krueger F, Pardini M, Huey ED, Raymont V, Solomon J, Lipsky RH, et al. The role of the Met66 brain-derived neurotrophic factor allele in the recovery of executive functioning after combat-related traumatic brain injury. J Neurosci Off J Soc Neurosci. 2011 Jan 12;31(2):598–606.

12. Heneka MT, Carson MJ, El Khoury J, Landreth GE, Brosseron F, Feinstein DL, et al. Neuroinflammation in Alzheimer's Disease. Lancet Neurol. 2015 Apr;14(4):388–405.

13. Bower JH, Maraganore DM, Peterson BJ, McDonnell SK, Ahlskog JE, Rocca WA. Head trauma preceding PD: a case-control study. Neurology. 2003 May 27;60(10):1610–5.

14. Uryu K, Giasson BI, Longhi L, Martinez D, Murray I, Conte V, et al. Age-dependent synuclein pathology following traumatic brain injury in mice. Exp Neurol. 2003 Nov;184(1):214–24.

15. Tansey MG, Goldberg MS. Neuroinflammation in Parkinson's disease: its role in neuronal death and implications for therapeutic intervention. Neurobiol Dis. 2010 Mar;37(3):510–8.

16. Simon DW, McGeachy MJ, Bayır H, Clark RSB, Loane DJ, Kochanek PM. The far-reaching scope of neuroinflammation after traumatic brain injury. Nat Rev Neurol. 2017 Mar;13(3):171–91.

17. Schimmel SJ, Acosta S, Lozano D. Neuroinflammation in traumatic brain injury: A chronic response to an acute injury. Brain Circ. 2017;3(3):135–42.

18. Morganti-Kossmann MC, Satgunaseelan L, Bye N, Kossmann T. Modulation of immune response by head injury. Injury. 2007 Dec;38(12):1392–400.

19. Loane DJ, Kumar A, Stoica BA, Cabatbat R, Faden AI. Progressive neurodegeneration after experimental brain trauma: association with chronic microglial activation. J Neuropathol Exp Neurol. 2014 Jan;73(1):14–29.

20. Bermpohl D, You Z, Lo EH, Kim HH, Whalen MJ. TNF alpha and Fas mediate tissue damage and functional outcome after traumatic brain injury in mice. J Cereb Blood Flow Metab Off J Int Soc Cereb Blood Flow Metab. 2007 11;27(11):1806–18.

21. Ebert SE, Jensen P, Ozenne B, Armand S, Svarer C, Stenbaek DS, et al. Molecular imaging of neuroinflammation in patients after mild traumatic brain injury: a longitudinal 123I-CLINDE single photon emission computed tomography study. Eur J Neurol. 2019;26(12):1426–32.

22. Perez-Polo JR, Rea HC, Johnson KM, Parsley MA, Unabia GC, Xu G, et al. Inflammatory consequences in a rodent model of mild traumatic brain injury. J Neurotrauma. 2013 May 1;30(9):727–40.

23. Mountney A, Boutté AM, Cartagena CM, Flerlage WF, Johnson WD, Rho C, et al. Functional and Molecular Correlates after Single and Repeated Rat Closed-Head Concussion: Indices of Vulnerability after Brain Injury. J Neurotrauma. 2017 Oct 1;34(19):2768–89.

24. Vállez García D, Otte A, Dierckx RAJO, Doorduin J. Three Month Follow-Up of Rat Mild Traumatic Brain Injury: A Combined [18F]FDG and [11C]PK11195 Positron Emission Study. J Neurotrauma. 2016 Oct 15;33(20):1855–65.

25. Rathbone ATL, Tharmaradinam S, Jiang S, Rathbone MP, Kumbhare DA. A review of the neuro- and systemic inflammatory responses in post concussion symptoms: Introduction of the "post-inflammatory brain syndrome" PIBS. Brain Behav Immun. 2015 May;46:1–16.

26. Giza CC, Hovda DA. The Neurometabolic Cascade of Concussion. J Athl Train. 2001 Sep;36(3):228–35.

27. Giza CC, Hovda DA. The New Neurometabolic Cascade of Concussion. Neurosurgery. 2014 Oct;75(0 4):S24–33.

28. Burda JE, Bernstein AM, Sofroniew MV. Astrocyte roles in traumatic brain injury. Exp Neurol. 2016 Jan;275(0 3):305–15.

29. Loane DJ, Kumar A. Microglia in the TBI Brain: The Good, The Bad, And The Dysregulated. Exp Neurol. 2016 01;275(0 3):316–27.

30. Witcher KG, Bray CE, Chunchai T, Zhao F, O'Neil SM, Gordillo AJ, et al. Traumatic Brain Injury Causes Chronic Cortical Inflammation and Neuronal Dysfunction Mediated by Microglia. J Neurosci. 2021 Feb 17;41(7):1597–616.

31. Kumar A, Loane DJ. Neuroinflammation after traumatic brain injury: Opportunities for therapeutic intervention. Brain Behav Immun. 2012 Nov 1;26(8):1191–201.

32. Ahmed SM, Rzigalinski BA, Willoughby KA, Sitterding HA, Ellis EF. Stretch-induced injury alters mitochondrial membrane potential and cellular ATP in cultured astrocytes and neurons. J Neurochem. 2000 May;74(5):1951–60.

33. Verderio C, Matteoli M. ATP mediates calcium signaling between astrocytes and microglial cells: modulation by IFN-gamma. J Immunol Baltim Md 1950. 2001 May 15;166(10):6383–91.

34. Neary JT, Kang Y, Willoughby KA, Ellis EF. Activation of Extracellular Signal-Regulated Kinase by Stretch-Induced Injury in Astrocytes Involves Extracellular ATP and P2 Purinergic Receptors. J Neurosci. 2003 Mar 15;23(6):2348–56.

35. Huang T, Solano J, He D, Loutfi M, Dietrich WD, Kuluz JW. Traumatic Injury Activates MAP Kinases in Astrocytes: Mechanisms of Hypothermia and Hyperthermia. J Neurotrauma. 2009 Sep;26(9):1535–45.

36. Neary JT, Kang Y, Tran M, Feld J. Traumatic injury activates protein kinase B/Akt in cultured astrocytes: role of extracellular ATP and P2 purinergic receptors. J Neurotrauma. 2005 Apr;22(4):491–500.

37. Floyd CL, Gorin FA, Lyeth BG. Mechanical strain injury increases intracellular sodium and reverses Na+/Ca2+ exchange in cortical astrocytes. Glia. 2005 Jul;51(1):35–46.

38. Bowman CL, Ding JP, Sachs F, Sokabe M. Mechanotransducing ion channels in astrocytes. Brain Res. 1992 Jul 3;584(1–2):272–86.

39. Ojo JO, Mouzon BC, Crawford F. Repetitive head trauma, chronic traumatic encephalopathy and tau: Challenges in translating from mice to men. Exp Neurol. 2016 Jan 1;275:389–404.

40. Bolton-Hall AN, Hubbard WB, Saatman KE. Experimental Designs for Repeated Mild Traumatic Brain Injury: Challenges and Considerations. J Neurotrauma. 2019 Apr 15;36(8):1203–21.

41. McAteer KM, Turner RJ, Corrigan F. Animal models of chronic traumatic encephalopathy. Concussion [Internet]. 2017 May 19 [cited 2021 Jan 12];2(2). Available from: https://www.ncbi.nlm.nih.gov/pmc/articles/PMC6093772/

42. Washington PM, Morffy N, Parsadanian M, Zapple DN, Burns MP. Experimental traumatic brain injury induces rapid aggregation and oligomerization of amyloid-beta in an Alzheimer's disease mouse model. J Neurotrauma. 2014 Jan 1;31(1):125–34.

43. Tran HT, LaFerla FM, Holtzman DM, Brody DL. Controlled Cortical Impact Traumatic Brain Injury in 3xTg-AD Mice Causes Acute Intra-Axonal Amyloid-β Accumulation and Independently Accelerates the Development of Tau Abnormalities. J Neurosci. 2011 Jun 29;31(26):9513–25.

44. Winston CN, Noël A, Neustadtl A, Parsadanian M, Barton DJ, Chellappa D, et al. Dendritic Spine Loss and Chronic White Matter Inflammation in a Mouse Model of Highly Repetitive Head Trauma. Am J Pathol. 2016 Mar 1;186(3):552–67.

45. Tran HT, Sanchez L, Esparza TJ, Brody DL. Distinct Temporal and Anatomical Distributions of Amyloid-β and Tau Abnormalities following Controlled Cortical Impact in Transgenic Mice. PLOS ONE. 2011 Sep 29;6(9):e25475.

46. Saber M, Murphy SM, Cho Y, Lifshitz J, Rowe RK. Experimental diffuse brain injury and a model of Alzheimer's disease exhibit disease-specific changes in sleep and incongruous peripheral inflammation. J Neurosci Res. 2021;99(4):1136–60.

47. Wu Z, Wang ZH, Liu X, Zhang Z, Gu X, Yu SP, et al. Traumatic brain injury triggers APP and Tau cleavage by delta-secretase, mediating Alzheimer's disease pathology. Prog Neurobiol. 2020;185.

48. Bennett RE, Esparza TJ, Lewis HA, Kim E, Mac Donald CL, Sullivan PM, et al. Human apolipoprotein E4 worsens acute axonal pathology but not amyloid-β immunoreactivity after traumatic brain injury in 3xTG-AD mice. J Neuropathol Exp Neurol. 2013;72(5):396–403.

49. Hu W, Tung YC, Zhang Y, Liu F, Iqbal K. Involvement of activation of asparaginyl endopeptidase in tau hyperphosphorylation in repetitive mild traumatic brain injury. J Alzheimers Dis. 2018;64(3):709–22.

50. Meehan WP 3rd, Zhang J, Mannix R, Whalen MJ. Increasing recovery time between injuries improves cognitive outcome after repetitive mild concussive brain injuries in mice. Neurosurgery. 2012 Oct;71(4):885–91.

51. Brothers RO, Bitarafan S, Pybus AF, Wood LB, Buckley EM. Systems Analysis of the Neuroinflammatory and Hemodynamic Response to Traumatic Brain Injury. J Vis Exp JoVE. 2022 May 27;(183).

52. Wickham H, Averick M, Bryan J, Chang W, McGowan LD, François R, et al. Welcome to the Tidyverse. J Open Source Softw. 2019 Nov 21;4(43):1686.

53. Zhao S, Guo Y, Sheng Q, Shyr Y. Advanced heat map and clustering analysis using heatmap3. BioMed Res Int. 2014;2014:986048.

54. Wickham H, Chang W, Henry L, Pedersen TL, Takahashi K, Wilke C, et al. ggplot2: Create Elegant Data Visualisations Using the Grammar of Graphics [Internet]. 2022 [cited 2022 Oct 7]. Available from: https://CRAN.R-project.org/package=ggplot2

55. Kassambara A. ggpubr: "ggplot2" Based Publication Ready Plots [Internet]. 2020 [cited 2022 Oct 7]. Available from: https://CRAN.R-project.org/package=ggpubr

56. Hänzelmann S, Castelo R, Guinney J. GSVA: gene set variation analysis for microarray and RNA-seq data. BMC Bioinformatics. 2013 Jan 16;14:7.

57. Coombes KR. Object Oriented Microarray and Proteomics Analysis (OOMPA). :6.

58. Love MI, Huber W, Anders S. Moderated estimation of fold change and dispersion for RNA-seq data with DESeq2. Genome Biol. 2014 Dec 5;15(12):550.

59. Langfelder P, Horvath S. WGCNA: an R package for weighted correlation network analysis. BMC Bioinformatics. 2008 Dec;9(1):1–13.

60. Johnson ECB, Carter EK, Dammer EB, Duong DM, Gerasimov ES, Liu Y, et al. Large-scale deep multi-layer analysis of Alzheimer's disease brain reveals strong proteomic disease-related changes not observed at the RNA level. Nat Neurosci. 2022 Feb;25(2):213–25.

61. Johnson ECB, Dammer EB, Duong DM, Ping L, Zhou M, Yin L, et al. Large-scale proteomic analysis of Alzheimer's disease brain and cerebrospinal fluid reveals early changes in energy metabolism associated with microglia and astrocyte activation. Nat Med. 2020 May;26(5):769–80.

62. Seyfried NT, Dammer EB, Swarup V, Nandakumar D, Duong DM, Yin L, et al. A Multi-network Approach Identifies Protein-Specific Co-expression in Asymptomatic and Symptomatic Alzheimer's Disease. Cell Syst. 2017 Jan 25;4(1):60-72.e4.

63. Sharma K, Schmitt S, Bergner CG, Tyanova S, Kannaiyan N, Manrique-Hoyos N, et al. Cell type- and brain region-resolved mouse brain proteome. Nat Neurosci. 2015 Dec;18(12):1819–31.

64. Zhang Y, Chen K, Sloan SA, Bennett ML, Scholze AR, O'Keeffe S, et al. An RNA-Sequencing Transcriptome and Splicing Database of Glia, Neurons, and Vascular Cells of the Cerebral Cortex. J Neurosci. 2014 09-03;34(36):11929–47.

65. Leeuw CA de, Mooij JM, Heskes T, Posthuma D. MAGMA: Generalized Gene-Set Analysis of GWAS Data. PLOS Comput Biol. 2015 Apr 17;11(4):e1004219.

66. Kunkle BW, Grenier-Boley B, Sims R, Bis JC, Damotte V, Naj AC, et al. Genetic meta-analysis of diagnosed Alzheimer's disease identifies new risk loci and implicates Aβ, tau, immunity and lipid processing. Nat Genet. 2019 Mar;51(3):414–30.

67. Lambert JC, Ibrahim-Verbaas CA, Harold D, Naj AC, Sims R, Bellenguez C, et al. Meta-analysis of 74,046 individuals identifies 11 new susceptibility loci for Alzheimer's disease. Nat Genet. 2013 Dec;45(12):1452–8.

68. Bellenguez C, Küçükali F, Jansen IE, Kleineidam L, Moreno-Grau S, Amin N, et al. New insights into the genetic etiology of Alzheimer's disease and related dementias. Nat Genet. 2022 Apr;54(4):412–36.

69. Subramanian A, Tamayo P, Mootha VK, Mukherjee S, Ebert BL, Gillette MA, et al. Gene set enrichment analysis: a knowledge-based approach for interpreting genome-wide expression profiles. Proc Natl Acad Sci U S A. 2005 10-25;102(43):15545–50.

70. Liberzon A, Subramanian A, Pinchback R, Thorvaldsdóttir H, Tamayo P, Mesirov JP. Molecular signatures database (MSigDB) 3.0. Bioinformatics. 2011 Jun 15;27(12):1739–40.

71. Galea E, Weinstock LD, Larramona-Arcas R, Pybus AF, Giménez-Llort L, Escartin C, et al. Multi-transcriptomic analysis points to early organelle dysfunction in human astrocytes in Alzheimer's disease. Neurobiol Dis. 2022 May;166:105655.

72. Dennison JL, Ricciardi NR, Lohse I, Volmar CH, Wahlestedt C. Sexual Dimorphism in the 3xTg-AD Mouse Model and Its Impact on Pre-Clinical Research. J Alzheimers Dis. 2021 Jan 1;80(1):41–52.

73. Hirata-Fukae C, Li HF, Hoe HS, Gray AJ, Minami SS, Hamada K, et al. Females exhibit more extensive amyloid, but not tau, pathology in an Alzheimer transgenic model. Brain Res. 2008 Jun 24;1216:92–103.

74. Goetzl EJ, Elahi FM, Mustapic M, Kapogiannis D, Pryhoda M, Gilmore A, et al. Altered levels of plasma neuron-derived exosomes and their cargo proteins characterize acute and chronic mild traumatic brain injury. FASEB J. 2019;33(4):5082–8.

75. Witcher KG, Eiferman DS, Godbout JP. Priming the Inflammatory Pump of the CNS after Traumatic Brain Injury. Trends Neurosci. 2015 Oct;38(10):609–20.

76. Papa L, Silvestri S, Brophy GM, Giordano P, Falk JL, Braga CF, et al. GFAP Out-Performs S100β in Detecting Traumatic Intracranial Lesions on Computed Tomography in Trauma Patients with Mild Traumatic Brain Injury and Those with Extracranial Lesions. J Neurotrauma. 2014 Nov 15;31(22):1815–22.

77. Papa L, Lewis LM, Falk JL, Zhang Z, Silvestri S, Giordano P, et al. Elevated levels of serum glial fibrillary acidic protein breakdown products in mild and moderate traumatic brain injury are associated with intracranial lesions and neurosurgical intervention. Ann Emerg Med. 2012 Jun;59(6):471–83.

78. Papa L, Brophy GM, Welch RD, Lewis LM, Braga CF, Tan CN, et al. Time Course and Diagnostic Accuracy of Glial and Neuronal Blood Biomarkers GFAP and UCH-L1 in a Large Cohort of Trauma Patients With and Without Mild Traumatic Brain Injury. JAMA Neurol. 2016 May 1;73(5):551–60.

79. Papa L, Zonfrillo MR, Welch RD, Lewis LM, Braga CF, Tan CN, et al. Evaluating glial and neuronal blood biomarkers GFAP and UCH-L1 as gradients of brain injury in concussive, subconcussive and non-concussive trauma: a prospective cohort study. BMJ Paediatr Open. 2019 Aug 1;3(1):e000473.

80. Žurek J, Fedora M. The usefulness of S100B, NSE, GFAP, NF-H, secretagogin and Hsp70 as a predictive biomarker of outcome in children with traumatic brain injury. Acta Neurochir (Wien). 2012 Jan 1;154(1):93–103.

81. Liddelow SA, Guttenplan KA, Clarke LE, Bennett FC, Bohlen CJ, Schirmer L, et al. Neurotoxic reactive astrocytes are induced by activated microglia. Nature. 2017 Jan;541(7638):481–7.

82. Xiong XY, Tang Y, Yang QW. Metabolic changes favor the activity and heterogeneity of reactive astrocytes. Trends Endocrinol Metab. 2022 Jun 1;33(6):390–400.

83. Gupte R, Brooks W, Vukas R, Pierce J, Harris J. Sex Differences in Traumatic Brain Injury: What We Know and What We Should Know. J Neurotrauma. 2019 Nov 15;36(22):3063–91.

84. Schäfer S, Wirths O, Multhaup G, Bayer TA. Gender dependent APP processing in a transgenic mouse model of Alzheimer's disease. J Neural Transm. 2007 Mar 1;114(3):387–94.

85. Jankowsky JL, Zheng H. Practical considerations for choosing a mouse model of Alzheimer's disease. Mol Neurodegener. 2017 Dec 22;12(1):89.

86. Kapadia M, Mian MF, Michalski B, Azam AB, Ma D, Salwierz P, et al. Sex-Dependent Differences in Spontaneous Autoimmunity in Adult 3xTg-AD Mice. J Alzheimers Dis JAD. 2018;63(3):1191–205.

87. Prieto GA, Cotman CW. Cytokines and cytokine networks target neurons to modulate long-term potentiation. Cytokine Growth Factor Rev. 2017 Apr;34:27–33.

88. Talbot S, Foster SL, Woolf CJ. Neuroimmunity: Physiology and Pathology. Annu Rev Immunol. 2016;34(1):421–47.

89. Fukunaga K, Miyamoto E. Role of MAP kinase in neurons. Mol Neurobiol. 1998 Feb;16(1):79–95.

90. Asih PR, Prikas E, Stefanoska K, Tan ARP, Ahel HI, Ittner A. Functions of p38 MAP Kinases in the Central Nervous System. Front Mol Neurosci [Internet]. 2020 [cited 2023 May 3];13. Available from: https://www.frontiersin.org/articles/10.3389/fnmol.2020.570586

91. Schnöder L, Hao W, Qin Y, Liu S, Tomic I, Liu X, et al. Deficiency of Neuronal p38α MAPK Attenuates Amyloid Pathology in Alzheimer Disease Mouse and Cell Models through Facilitating Lysosomal Degradation of BACE1. J Biol Chem. 2016 Jan 29;291(5):2067–79.

92. Shih RH, Wang CY, Yang CM. NF-kappaB Signaling Pathways in Neurological Inflammation: A Mini Review. Front Mol Neurosci. 2015 Dec 18;8:77.

93. Di Cesare Mannelli L, Micheli L, Cervetto C, Toti A, Lucarini E, Parisio C, et al. Neuronal alarmin IL-1α evokes astrocyte-mediated protective signals: Effectiveness in chemotherapy-induced neuropathic pain. Neurobiol Dis. 2022 Jun 15;168:105716.

94. Michael BD, Bricio-Moreno L, Sorensen EW, Miyabe Y, Lian J, Solomon T, et al. Astrocyte- and Neuron-Derived CXCL1 Drives Neutrophil Transmigration and Blood-Brain Barrier Permeability in Viral Encephalitis. Cell Rep. 2020 Sep 15;32(11):108150.

95. Hallett H, Churchill L, Taishi P, De A, Krueger JM. Whisker stimulation increases expression of nerve growth factor- and interleukin-1beta-immunoreactivity in the rat somatosensory cortex. Brain Res. 2010 May 28;1333:48–56.

96. Ravizza T, Boer K, Redeker S, Spliet WGM, van Rijen PC, Troost D, et al. The IL-1β system in epilepsy-associated malformations of cortical development. Neurobiol Dis. 2006 Oct 1;24(1):128–43.

97. Meola D, Huang Z, Petitto JM. Selective Neuronal and Brain Regional Expession of IL-2 in IL2P 8-GFP Transgenic Mice: Relation to Sensorimotor Gating. J Alzheimers Dis Park. 2013 Oct 28;3(4):1000127.

98. Guo W, Zheng DH, Sun FJ, Yang JY, Zang ZL, Liu SY, et al. Expression and Cellular Distribution of the Interleukin 2 Signaling System in Cortical Lesions From Patients With Focal Cortical Dysplasia. J Neuropathol Exp Neurol. 2014 Mar 1;73(3):206–22.

99. Fontaine RH, Cases O, Lelièvre V, Mesplès B, Renauld JC, Loron G, et al. IL-9/IL-9 receptor signaling selectively protects cortical neurons against developmental apoptosis. Cell Death Differ. 2008 Oct;15(10):1542–52.

100. olde Heuvel F, Holl S, Chandrasekar A, Li Z, Wang Y, Rehman R, et al. STAT6 mediates the effect of ethanol on neuroinflammatory response in TBI. Brain Behav Immun. 2019 Oct 1;81:228–46.

101. Li S, olde Heuvel F, Rehman R, Aousji O, Froehlich A, Li Z, et al. Interleukin-13 and its receptor are synaptic proteins involved in plasticity and neuroprotection. Nat Commun. 2023 Jan 13;14(1):200.

102. Mori S, Sugama S, Nguyen W, Michel T, Sanna MG, Sanchez-Alavez M, et al. Lack of interleukin-13 receptor α1 delays the loss of dopaminergic neurons during chronic stress. J Neuroinflammation. 2017 Apr 21;14(1):88.

103. Xia M, Hyman BT. GROα/KC, a chemokine receptor CXCR2 ligand, can be a potent trigger for neuronal ERK1/2 and PI-3 kinase pathways and for tau hyperphosphorylation—a role in Alzheimer's disease? J Neuroimmunol. 2002 Jan 1;122(1):55–64.

104. Carroll SL, Frohnert PW. Expression of JE (Monocyte Chemoattractant Protein-1) Is Induced by Sciatic Axotomy in Wild Type Rodents but Not in C57BL/Wlds Mice. J Neuropathol Exp Neurol. 1998 Oct 1;57(10):915–30.

105. Sankar SB, Pybus AF, Liew A, Sanders B, Shah KJ, Wood LB, et al. Low cerebral blood flow is a non-invasive biomarker of neuroinflammation after repetitive mild traumatic brain injury. Neurobiol Dis. 2019;124:544–54.

106. Lei J, Gao G, Feng J, Jin Y, Wang C, Mao Q, et al. Glial fibrillary acidic protein as a biomarker in severe traumatic brain injury patients: a prospective cohort study. Crit Care. 2015 Dec 1;19(1):362.

107. Thelin E, Al Nimer F, Frostell A, Zetterberg H, Blennow K, Nyström H, et al. A Serum Protein Biomarker Panel Improves Outcome Prediction in Human Traumatic Brain Injury. J Neurotrauma. 2019 Oct 15;36(20):2850–62.

108. McCrea M, Broglio SP, McAllister TW, Gill J, Giza CC, Huber DL, et al. Association of Blood Biomarkers With Acute Sport-Related Concussion in Collegiate Athletes: Findings From the NCAA and Department of Defense CARE Consortium. JAMA Netw Open. 2020 Jan 3;3(1):e1919771.

109. Xu X, Cowan M, Beraldo F, Schranz A, McCunn P, Geremia N, et al. Repetitive mild traumatic brain injury in mice triggers a slowly developing cascade of long-term and persistent behavioral deficits and pathological changes. Acta Neuropathol Commun. 2021 Apr 6;9(1):60.

110. Button EB, Cheng WH, Barron C, Cheung H, Bashir A, Cooper J, et al. Development of a novel, sensitive translational immunoassay to detect plasma glial fibrillary acidic protein (GFAP) after murine traumatic brain injury. Alzheimers Res Ther. 2021 Mar 7;13(1):58.

111. Shandra O, Winemiller AR, Heithoff BP, Munoz-Ballester C, George KK, Benko MJ, et al. Repetitive Diffuse Mild Traumatic Brain Injury Causes an Atypical Astrocyte Response and Spontaneous Recurrent Seizures. J Neurosci Off J Soc Neurosci. 2019 Mar 6;39(10):1944–63.

112. Singh K, Trivedi R, Devi MM, Tripathi RP, Khushu S. Longitudinal changes in the DTI measures, anti-GFAP expression and levels of serum inflammatory cytokines following mild traumatic brain injury. Exp Neurol. 2016 Jan 1;275:427–35.

113. Michinaga S, Koyama Y. Pathophysiological Responses and Roles of Astrocytes in Traumatic Brain Injury. Int J Mol Sci. 2021 Jun 15;22(12):6418.

114. Villapol S, Byrnes KR, Symes AJ. Temporal dynamics of cerebral blood flow, cortical damage, apoptosis, astrocyte-vasculature interaction and astrogliosis in the pericontusional region after traumatic brain injury. Front Neurol. 2014;5:82.

115. Todd BP, Chimenti MS, Luo Z, Ferguson PJ, Bassuk AG, Newell EA. Traumatic brain injury results in unique microglial and astrocyte transcriptomes enriched for type I interferon response. J Neuroinflammation. 2021 Jul 5;18:151.

116. Arneson D, Zhang G, Ying Z, Zhuang Y, Byun HR, Ahn IS, et al. Single cell molecular alterations reveal target cells and pathways of concussive brain injury. Nat Commun. 2018 Sep 25;9(1):3894.

117. Choudhury GR, Ryou MG, Poteet E, Wen Y, He R, Sun F, et al. INVOLVEMENT OF P38 MAPK IN REACTIVE ASTROGLIOSIS INDUCED BY ISCHEMIC STROKE. Brain Res. 2014 Mar 3;1551:45.

118. Mandell JW, VandenBerg SR. ERK/MAP kinase is chronically activated in human reactive astrocytes. Neuroreport. 1999 Nov 26;10(17):3567–72.

119. Kaminska B, Gozdz A, Zawadzka M, Ellert-Miklaszewska A, Lipko M. MAPK Signal Transduction Underlying Brain Inflammation and Gliosis as Therapeutic Target. Anat Rec. 2009;292(12):1902–13.

120. Oddo S, Caccamo A, Shepherd JD, Murphy MP, Golde TE, Kayed R, et al. Triple-transgenic model of Alzheimer's disease with plaques and tangles: intracellular Abeta and synaptic dysfunction. Neuron. 2003 Jul 31;39(3):409–21.

121. Billings LM, Oddo S, Green KN, McGaugh JL, LaFerla FM. Intraneuronal Abeta causes the onset of early Alzheimer's disease-related cognitive deficits in transgenic mice. Neuron. 2005 Mar 3;45(5):675–88.

ACKNOWLEDGEMENTS

We wish to acknowledge fruitful discussions with Michelle LaPlaca, and Manu Platt. We also thank the core facilities at the Parker H. Petit Institute for Bioengineering and Bioscience at the Georgia Institute of Technology for use of their shared equipment, services, and expertise.

FUNDING

This work was supported by the U.S. Department of Defense through the Congressionally Directed Medical Research Programs (CDMRP) under Award No. W81XWH-18-1-0669 (LBW/EMB). Opinions, interpretations, conclusions, and recommendations are those of the author and are not necessarily endorsed by the Department of Defense. It was also supported by the National Institutes of Health under Award Nos. 1R01NS115994 (LBW/EB), 1R01AG075820 (SR/LBW), 1R01NS114130 (SR), 1RF1AG071587 (SR). AFP was supported in part by the National Institutes of Health Cell and Tissue Engineering Biotechnology Training Grant (T32-GM008433).

AUTHOR INFORMATION

Contributions

AFP conducted data analysis, prepared all figures, and wrote the manuscript. ROB and AR conducted animal experiments, curated animal data, and conducted cerebral blood flow measurements. AFP, SB, AK, FRM, KU, and BD conducted molecular assays and experimentation. ED and SR contributed to informatic analysis. LBW and EMB conceived the study, supervised research, and revised the manuscript. All authors reviewed the manuscript.

Corresponding Authors

Correspondence to Levi B. Wood and Erin M. Buckley.

ETHICS DECLARATIONS

Ethics approval and consent to participate

All protocols were approved by the U.S. Army Medical Research and Development Command (MRDC) Animal Care and Use Review Office (ACURO) and the Emory University Institutional Animal Care and Use Committee (IACUC) in accordance with National Institutes of Health guidelines.

Consent for publication

Not applicable.

Competing interests

The authors have no conflicts of interest to disclose.

SUPPLEMENTARY INFORMATION

Additional file 1.

Supplementary Figures.

Profiling the neuroimmune cascade in 3xTg mice exposed to successive mild traumatic brain injuries

Alyssa F. Pybus[1], Sara Bitarafan[2], Rowan O. Brothers[1], Alivia Rohrer[1], Arushi Khaitan[1], Felix Rivera Moctezuma[2], Kareena Udeshi[2], Brae Davies[2], Sydney Triplett[1], Eric Dammer[3], Srikant Rangaraju[4], Erin M. Buckley[1,5,6,¥,], Levi B. Wood[1,2,6,¥,] *

[1]Wallace H. Coulter Department of Biomedical Engineering, Georgia Institute of Technology and Emory University
[2]George W. Woodruff School of Mechanical Engineering, Georgia Institute of Technology
[3]Center for Neurodegenerative Diseases, School of Medicine, Emory University
[4]Department of Neurology, School of Medicine, Emory University
[5]Department of Pediatrics, School of Medicine, Emory University
[6]Parker H. Petit Institute for Bioengineering and Bioscience, Georgia Institute of Technology

[¥]*Equally contributing corresponding authors*
To whom correspondence should be addressed

Erin M. Buckley, PhD[¥, *] Assistant Professor Wallace H. Coulter Department of Biomedical Engineering, Georgia Institute of Technology and Emory University; Department of Pediatrics, School of Medicine, Emory University 1760 Haygood Dr NE Atlanta, GA 30322 E-mail: erin.buckley@emory.edu	**Levi B. Wood**, PhD [¥, *] Assistant Professor George W. Woodruff School of Mechanical Engineering, Wallace H. Coulter Department of Biomedical Engineering, and Parker H. Petit Institute for Bioengineering and Bioscience, Georgia Institute of Technology 315 Ferst Dr, Rm 3311 Atlanta, GA 30332 E-mail: levi.wood@me.gatech.edu

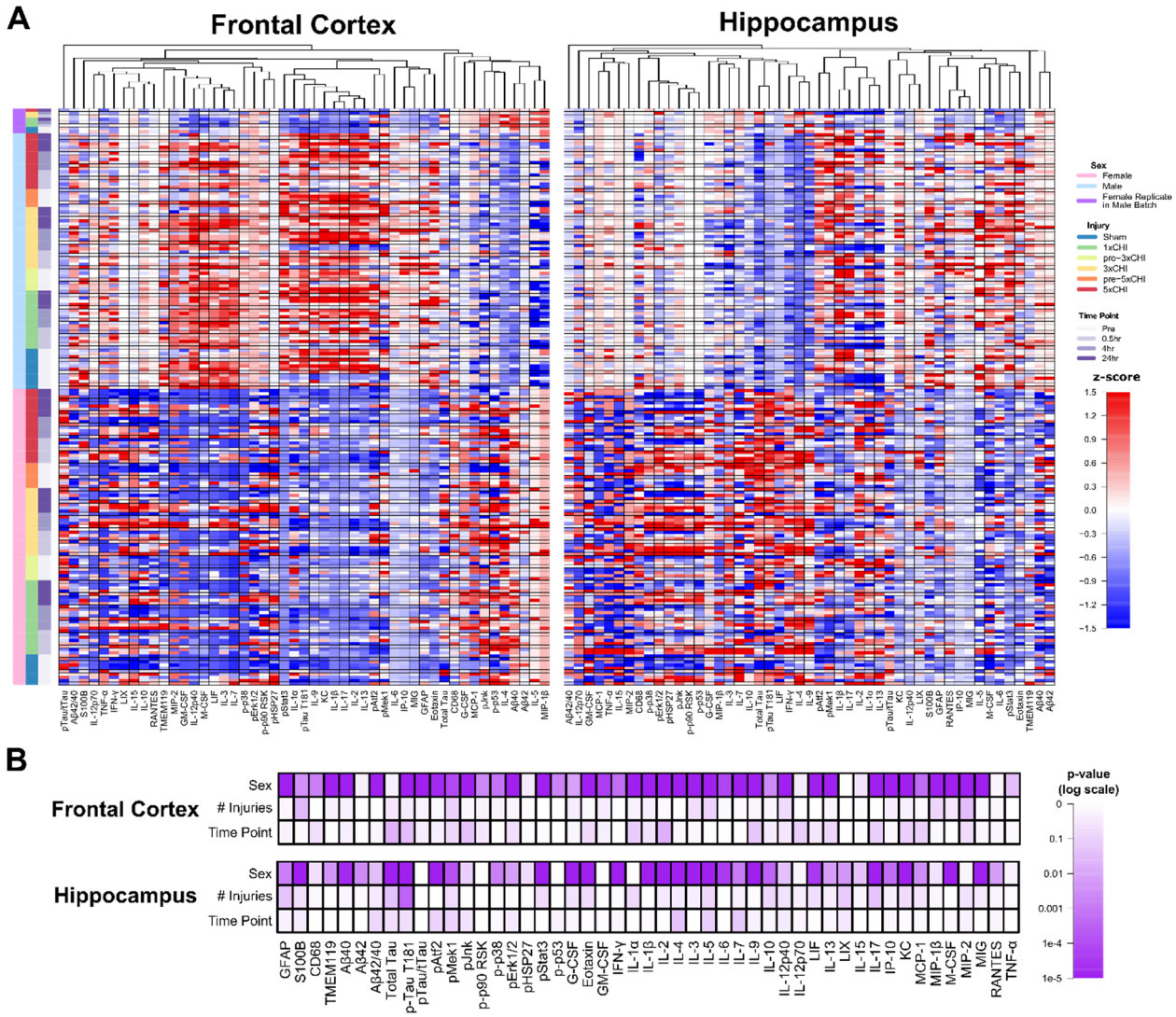
Supplementary Table S1. Sample sizes of each experimental group. Tables are separated by Female (top) and Male (bottom) samples by injury group (1x,3x,5xCHI) and time point (pre-injury, 30min, 4hr, 24hr). Sample size is indicated in n column. In total, 96 females and 83 males were used in the protein analysis and 39 females in RNAseq analysis.

Protein Data

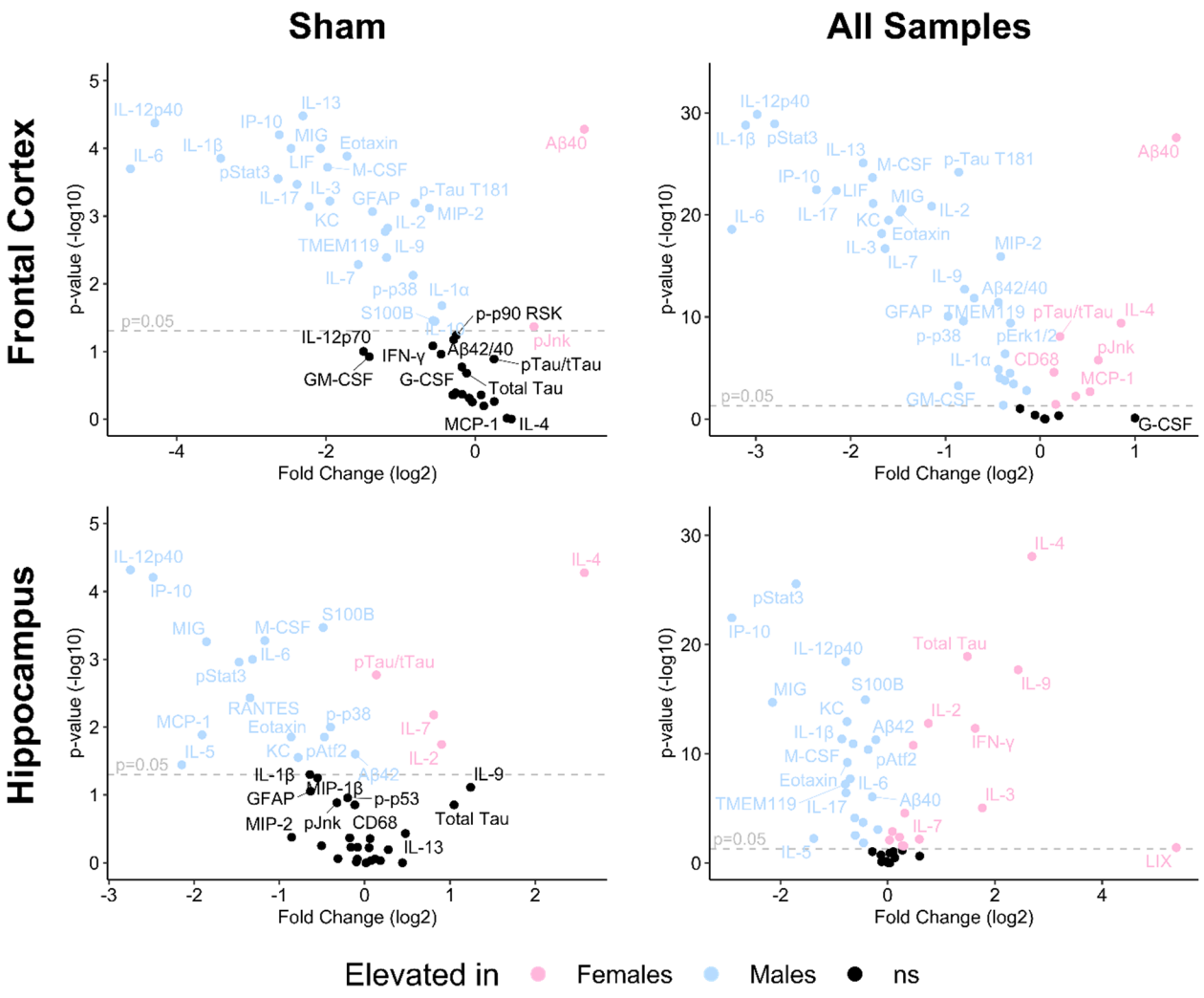
Sex	Injury	Time Point	Total Time	n
Females	1xCHI	Pre-Injury	0	10
		30min	0.5	8
		4hr	4	8
		24hr	24	8
	3xCHI	Pre-Injury	48	8
		30min	48.5	8
		4hr	52	6
		24hr	72	8
	5xCHI	Pre-Injury	96	8
		30min	96.5	8
		4hr	100	7
		24hr	120	9
			Female Total:	**96**
Males	1xCHI	Pre-Injury	0	13
		30min	0.5	7
		4hr	4	6
		24hr	24	6
	3xCHI	Pre-Injury	48	7
		30min	48.5	6
		4hr	52	7
		24hr	72	7
	5xCHI	Pre-Injury	96	6
		30min	96.5	6
		4hr	100	6
		24hr	120	6
			Male Total:	**83**

RNAseq Data

Sex	Injury	Time Point	Total Time	n
Females	1xCHI	Pre-Injury	0	4
		30min	0.5	3
		4hr	4	3
		24hr	24	4
	3xCHI	Pre-Injury	48	3
		30min	48.5	3
		4hr	52	2
		24hr	72	4
	5xCHI	Pre-Injury	96	3
		30min	96.5	3
		4hr	100	3
		24hr	120	4
			Female Total:	**39**



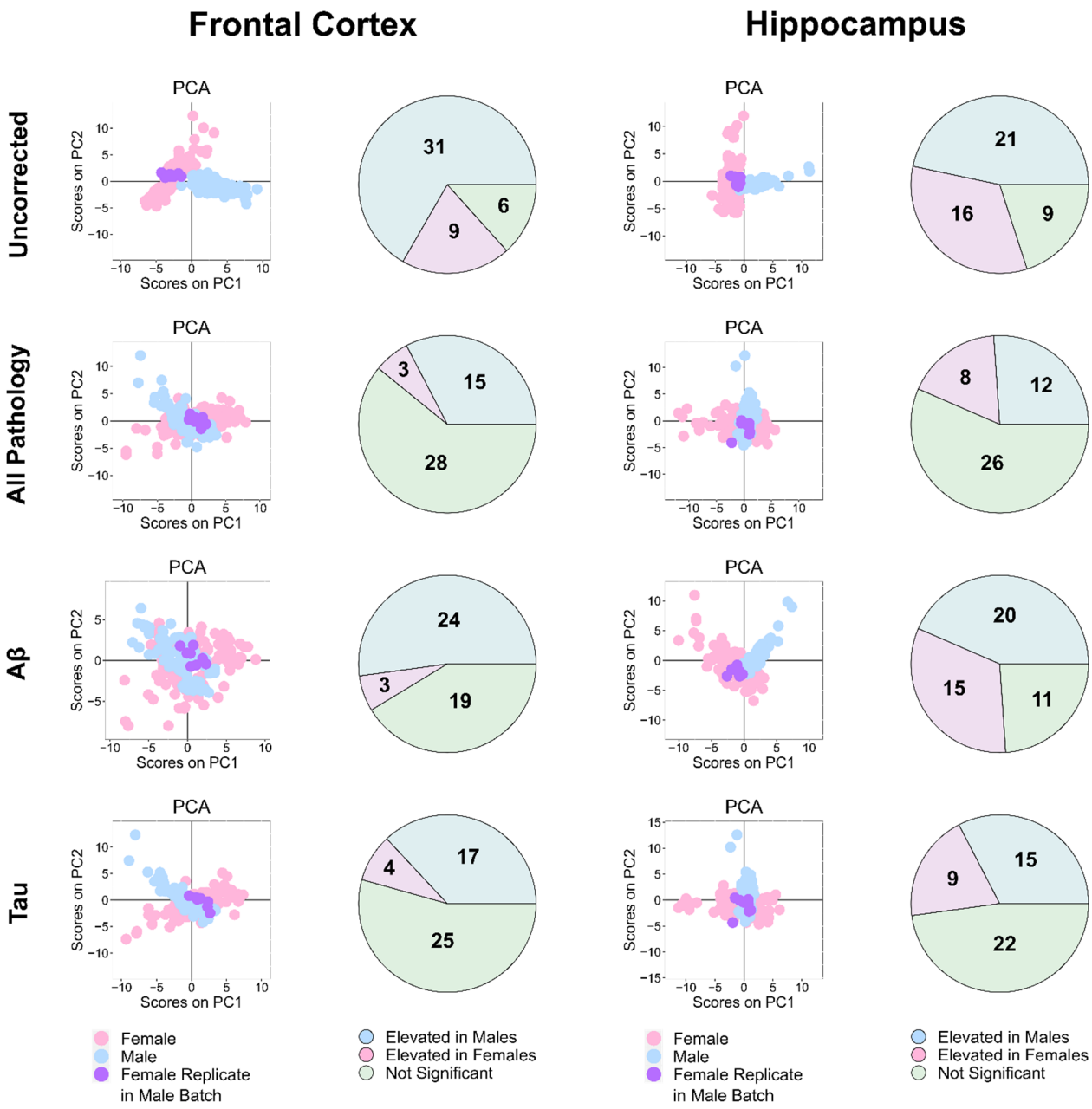
Supplementary Figure S1. Pronounced sexual dimorphism of immune signaling, glial markers, and molecular markers of pathology in 3xTg-AD mice: all-samples heatmap and multiple linear regression model. A) 30 cytokines, 6 MAPK phospho-proteins, amyloid beta 40 and 42, total and phospho-tau, GFAP, S100B, CD68, and TMEM119 were measured by multiplex and traditional ELISA in both frontal cortex (left) and hippocampus (right) tissue of 96 female (pink) and 83 male (blue) 3xTg-AD mice aged 2-4mo. Eight female samples were run as replicates within male batch assays (purple) to allow transformation of male data to female space by linear regression. S100B, CD68, and TMEM119 were run with all samples at the same time while all other assays were run in separate batches for male and female samples. Each row represents data from an individual mouse z-scored along each column. Columns are clustered by Euclidean distance via unweighted pair group method with arithmetic mean. **B**) Multiple linear regression models were calculated for each measured protein using fixed effects of sex, number of injuries, and time point after most recent injury. The model shows that the effect of sex strongly outweighs injury-dependent changes for most proteins from both regions.



Supplementary Figure S2. Pronounced sexual dimorphism of immune signaling, glial markers, and molecular markers of pathology in 3xTg-AD mice: volcano plots. Volcano plots of male vs female comparative analysis show Wilcoxon rank-sum p-values (vertical axis, -log10 scale) and fold change (horizontal axis, log2 scale) of each measured protein. Proteins are considered significantly elevated in either male (blue) or female (pink) samples if $p<0.05$ by Wilcoxon rank-sum test. All significantly different proteins within sham-injured samples were also significant within all samples in the same direction. The all-samples analysis revealed a greater proportion of significantly different proteins by sex.

Supplementary Table S2. Sex differences by protein within each brain region among sham-injured and all samples. Proteins are considered significantly elevated in either male (blue) or female (pink) samples if $p<0.05$ by Wilcoxon rank-sum test. All significantly different proteins within sham-injured samples were also significant within all samples in the same direction. ns = not significant, *$p<0.05$, **$p<0.01$, ***$p<0.001$, ****$p<0.0001$. The all-samples analysis revealed a greater proportion of significantly different proteins by sex.

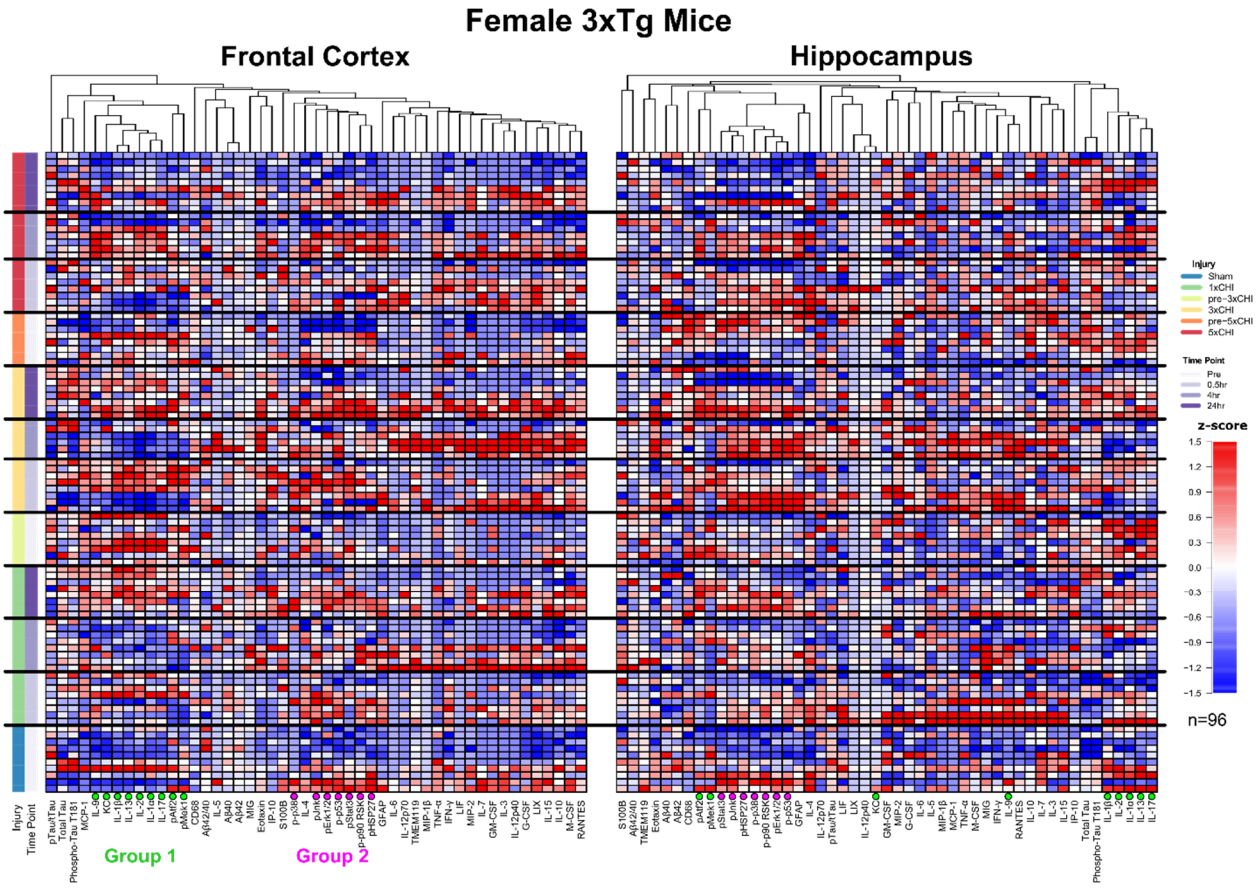
Protein	Frontal Cortex Sham	Frontal Cortex All	Hippocampus Sham	Hippocampus All
GFAP	Males ***	Males ****	ns	Males *
S100B	Males *	Males ***	Males ***	Males ****
CD68	ns	Females ****	ns	ns
TMEM119	Males **	Males ****	ns	Males ****
Aβ40	Females ****	Females ****	ns	Males ****
Aβ42	ns	Females *	Males *	Males ****
Total Tau	ns	ns	ns	Females ****
p-Tau	Males ***	Males ****	ns	Females ****
pAtf2	ns	Males ****	Males *	Males ****
pMek1	ns	Males ****	ns	Males ***
pJnk	Females *	Females ****	ns	ns
p-p90 RSK	ns	Males **	N/A	N/A
p-p38	Males **	Males ****	Males *	Males ***
pErk1/2	ns	Males ****	ns	Females **
pHSP27	ns	ns	ns	ns
pStat3	Males ***	Males ****	Males **	Males ****
p-p53	ns	Females **	ns	ns
G-CSF	ns	ns	Females **	Females ****
Eotaxin	Males ***	Males ****	Males *	Males ****
GM-CSF	ns	Males ***	ns	Females **
IFN-γ	ns	Males ***	ns	Females ****
IL-1α	Males *	Males ****	ns	ns
IL-1β	Males ***	Males ****	ns	Males ****
IL-2	Males **	Males ****	Females *	Females ****
IL-4	ns	Females ****	Females ****	Females ****
IL-3	Males ***	Males ****	Females *	Females ****
IL-5	Females *	Females ****	Males *	Males **
IL-6	Males ***	Males ****	Males **	Males ****
IL-7	Males **	Males ****	Females **	Females ****
IL-9	Males **	Males ****	ns	Females ****
IL-10	Males *	Males ****	ns	Females **
IL-12p40	Males ****	Males ****	Males ****	Males ****
IL-12p70	ns	Ns	ns	ns
LIF	Males ***	Males ****	ns	ns
IL-13	Males ****	Males ****	ns	Females *
LIX	N/A	N/A	ns	Females *
IL-15	ns	ns	ns	ns
IL-17	Males ***	Males ****	ns	Males ****
IP-10	Males ****	Males ****	Males ****	Males ****
KC	Males ***	Males ****	Males *	Males ****
MCP-1	ns	Females **	Males *	Males ****
MIP-1β	Females **	Females ****	ns	Females *
M-CSF	Males ***	Males ****	Males ***	Males ****
MIP-2	Males ***	Males ****	ns	Females **
MIG	Males ***	Males ****	Males ***	Males ****
RANTES	ns	ns	Males **	Males **
TNF-α	ns	Males *	ns	ns



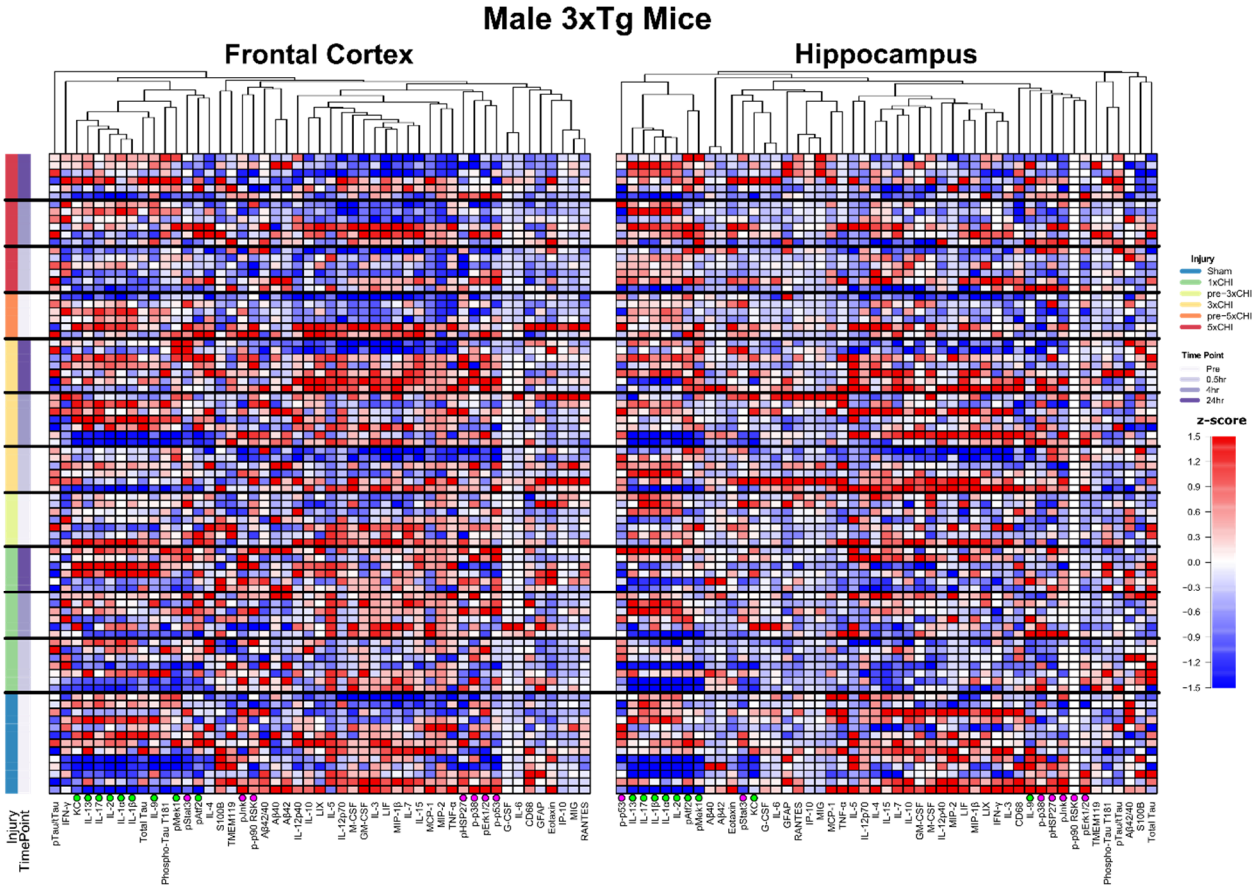
Supplementary Figure S3. Sex differences within pathology-adjusted data. Adjusted data is defined as the residual of a linear regression of Aβ markers (Aβ40 + Aβ42), tau markers (total tau + phospho-tau T181), or all pathological markers (Aβ and tau combined) against all combined protein data. From top to bottom, the graphic shows uncorrected data, all pathology-, Aβ-, and tau-adjusted data for both the frontal cortex (left) and hippocampus (right). A principal component analysis (PCA) scores plot of the first two PCs is shown to illustrate changes in variance between the samples after adjustment. The pie charts are annotated with the number of differentially expressed proteins which are significantly upregulated in male (blue) and female (pink) samples, or not significantly different (green). Proteins are considered significantly different if $p<0.05$ by Wilcox Rank Sum test.

Supplementary Table S3. Sex differences by protein within each brain region before and after adjustment for pathological markers. Proteins are considered significantly elevated in either male (blue) or female (pink) samples if $p<0.05$ by Wilcoxon rank-sum test. Adjusted data is defined as the residual of a linear regression of Aβ markers (Aβ40 + Aβ42), tau markers (total tau + phospho-tau T181), or all pathological markers (Aβ and tau combined) against all combined protein data. Phospho-p90 RSK and LIX were measured below the detection limit among all eight female replicate samples within the male batch hippocampus and frontal cortex, respectively, disallowing conversion to female space.

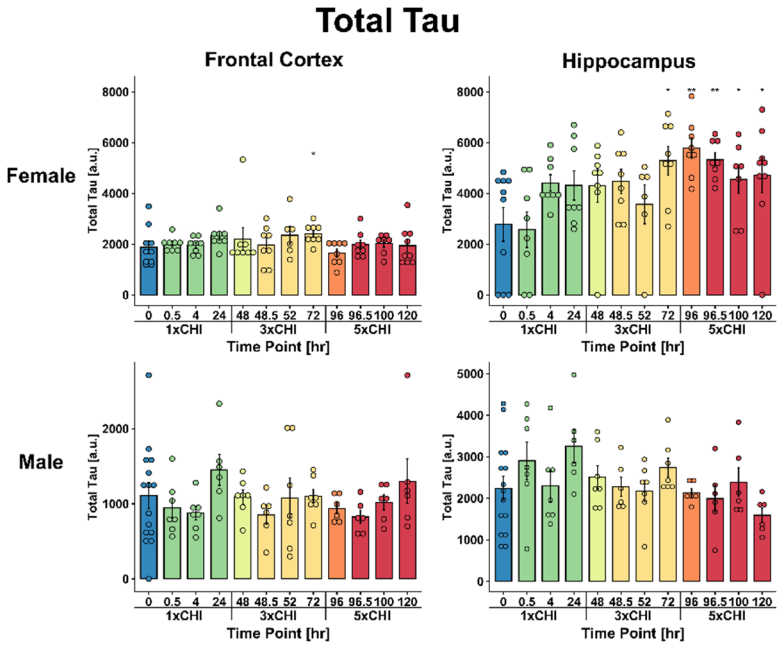
	Frontal Cortex				Hippocampus			
Protein	**Original**	**All**	**Aβ**	**Tau**	**Original**	**All**	**Aβ**	**Tau**
GFAP	M	ns	ns	M	M	ns	ns	ns
S100B	M	ns	ns	ns	M	M	M	M
CD68	F	F	F	F	ns	ns	ns	ns
TMEM119	M	M	ns	M	M	ns	M	ns
Aβ40	F	F	M	F	M	M	M	M
Aβ42	F	M	M	M	M	F	ns	M
Total Tau	ns	ns	ns	M	F	ns	F	M
Phospho-Tau	M	M	M	ns	F	ns	F	M
pAtf2	M	ns	M	ns	M	M	M	M
pMek1	M	ns	ns	ns	M	M	M	M
pJnk	F	ns	ns	ns	ns	ns	ns	ns
p-p90 RSK	M	ns	ns	ns	N/A	N/A	N/A	N/A
p-p38	M	M	M	M	M	ns	M	M
pErk1/2	M	M	M	M	F	ns	F	ns
pHSP27	ns	ns	ns	ns	ns	ns	F	ns
pStat3	M	ns	M	ns	M	M	M	M
p-p53	F	ns	ns	ns	ns	ns	ns	ns
G-CSF	ns	ns	ns	ns	F	ns	F	ns
Eotaxin	M	ns	ns	ns	M	ns	M	ns
GM-CSF	M	M	M	M	F	M	M	F
IFN-γ	M	ns	M	ns	F	F	F	F
IL-1α	M	ns	ns	ns	ns	ns	ns	ns
IL-1β	M	ns	M	ns	M	M	M	M
IL-2	M	ns	M	ns	F	F	F	F
IL-4	F	ns	F	F	F	F	F	F
IL-3	M	M	M	M	F	F	F	F
IL-5	F	ns	ns	ns	M	M	M	M
IL-6	M	ns	ns	M	M	ns	M	ns
IL-7	M	M	M	M	F	ns	F	ns
IL-9	M	ns	M	ns	F	F	F	F
IL-10	M	M	M	M	F	ns	F	ns
IL-12p40	M	M	M	M	M	ns	M	ns
IL-12p70	ns	M	ns	M	ns	ns	ns	ns
LIF	M	M	M	M	ns	F	ns	F
IL-13	M	ns	M	ns	F	ns	F	ns
LIX	N/A	N/A	N/A	N/A	F	ns	F	ns
IL-15	ns	ns	ns	ns	ns	ns	ns	ns
IL-17	M	ns	M	ns	M	M	M	M
IP-10	M	M	ns	ns	M	ns	M	ns
KC	M	ns	M	ns	M	M	M	M
MCP-1	F	ns	ns	ns	M	M	M	M
MIP-1β	F	F	F	F	F	ns	ns	F
M-CSF	M	M	M	M	M	M	M	M
MIP-2	M	ns	M	M	F	F	F	F
MIG	M	ns	ns	M	M	ns	M	ns
RANTES	ns	M	M	ns	M	ns	M	ns
TNF-α	M	ns	M	ns	ns	ns	ns	ns



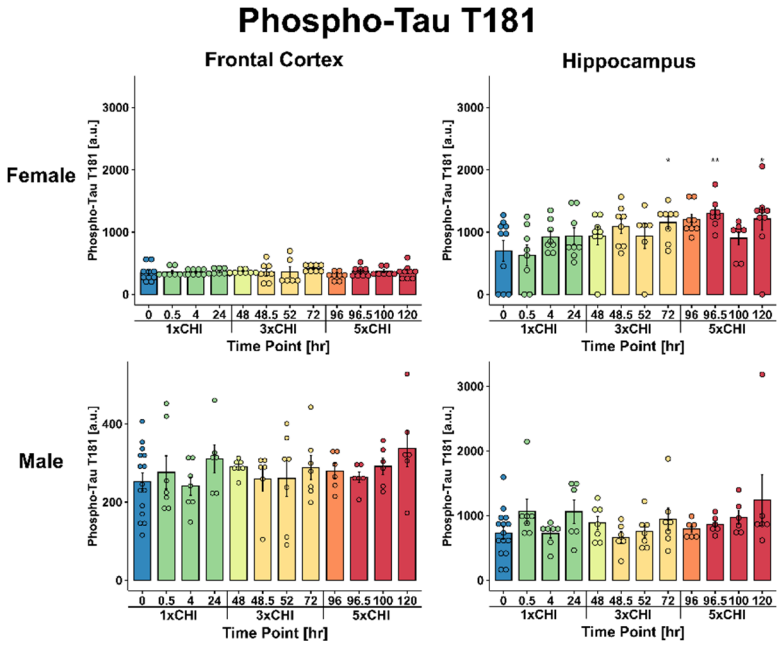
Supplementary Figure S4. Female protein data: Quantification of immune and pathological markers in female 3xTg-AD mice pre- and 30min, 4hr, & 24hr post-1x, 3x, and 5xCHI. 30 cytokines, 6 MAPK phospho-proteins, amyloid beta 40 and 42, total and phospho-tau, GFAP, S100B, CD68, and TMEM119 were measured by multiplex and traditional ELISA in both frontal cortex (left) and hippocampus (right) tissue of 96 female 3xTg-AD mice aged 2-4mo. Each row represents data from an individual mouse z-scored along each column. Columns are clustered by Euclidean distance via unweighted pair group method with arithmetic mean.



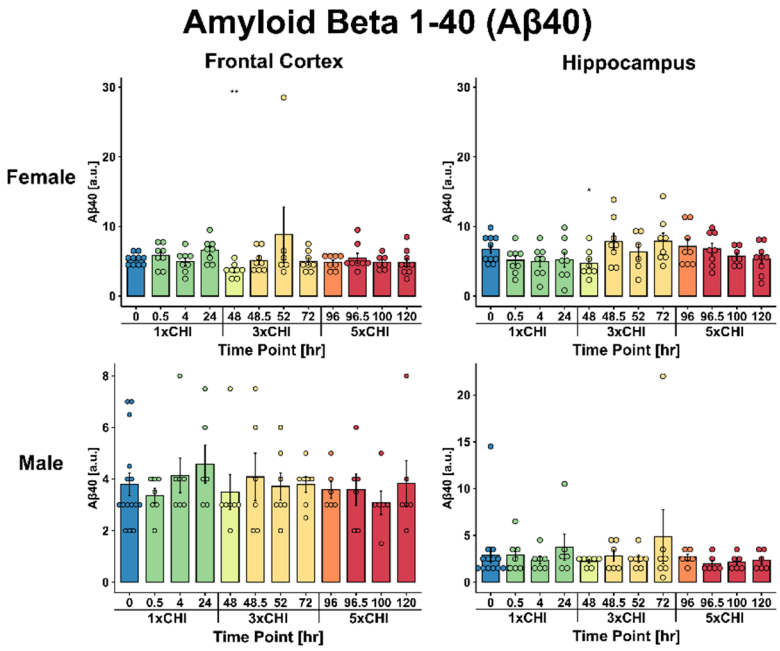
Supplementary Figure S5. Male protein data: Quantification of immune and pathological markers in male 3xTg-AD mice pre- and 30min, 4hr, & 24hr post-1x, 3x, and 5xCHI. 30 cytokines, 6 MAPK phospho-proteins, amyloid beta 40 and 42, total and phospho-tau, GFAP, S100B, CD68, and TMEM119 were measured by multiplex and traditional ELISA in both frontal cortex (left) and hippocampus (right) tissue of 83 male 3xTg-AD mice aged 2-4mo. Each row represents data from an individual mouse z-scored along each column. Columns are clustered by Euclidean distance via unweighted pair group method with arithmetic mean.



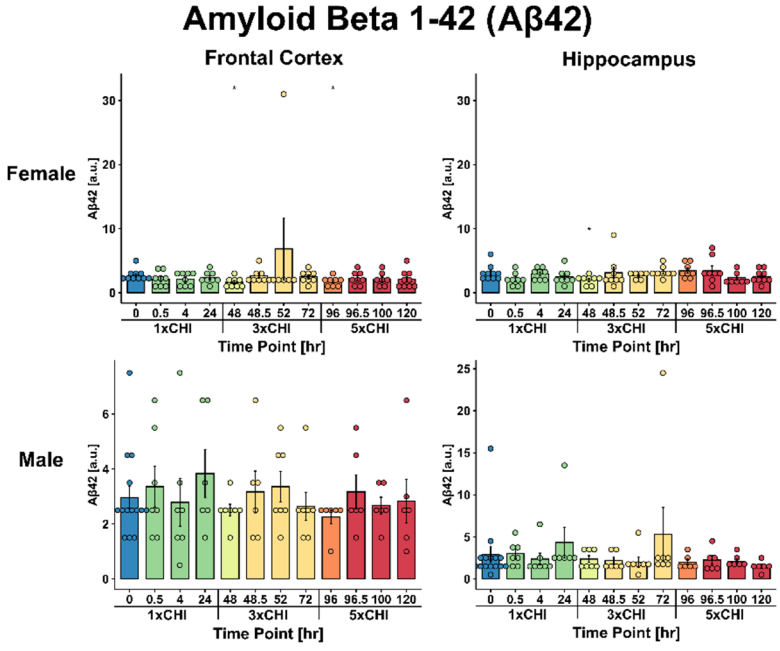
Supplementary Figure S6. Total tau by sex and brain region. Total tau was measured by Luminex ELISA (Millipore Sigma HNABTMAG-68K) in male and female frontal cortex and hippocampus tissue (*p<0.05, **p<0.01, Wilcox test vs sham) (mean ± SEM). Male and female samples run separately.



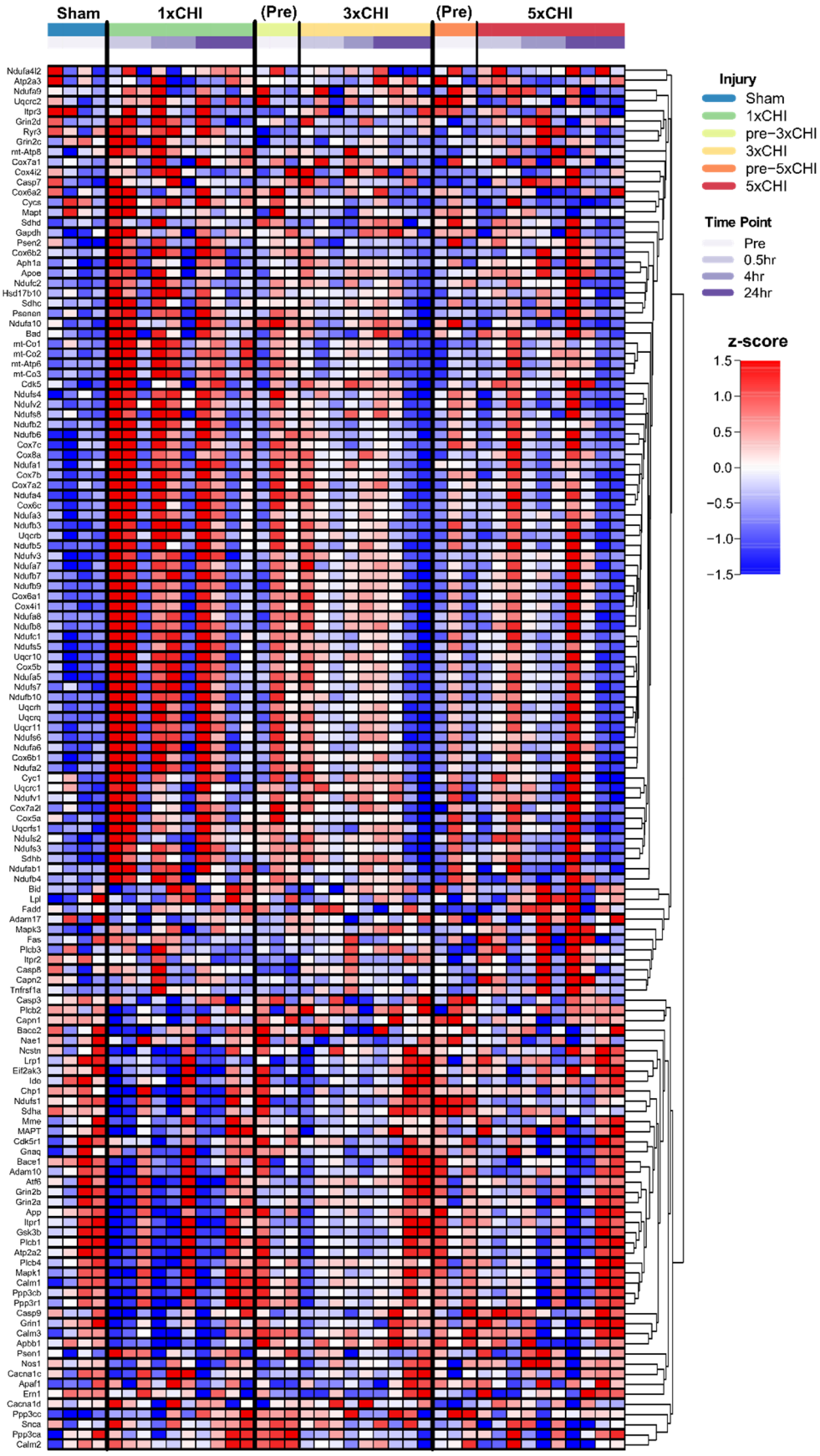
Supplementary Figure S7. Phospho-tau T181 by sex and brain region. Phospho-tau T181 was measured by Luminex ELISA (Millipore Sigma HNABTMAG-68K) in male and female frontal cortex and hippocampus tissue (*p<0.05, **p<0.01, Wilcox test vs sham) (mean ± SEM). Male and female samples run separately.



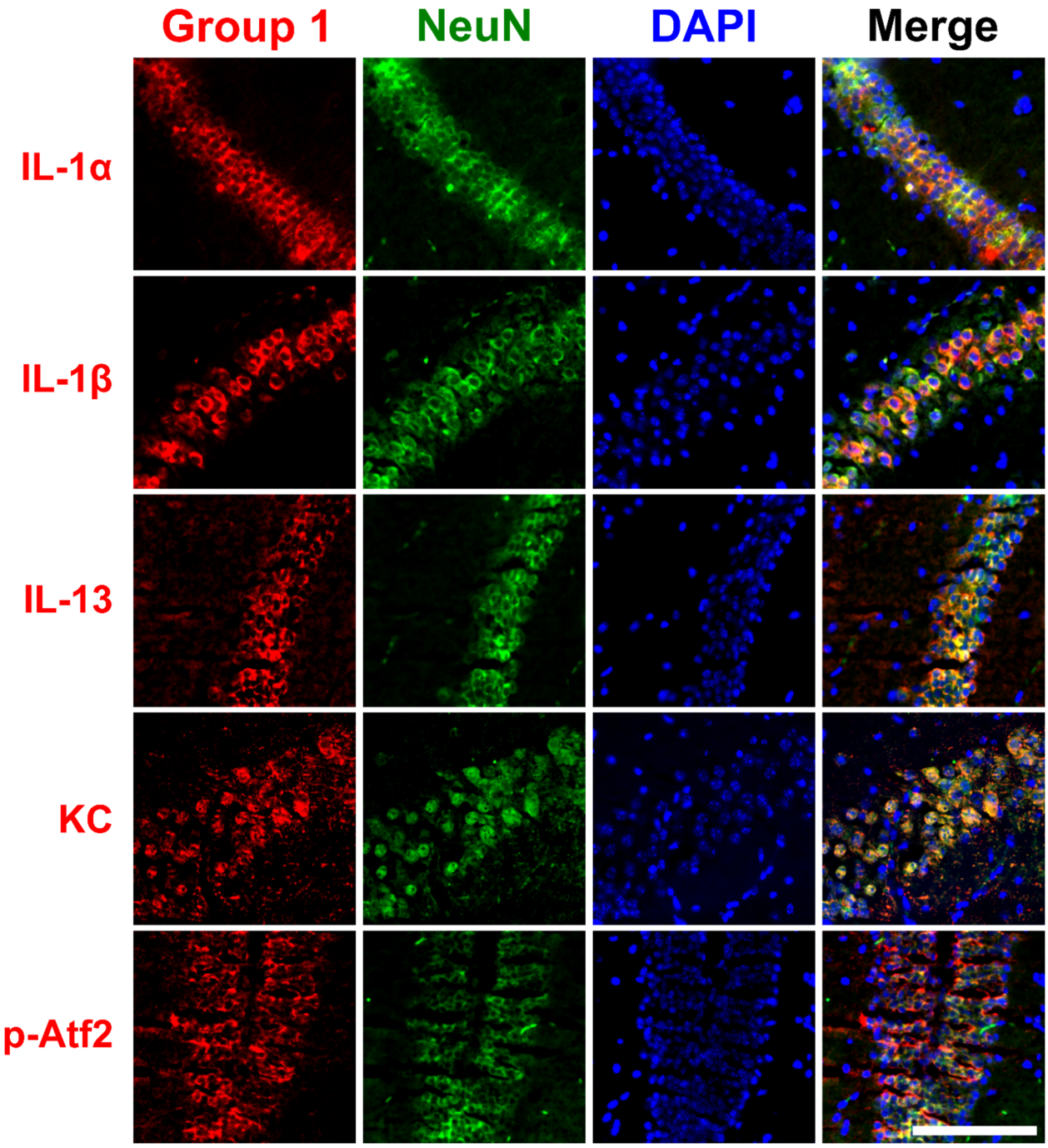
Supplementary Figure S8. Amyloid Beta 1-40 (Aβ40) by sex and brain region. Aβ40 was measured by Luminex ELISA (Millipore Sigma HNABTMAG-68K) in male and female frontal cortex and hippocampus tissue (*p<0.05, **p<0.01, Wilcox test vs sham) (mean ± SEM). Male and female samples run separately.



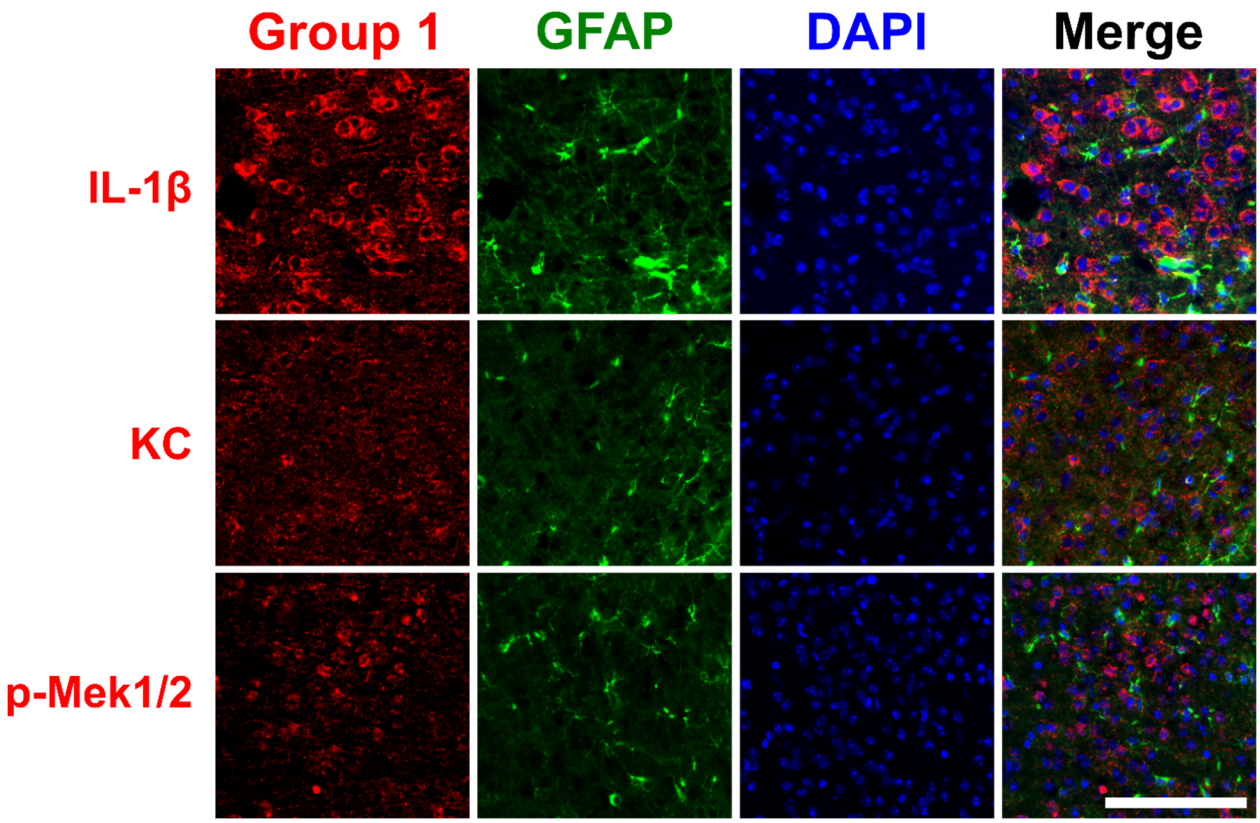
Supplementary Figure S9. Amyloid Beta 1-42 (Aβ42) by sex and brain region. Aβ42 was measured by Luminex ELISA (Millipore Sigma HNABTMAG-68K) in male and female frontal cortex and hippocampus tissue (*p<0.05, Wilcox test vs sham) (mean ± SEM). Male and female samples run separately.


Sham
1xCHI
(Pre)
3xCHI
(Pre)
5xCHI
Ndufa4l2
Atp2a3
Ndufa9
Uqcrc2
Itpr3
Grin2d
Ryr3
Grin2c
mt-Atp8
Cox7a1
Cox4i2
Casp7
Cox6a2
Cycs
Mapt
Sdhd
Gapdh
Psen2
Cox6b2
Aph1a
Apoe
Ndufc2
Hsd17b10
Sdhc
Psenen
Ndufa10
Bad
mt-Co1
mt-Co2
mt-Atp6
mt-Co3
Cdk5
Ndufs4
Ndufv2
Ndufs8
Ndufb2
Ndufb6
Cox7c
Cox8a
Ndufa1
Cox7b
Cox7a2
Ndufa4
Cox6c
Ndufa3
Ndufb3
Uqcrb
Ndufb5
Ndufv3
Ndufa7
Ndufb7
Ndufb9
Cox6a1
Cox4i1
Ndufa8
Ndufb8
Ndufc1
Ndufs5
Uqcr10
Cox5b
Ndufa5
Ndufs7
Ndufb10
Uqcrh
Uqcrq
Uqcr11
Ndufs6
Ndufa6
Cox6b1
Ndufa2
Cyc1
Uqcrc1
Ndufv1
Cox7a2l
Cox5a
Uqcrfs1
Ndufs2
Ndufs3
Sdhb
Ndufab1
Ndufb4
Bid
Lpl
Fadd
Adam17
Mapk3
Fas
Plcb3
Itpr2
Casp8
Capn2
Tnfrsf1a
Casp3
Plcb2
Capn1
Baco2
Nae1
Ncstn
Lrp1
Eif2ak3
Ido
Chp1
Ndufs1
Sdha
Mme
MAPT
Cdk5r1
Gnaq
Bace1
Adam10
Atf6
Grin2b
Grin2a
App
Itpr1
Gsk3b
Plcb1
Atp2a2
Plcb4
Mapk1
Calm1
Ppp3cb
Ppp3r1
Casp9
Grin1
Calm3
Apbb1
Psen1
Nos1
Cacna1c
Apaf1
Ern1
Cacna1d
Ppp3cc
Snca
Ppp3ca
Calm2
Injury
Sham
1xCHI
pre−3xCHI
3xCHI
pre−5xCHI
5xCHI
Time Point
Pre
0.5hr
4hr
24hr
z-score
1.5
1.0
0.5
0.0
−0.5
−1.0
−1.5

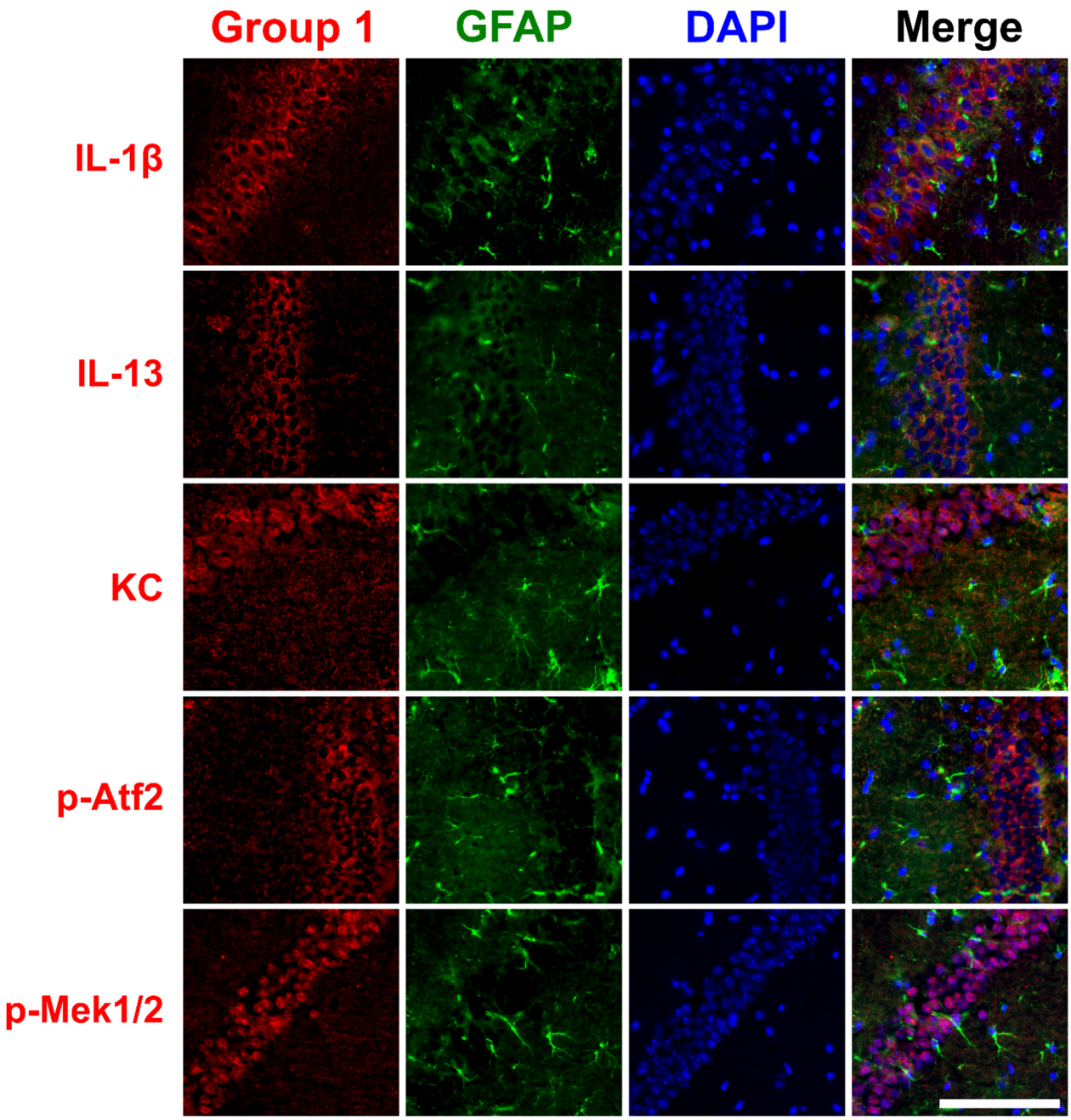
Supplementary Figure S10. Kyoto Encyclopedia of Genes and Genomes (KEGG) Alzheimer's disease gene set. RNAseq data from 204mo female 3xTg somato-motor cortex lysate pre- and 30min, 4hr, and 24hr post- 1x, 3x, and 5xCHI (n=2-4). Heatmap shows subset of all expressed genes from the KEGG Alzheimer's disease gene set (MSigDB C2 collection). RNAseq data is normalized, variance stabilized (**Methods**), then z-scored within each gene (rows) across all animals (columns). Genes are clustered by unweighted pair group method with arithmetic mean using Euclidean distance.



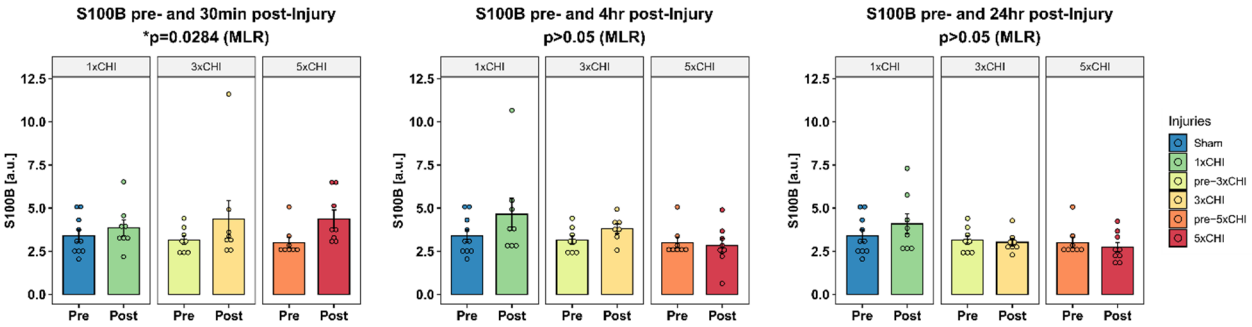
Supplementary Figure S11. Group 1 cytokines and phospho-proteins co-localize with NeuN in hippocampus 24hr post-CHI. Group 1 cytokines (IL-1α, IL-1β, IL-13, and KC) and MAPK phospho-protein phospho-Atf2 (red) co-stained with NeuN (green) and DAPI (blue) show extensive neuronal localization in the hippocampus 24h post-CHI in female 3xTg mice aged 2-4mo (scale bar: 500μm).



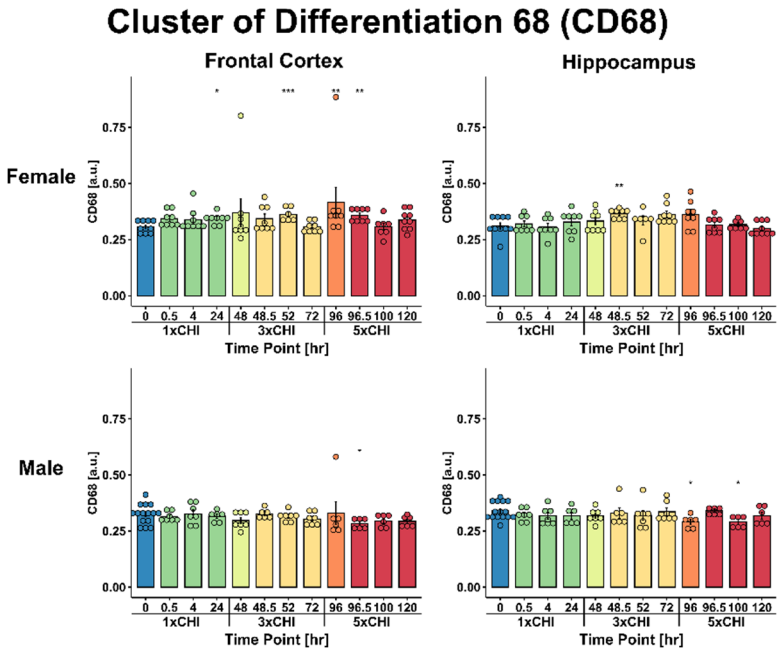
Supplementary Figure S12. Group 1 cytokines and phospho-proteins do not co-localize with astrocyte marker GFAP in the cortex 24hr post-CHI. Group 1 cytokines (IL-1β and KC) and MAPK phospho-protein phospho-Mek1/2 (red) co-stained with GFAP (green) and DAPI (blue) showed minimal astrocyte co-localization in the cortex 24h post-CHI in female 3xTg mice aged 2-4mo (scale bar: 500μm).



Supplementary Figure S13. Group 1 cytokines and phospho-proteins do not co-localize with astrocyte marker GFAP in the hippocampus 24hr post-CHI. Group 1 cytokines (IL-1β, IL-13, and KC) and MAPK phospho-proteins (phospho-Atf2 and phospho-Mek1/2) (red) co-stained with GFAP (green) and DAPI (blue) showed minimal astrocyte co-localization in the hippocampus 24h post-CHI in female 3xTg mice aged 2-4mo (scale bar: 500μm).



Supplementary Figure S14. Cortical astrocytes become reactive following mild TBI: S100B. Cortical S100 calcium-binding protein B (S100B) is significantly upregulated 30min post-injury vs pre-injury but not 4hr or 24hr post-injury (*p<0.05; multiple linear regression model, pre/post and number of injuries) (mean ± SEM).



Supplementary Figure S15. CD68 was measured by ELISA in male and female frontal cortex and hippocampus tissue (*p<0.05, **p<0.01, ***p<0.001, Wilcox test vs sham) (mean ± SEM). Male and female samples run simultaneously.